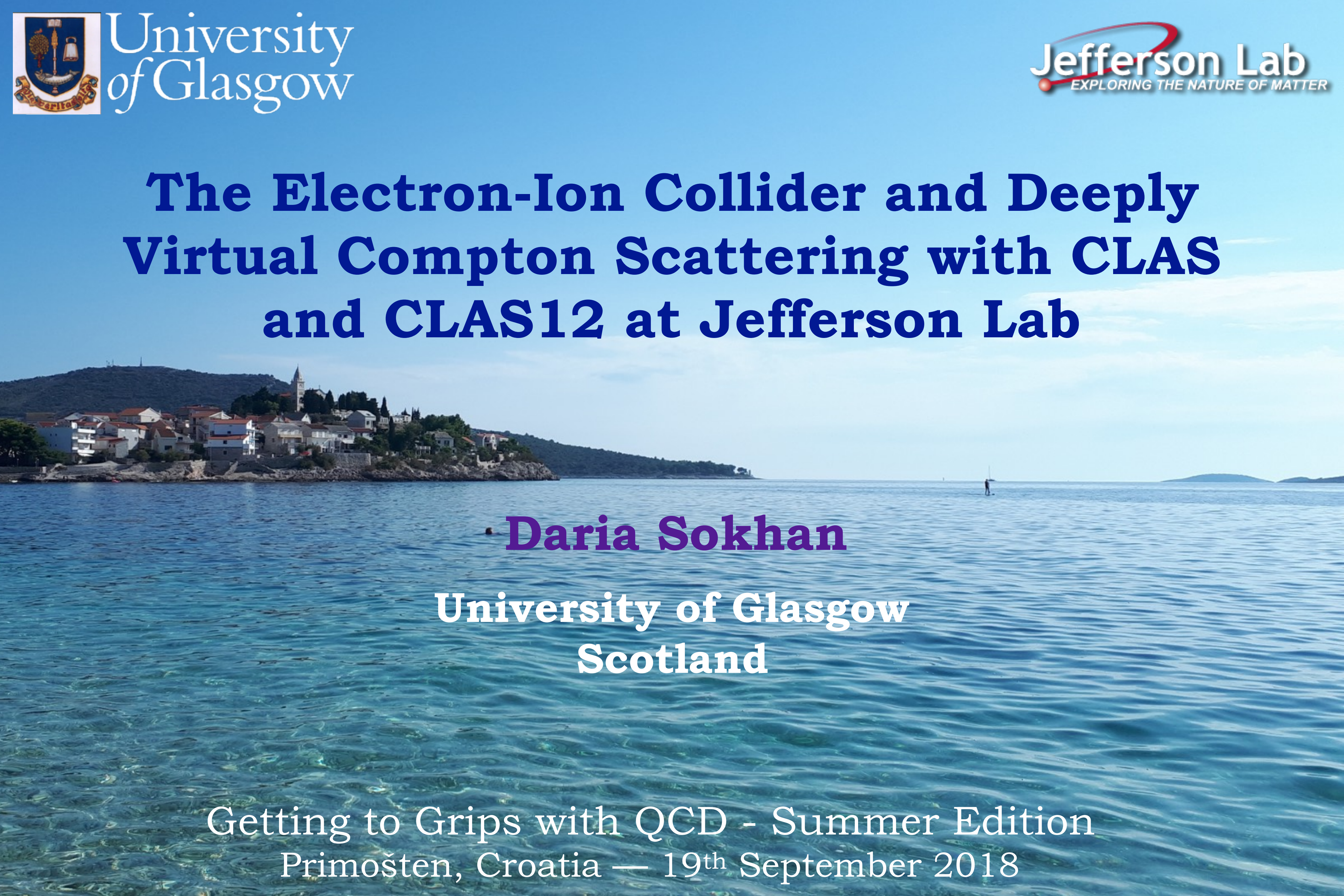

The Electron-Ion Collider and Deeply Virtual Compton Scattering with CLAS and CLAS12 at Jefferson Lab

Daria Sokhan

University of Glasgow
Scotland

Getting to Grips with QCD - Summer Edition
Primošten, Croatia — 19th September 2018

Nucleon Tomography: Intro

A constructivist view of the nucleon

Wigner distributions

$$\rho(x, \vec{k}_T, \vec{b}_T)$$

intuitive relation to experimental observables

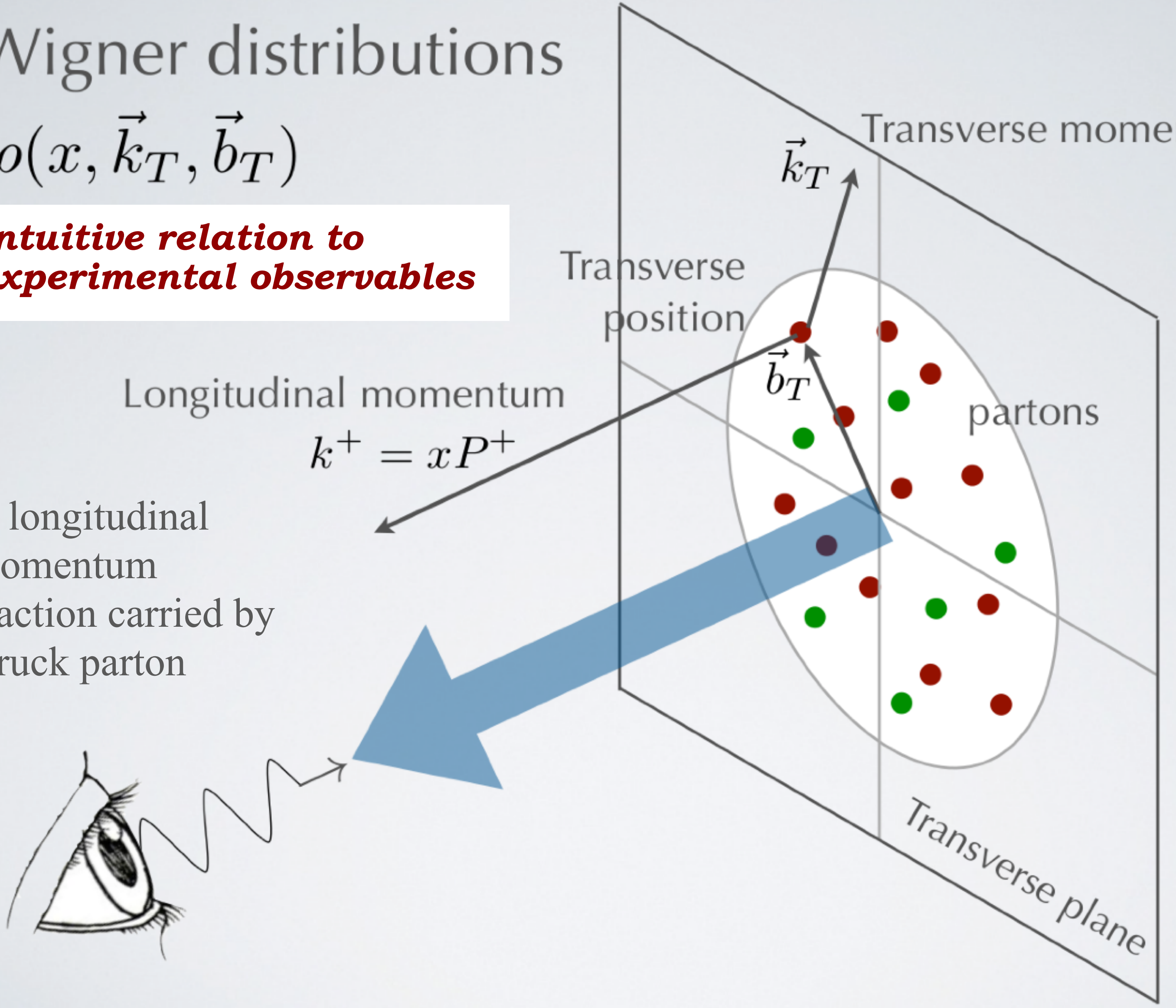

x: longitudinal momentum fraction carried by struck parton

A. Bacchetta

Images of the nucleon

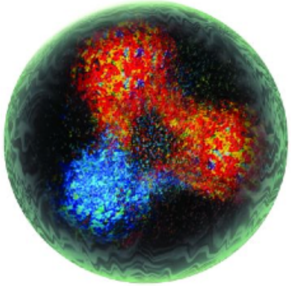

Wigner function:
full phase space parton
distribution of the nucleon

$$\int d^2 b_T$$

Transverse
Momentum
Distributions
(TMDs)

- Semi-inclusive Deep Inelastic Scattering (SIDIS)

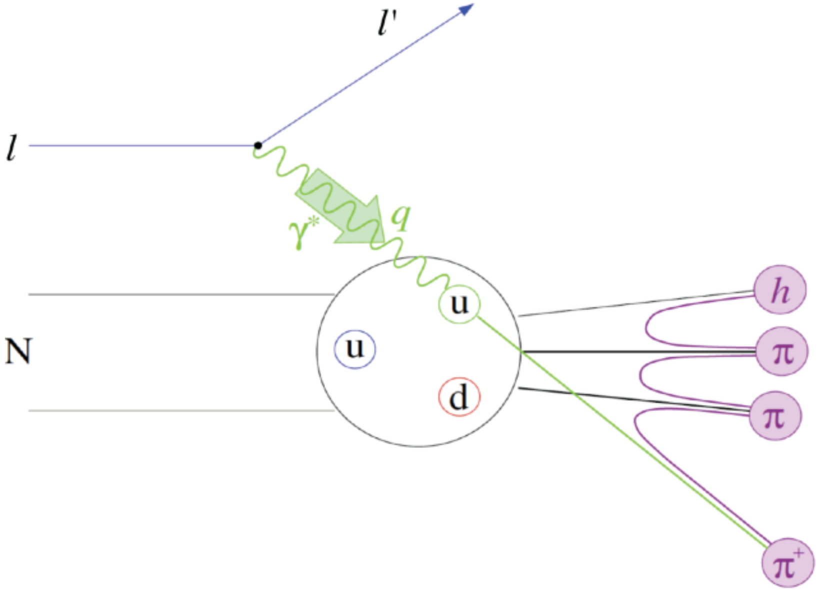

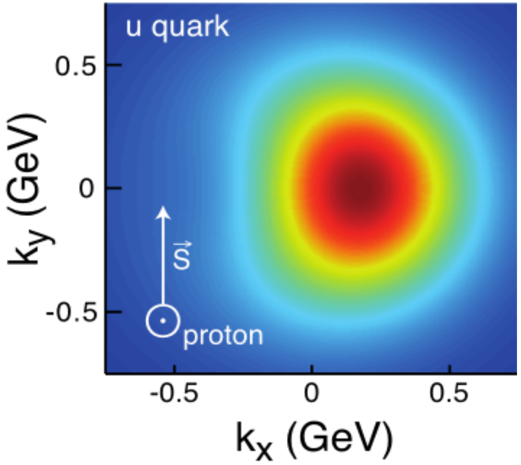

Sivers function: Alexei Prokudin, 2012
(using M. Anselmino et al., J. Phys. Conf. Ser. 295, 012062 (2011))

Images of the nucleon

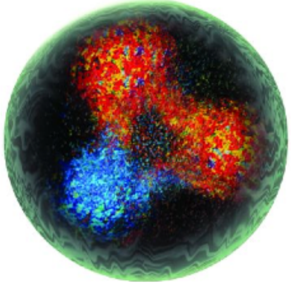

Wigner function:
full phase space parton
distribution of the nucleon

$$\int d^2 b_T$$

Transverse
Momentum
Distributions
(TMDs)

$$\int d^2 k_T$$

Parton Distribution
Functions (PDFs)

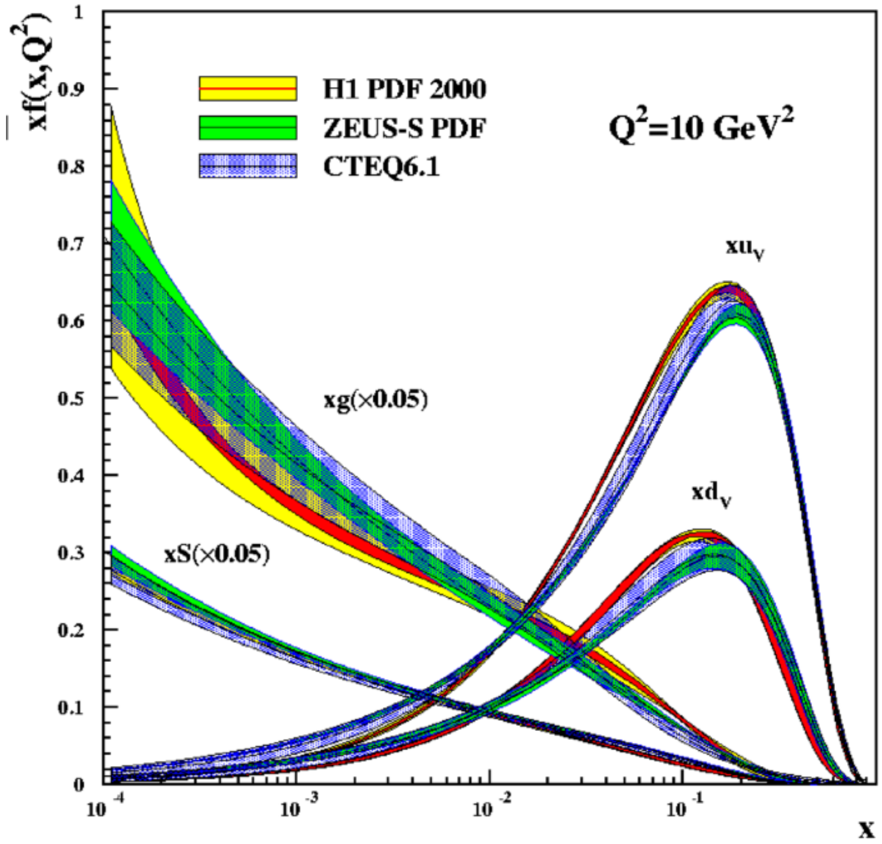

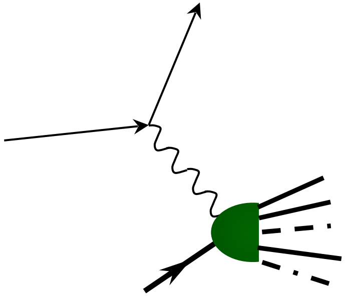

* Deep Inelastic
Scattering (DIS)

Images of the nucleon

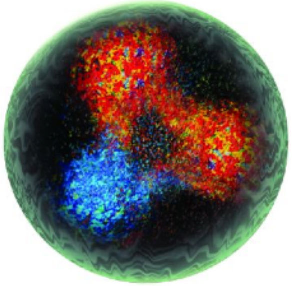

Wigner function:
full phase space parton
distribution of the nucleon

$$\int d^2 k_T$$

Generalised Parton
Distributions (GPDs)

- relate, in the infinite momentum frame, transverse position of partons ($b_\perp$) to longitudinal momentum (x).

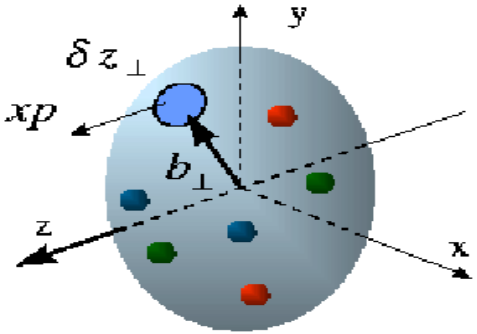

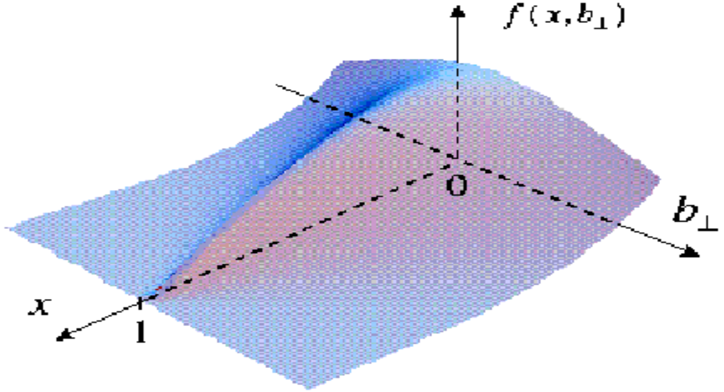

✱ Deep exclusive reactions, e.g.: Deeply Virtual Compton Scattering, Deeply Virtual Meson production, …

Images of the nucleon

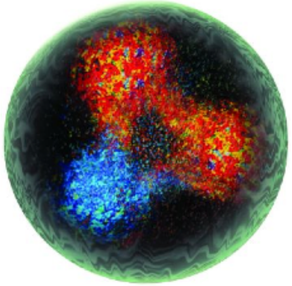

Wigner function:
full phase space parton
distribution of the nucleon

$\int d^2 k_T$

Generalised Parton
Distributions (GPDs)

$\int dx$

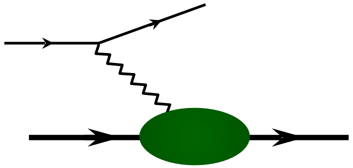

Elastic scattering

Form Factors
eg: G_{E}, G_{M}

Fourier Transform of electric Form Factor: transverse charge density of a nucleon

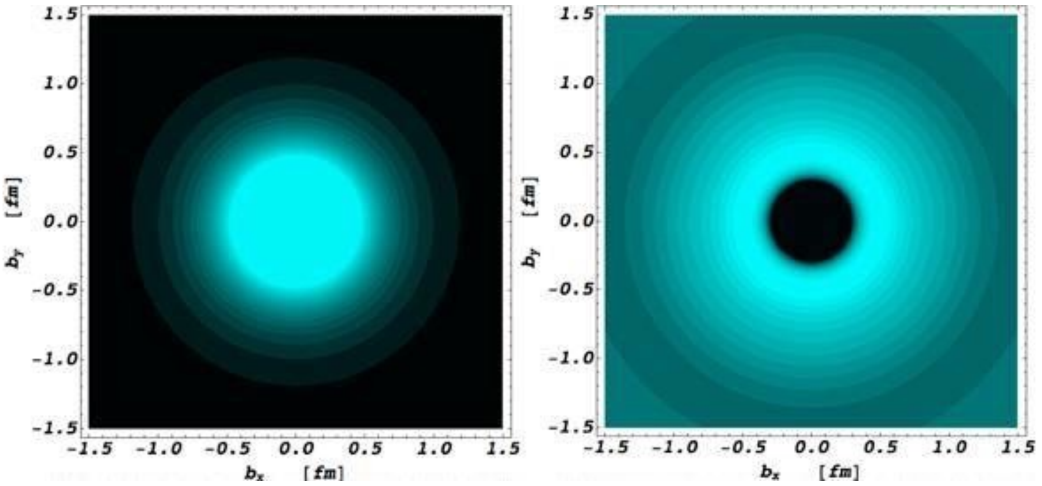

proton

neutron

C. Carlson, M. Vanderhaeghen
PRL 100, 032004 (2008)

Images of the nucleon

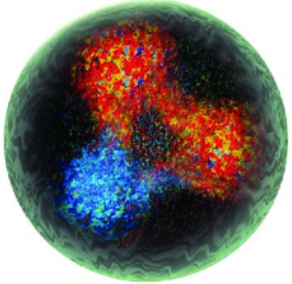

Wigner function:
full phase space parton
distribution of the nucleon

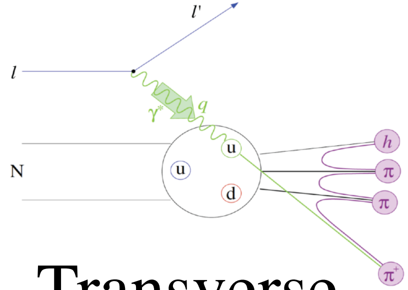

$\int d^2 k_T$

$\int d^2 b_T$

Transverse Momentum Distributions (TMDs)

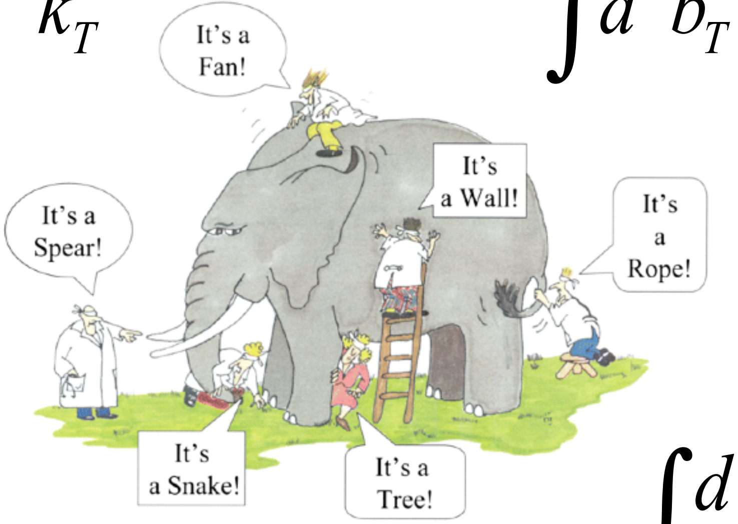

G. Renee Guzlas, artist.

Generalised Parton Distributions (GPDs)

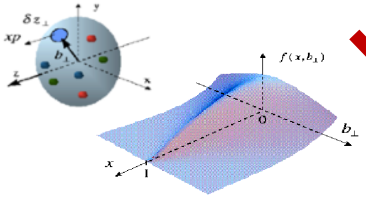

$\int dx$

$\int d^2 k_T$

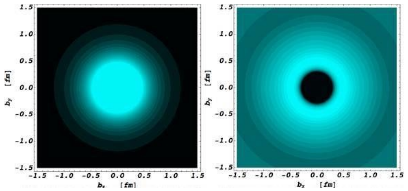

Form Factors
eg: G_E, G_M

Parton Distribution Functions (PDFs)

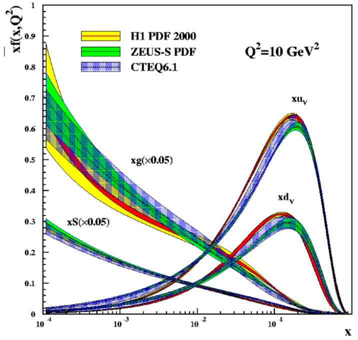

Images of the nucleon

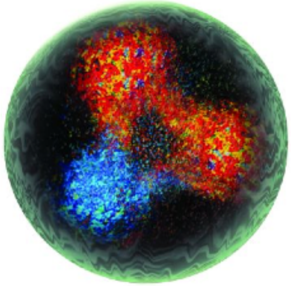

Wigner function:
full phase space parton distribution of the nucleon

$$\int d^2 k_T$$

$$\int d^2 b_T$$

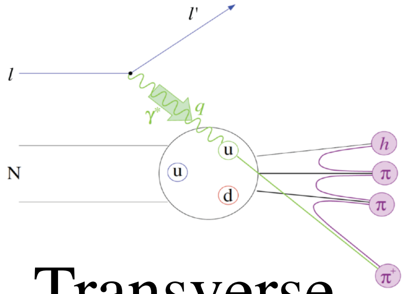

Transverse Momentum Distributions (TMDs)

Generalised Parton Distributions (GPDs)

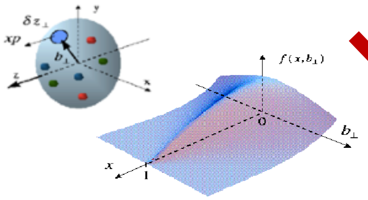

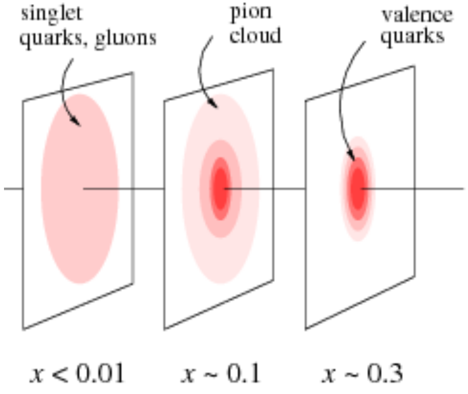

$$\int dx$$

$$\int d^2 k_T$$

Form Factors
eg: $G_{E,}\, G_M$

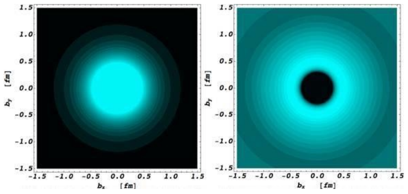

Parton Distribution Functions (PDFs)

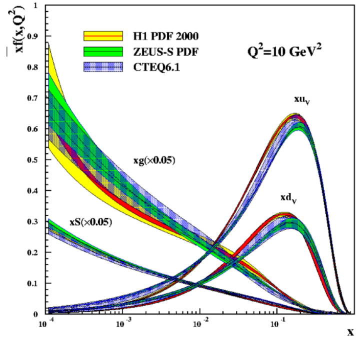

DVCS — an experimental window on GPDs

Experimental paths to GPDs

cliparts.co

Accessible in *exclusive* reactions, where all final state particles are detected.

Trodden paths, or ones starting to be explored:

- Deeply Virtual Compton Scattering (DVCS)
- Deeply Virtual Meson Production (DVMP)
- Time-like Compton Scattering (TCS)
- Double DVCS

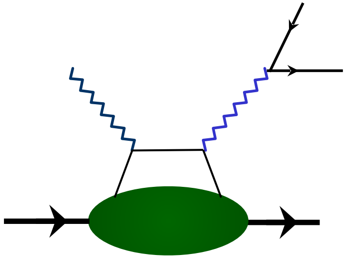

TCS

Virtual photon time-like

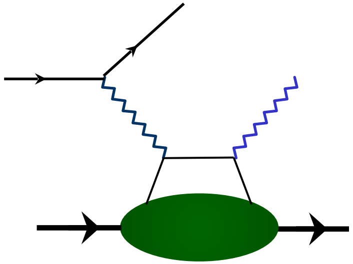

DVCS

Virtual photon space-like

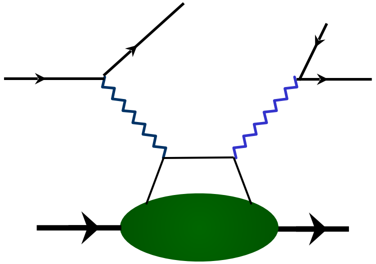

DDVCS

One time-like, one space-like virtual photon

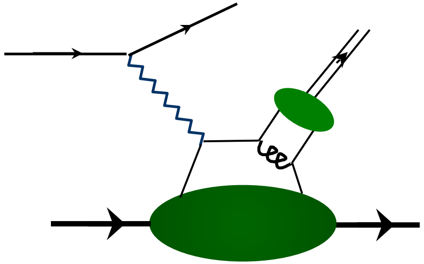

DVMP

GPDs and DVCS

- **Deeply Virtual Compton Scattering:** golden channel for the extraction of GPDs.

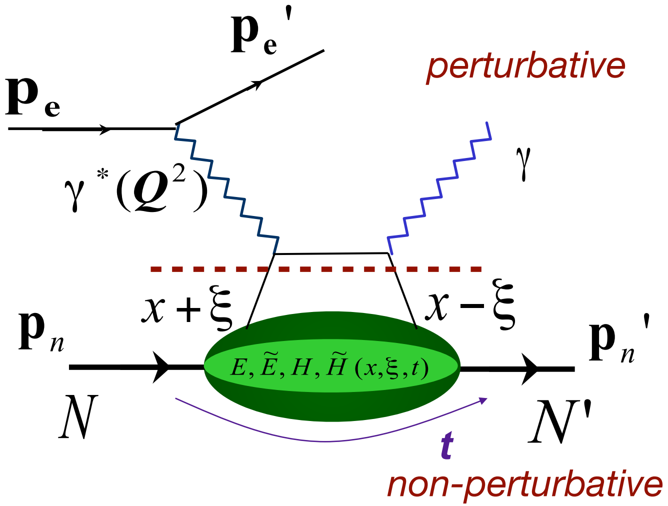

$$Q^2 = -(\mathbf{p}_e - \mathbf{p}_e')^2 \qquad t = (\mathbf{p}_n - \mathbf{p}_n')^2$$

Bjorken variable: $x_B = \dfrac{Q^2}{2\mathbf{p}_n \cdot \mathbf{q}}$

$x \pm \xi$ *longitudinal momentum fractions of the struck parton*

$$\xi \cong \frac{x_B}{2 - x_B}$$

- At high exchanged Q^2 and low t access to four chiral-even GPDs:

$$E^q, \tilde{E}^q, H^q, \tilde{H}^q(x, \xi, t)$$

- Can be related to PDFs:

$$H(x,0,0) = q(x) \quad \tilde{H}(x,0,0) = \Delta q(x)$$

and form factors:

$$\int_{-1}^{+1} H dx = F_1 \qquad \int_{-1}^{+1} \tilde{H}\, dx = G_A$$

$$\int_{-1}^{+1} E\, dx = F_2 \qquad \int_{-1}^{+1} \tilde{E}\, dx = G_P$$

- Small changes in nucleon transverse momentum allows mapping of transverse structure at large distances.

GPDs and nucleon spin

$$J_N = \frac{1}{2} = \frac{1}{2}\Sigma_q + L_q + J_g$$

- Ji's relation: $J^q = \frac{1}{2} - J^g = \frac{1}{2}\int_{-1}^{1} xdx \left\{H^q(x,\xi,0) + E^q(x,\xi,0)\right\}$

H accessible in DVCS off the proton, first experimental constraint on E, through neutron-DVCS:
M. Mazouz et al, PRL 99 (2007) 242501

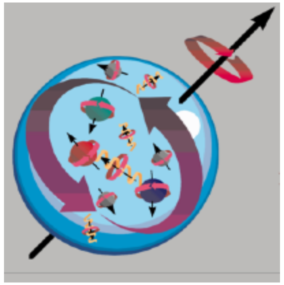

- GPDs can provide insight into the orbital angular momentum contribution to nucleon spin: **the spin puzzle**.

Measuring DVCS

- Process measured in experiment:

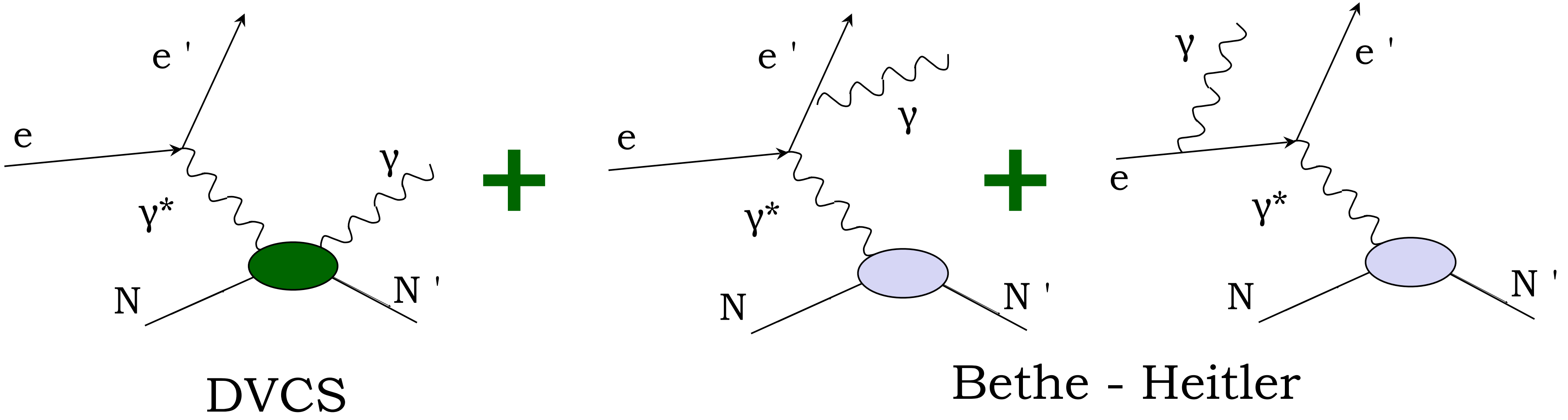

DVCS

Bethe - Heitler

$$d\sigma \propto \left|T_{DVCS}\right|^2 + \left|T_{BH}\right|^2 + T_{BH}T^*{}_{DVCS} + T_{DVCS}T^*{}_{BH}$$

Amplitude parameterised in terms of Compton Form Factors

Amplitude calculable from elastic Form Factors and QED

Interference term

$$\left|T_{DVCS}\right|^2 << \left|T_{BH}\right|^2$$

Compton Form Factors in DVCS

Experimentally accessible in DVCS cross-sections and spin asymmetries, eg:

$$A_{LU} = \frac{d\vec{\sigma} - d\overleftarrow{\sigma}}{d\vec{\sigma} + d\overleftarrow{\sigma}} = \frac{\Delta\sigma_{LU}}{d\vec{\sigma} + d\overleftarrow{\sigma}}$$

At leading twist, leading order:

$$T^{DVCS} \sim \int_{-1}^{+1} \frac{GPDs\,(x,\xi,t)}{x \pm \xi + i\varepsilon}\,dx \;+ \ldots \sim \quad P\int_{-1}^{+1} \frac{GPDs\,(x,\xi,t)}{x \pm \xi}\,dx \pm i\pi GPDs\,(\pm\xi,\xi,t) + \ldots$$

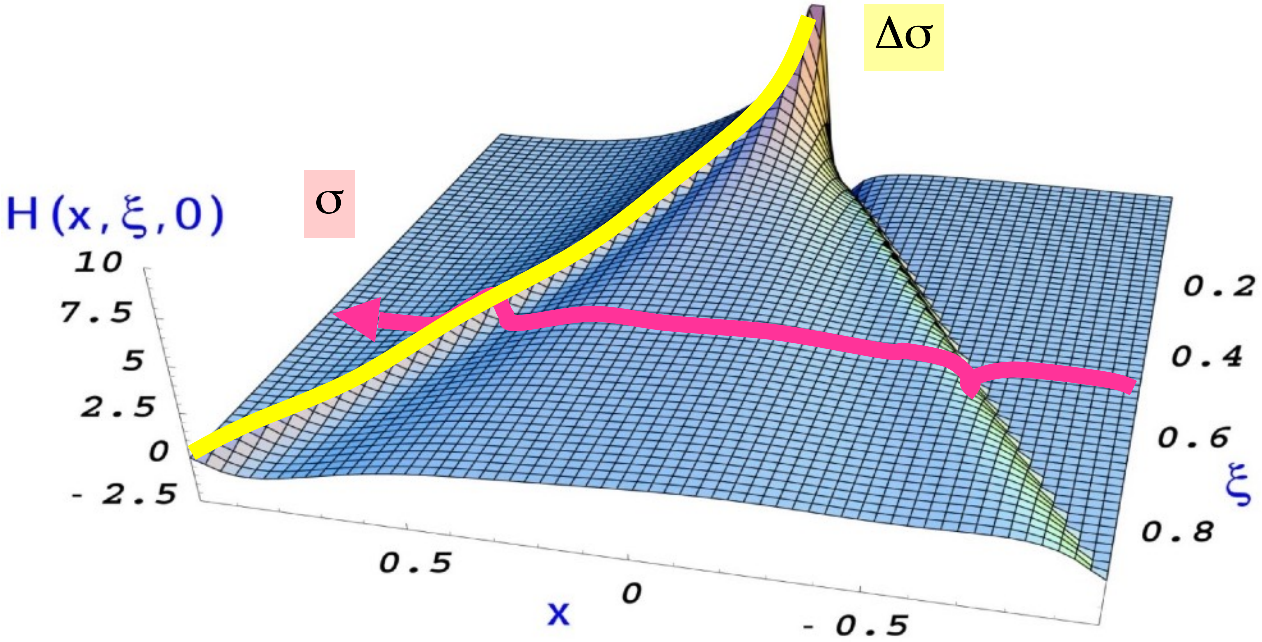

Only ξ and *t* are accessible experimentally!

To get information on *x* need extensive measurements in Q^2.

Need measurements off proton and neutron to get flavour separation of CFFs in DVCS.

Which DVCS experiment?

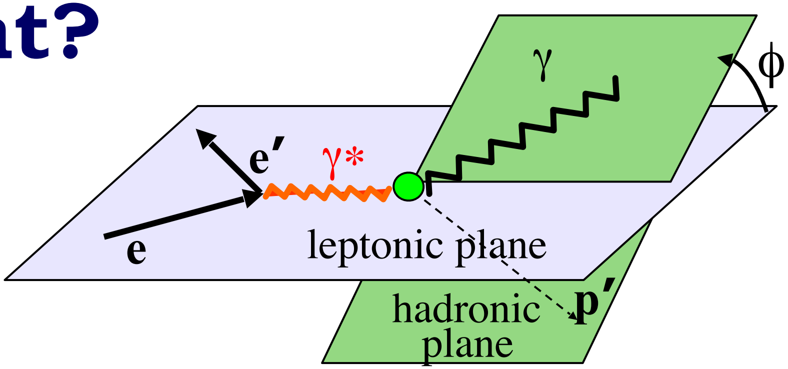

Real parts of CFFs accessible in cross-sections, beam-charge and double polarisation asymmetries,

imaginary parts of CFFs in single-spin asymmetries.

Beam, target polarisation

For example:

Proton Neutron

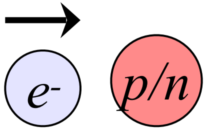

$$\Delta\sigma_{LU} \sim \sin\phi\; \Im(F_1 H + \xi G_M \tilde{H} - \frac{t}{4M^2} F_2 E)\; d\phi$$

$Im\{\boldsymbol{H}_{\mathbf{p}}, \tilde{H}_{\mathrm{p}}, E_{\mathrm{p}}\}$

$Im\{H_{\mathrm{n}}, \tilde{H}_{\mathrm{n}}, \boldsymbol{E}_{\mathbf{n}}\}$

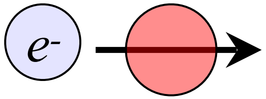

$$\Delta\sigma_{UL} \sim \sin\phi\; \Im(F_1 \tilde{H} + \xi G_M (H + \frac{x_B}{2} E) - \xi \frac{t}{4M^2} F_2 \tilde{E} + \ldots)\; d\phi$$

$Im\{\boldsymbol{H}_{\mathbf{p}}, \tilde{\boldsymbol{H}}_{\mathbf{p}}\}$

$Im\{\boldsymbol{H}_{\mathbf{n}}, E_{\mathrm{n}}, \tilde{E}_{\mathrm{n}}\}$

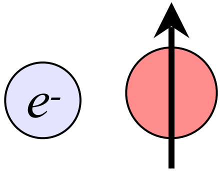

$$\Delta\sigma_{UT} \sim \cos\phi\; \Im(\frac{t}{4M^2}(F_2 H - F_1 E) + \ldots) d\phi$$

$Im\{\boldsymbol{H}_{\mathbf{p}}, \boldsymbol{E}_{\mathbf{p}}\}$

$Im\{\boldsymbol{H}_{\mathbf{n}}\}$

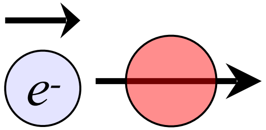

$$\Delta\sigma_{LL} \sim (A + B\cos\phi)\; \Re(F_1 \tilde{H} + \xi G_M (H + \frac{x_B}{2} E) + \ldots) d\phi$$

$Re\{\boldsymbol{H}_{\mathbf{p}}, \tilde{\boldsymbol{H}}_{\mathbf{p}}\}$

$Re\{\boldsymbol{H}_{\mathbf{n}}, E_{\mathrm{n}}, \tilde{E}_{\mathrm{n}}\}$

Jefferson Lab - Hall B

CLAS @ Jefferson Lab: 6 GeV era

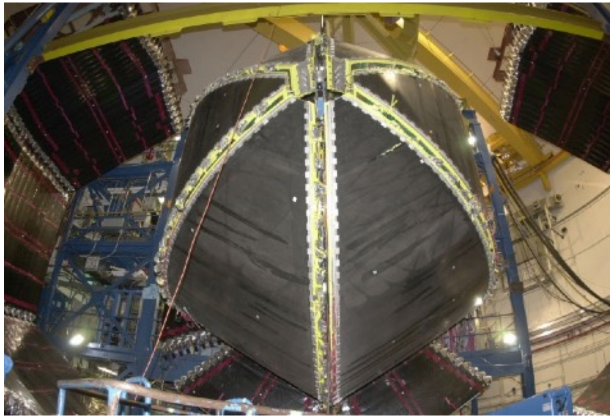

CEBAF: Continuous Electron Beam Accelerator Facility:

- Duty cycle: ~ 100%
- Electron polarisation up to ~85%
- Energy up to ~ 6 GeV

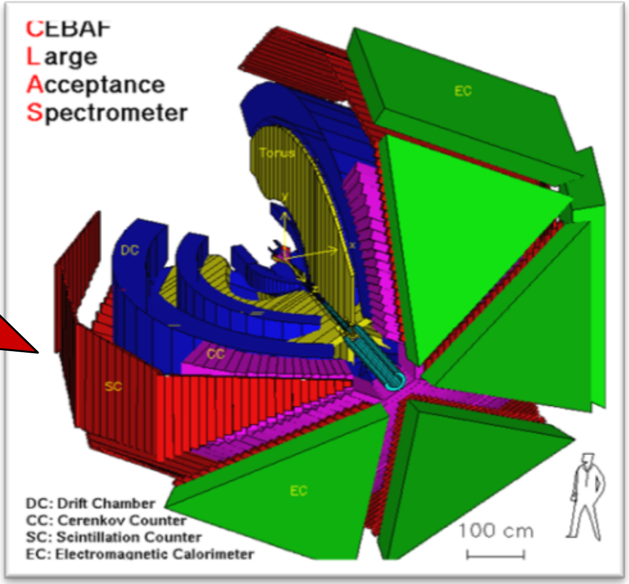

CLAS (CEBAF Large Acceptance Spectrometer) in Hall B:

- Drift chambers
- Toroidal magnetic field
- Cerenkov Counters
- Scintillator Time of Flight
- Electromagnetic Calorimeters

\+ a forward-angle Inner Calorimeter:

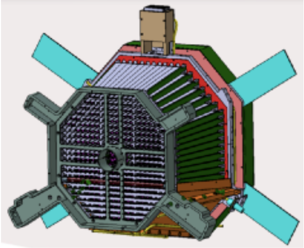

→ *Extremely large angular coverage*

JLab @ 12 GeV

- Energy up to 11 GeV (Halls A, B, C), 12 GeV Hall D
- Energy spread $\delta E/E_e \sim 10^{-4}$
- Electron polarisation up to ~80%, measured to 3%
- Beam size at target < 0.4 mm

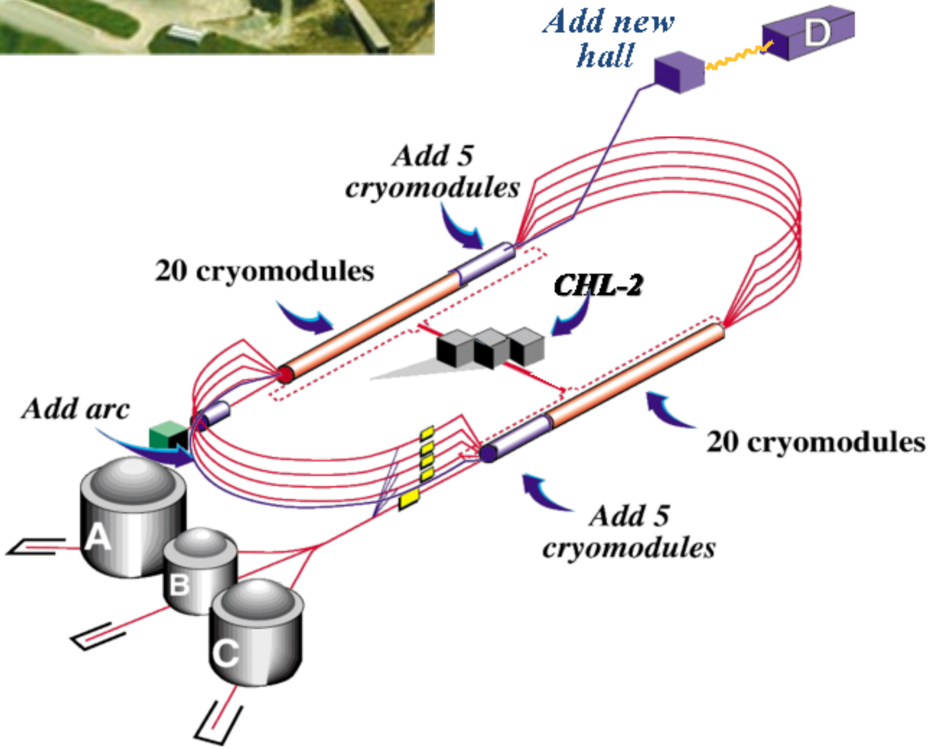

CLAS12

Design luminosity

$L \sim 10^{35}\ \mathrm{cm}^{-2}\ \mathrm{s}^{-1}$

High luminosity & large acceptance:
Concurrent measurement of exclusive, semi-inclusive, and inclusive processes

Acceptance for photons and electrons:

- $2.5^o < \theta < 125^o$

Acceptance for all charged particles:

- $5^o < \theta < 125^o$

Acceptance for neutrons:

- $5^o < \theta < 120^o$

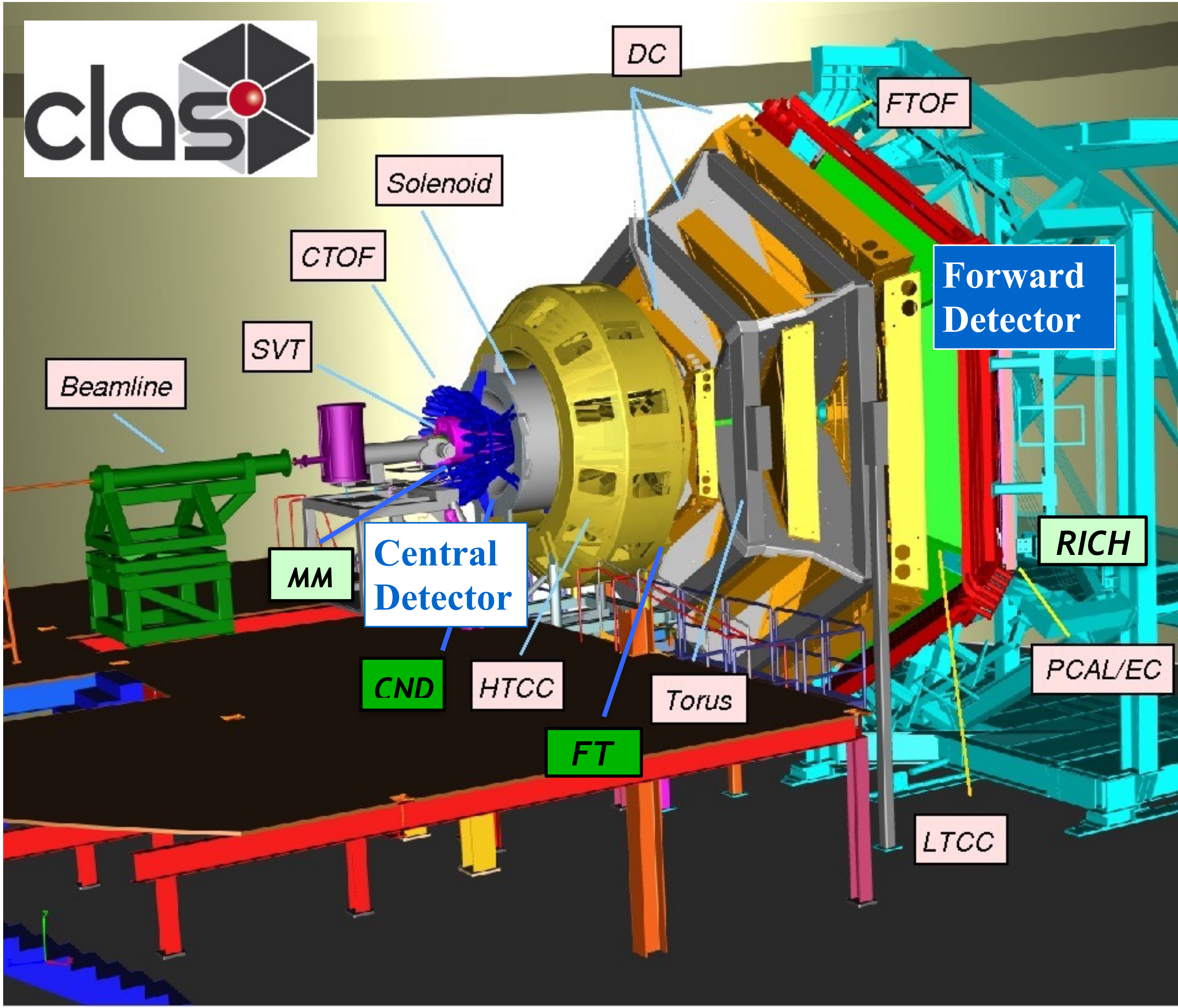

CLAS12 assembled

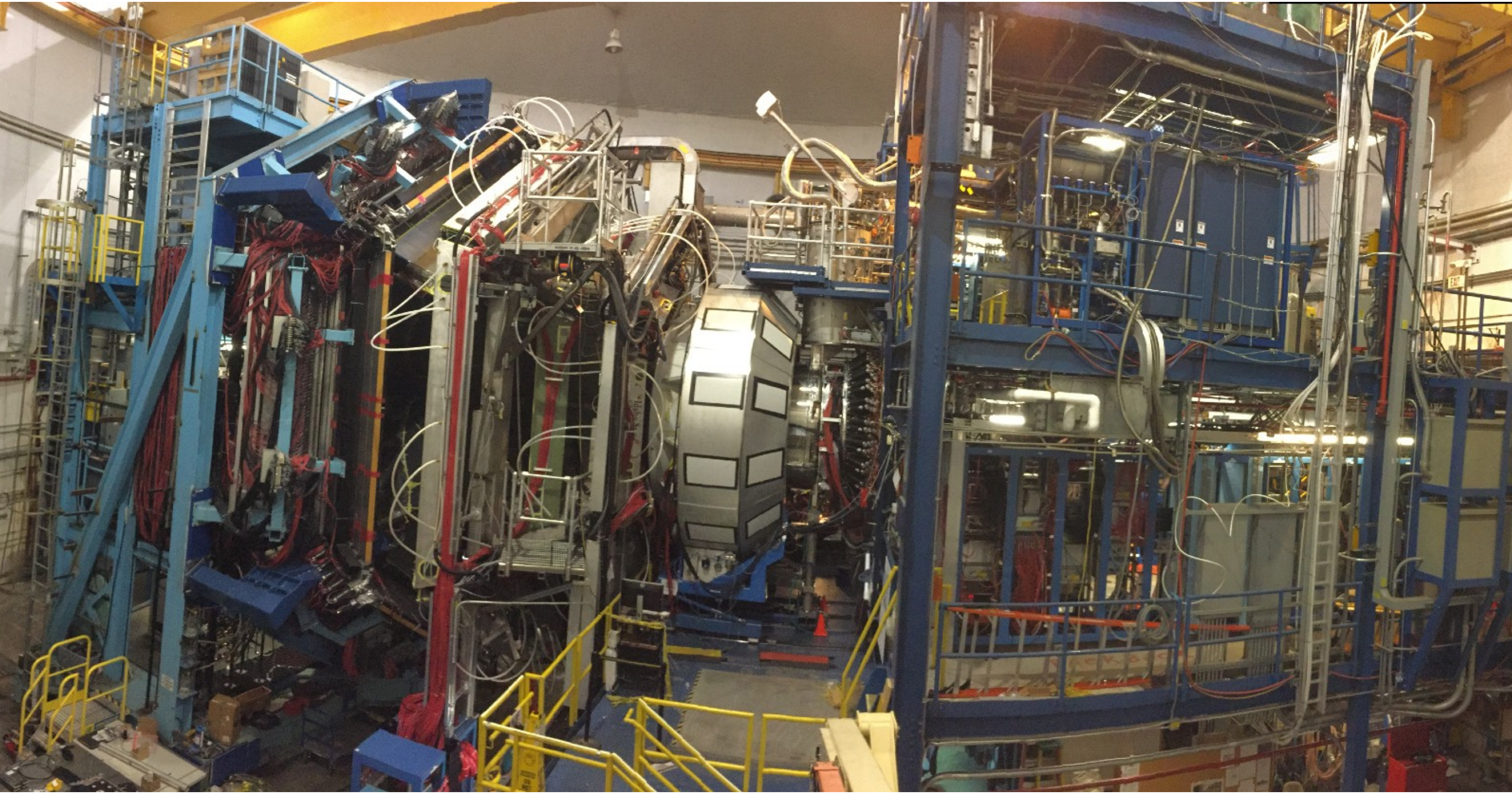

JLab @ 12 GeV

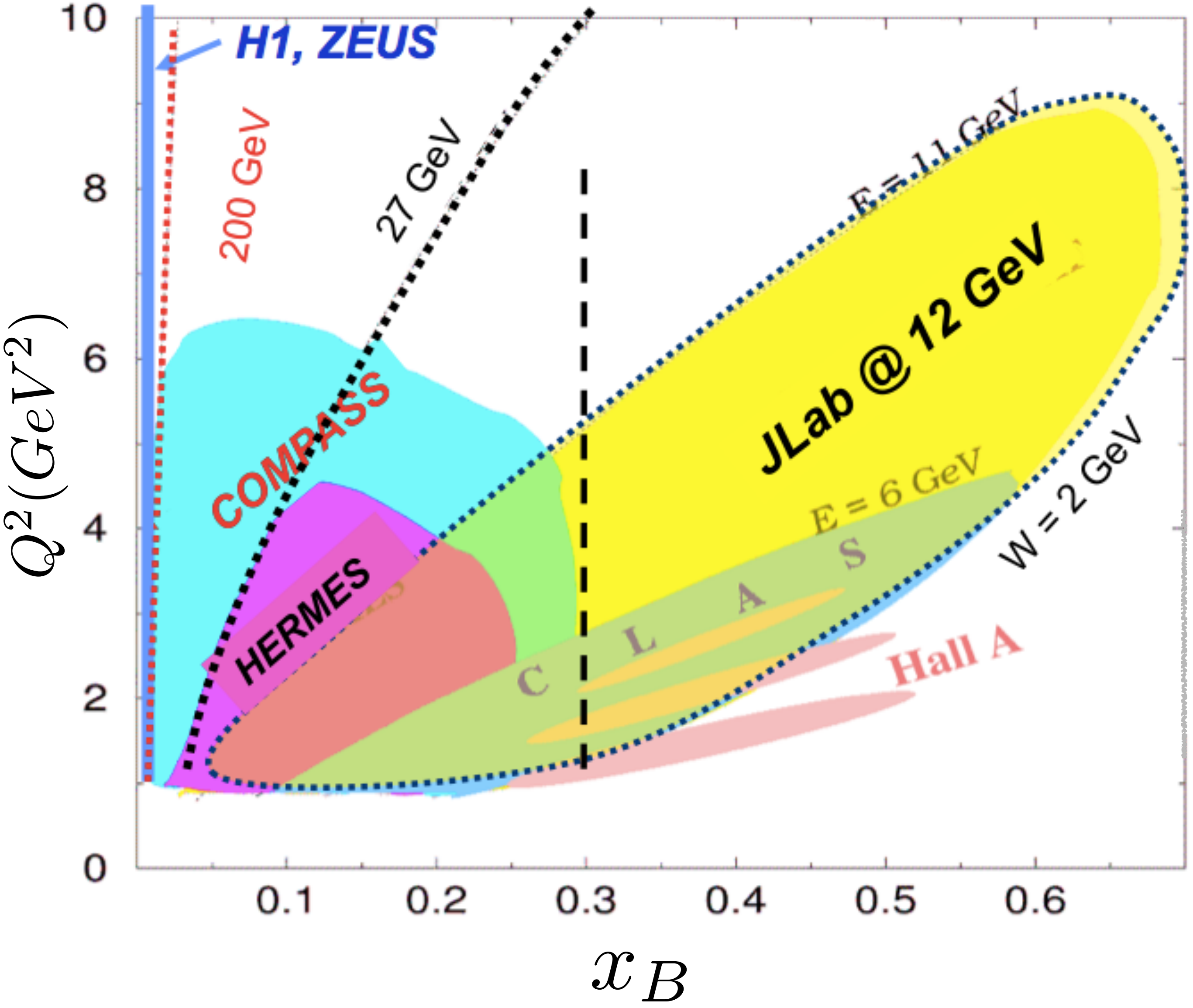
H1, ZEUS
200 GeV
27 GeV
COMPASS
HERMES
E = 11 GeV
JLab @ 12 GeV
E = 6 GeV
W = 2 GeV
C L A S
Hall A
$Q^2 (GeV^2)$
x_B
0
2
4
6
8
10
0.1
0.2
0.3
0.4
0.5
0.6

CLAS highlights from the 6 GeV era

CLAS unpolarised cross-sections

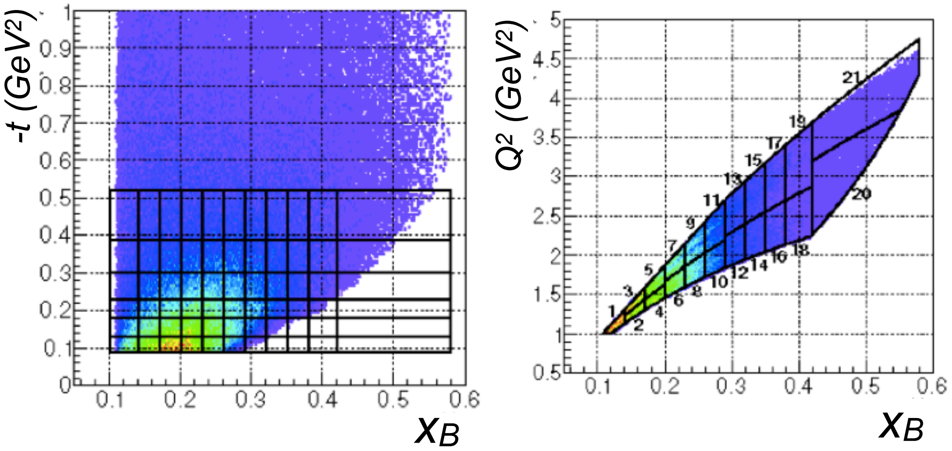

- BH only
- VGG *(Vanderhaeghen, Guichon, Guidal) - H only*
- KM10 (Kumericki, Mueller) *includes strong* $\tilde{H}$
- KM10a *(sets* $\tilde{H}$ *to zero)*
- KMS *(Kroll, Moutarde, Sabatié, tuned on low* x_B *meson-production data)*

- Widest phase space coverage in valence quark region: CFF constraints.
- Dominance of GPD *H* in unpolarised cross-section.

$$\frac{d^4\sigma_{ep\to ep\gamma}}{dQ^2dx_Bdtd\Phi}$$

$$\frac{1}{2}\left(\frac{d^4\overrightarrow{\sigma}_{ep\to ep\gamma}}{dQ^2dx_Bdtd\Phi}-\frac{d^4\overleftarrow{\sigma}_{ep\to ep\gamma}}{dQ^2dx_Bdtd\Phi}\right)$$

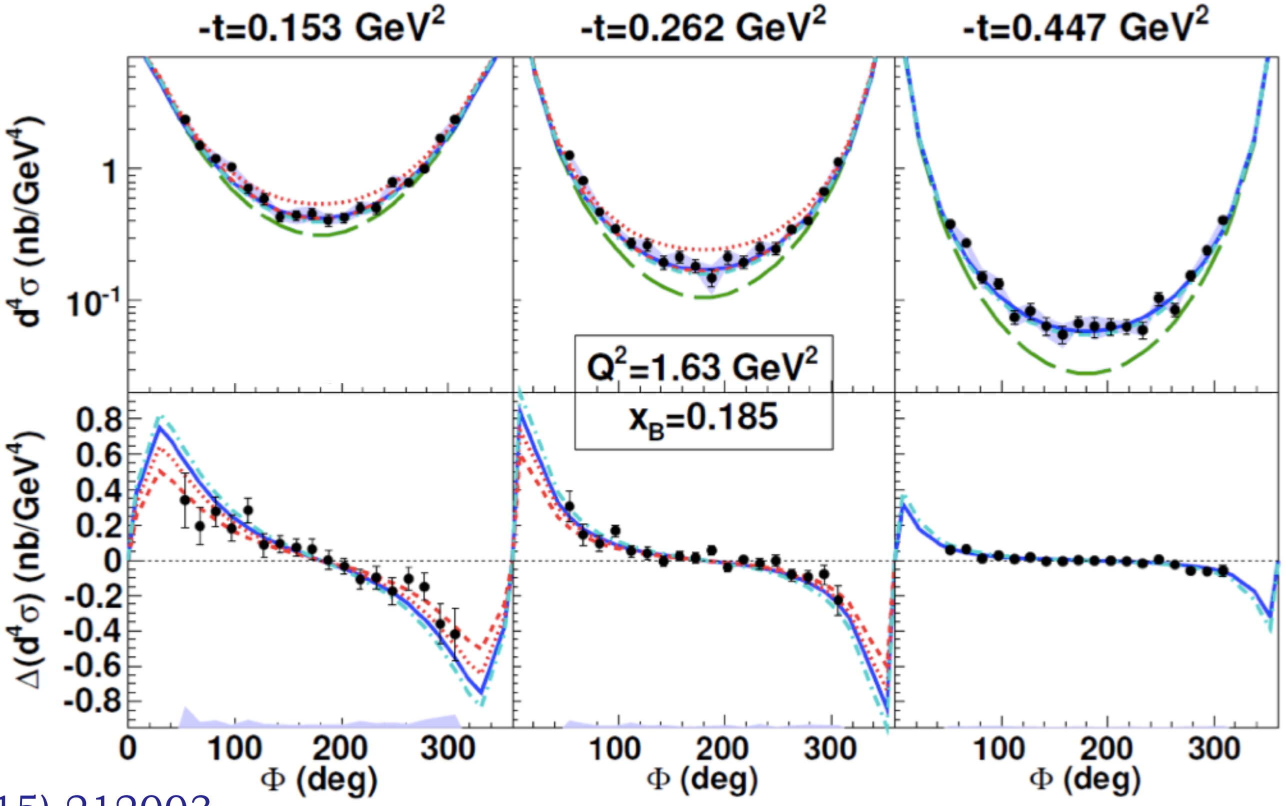

H.-S. Jo *et al* (CLAS), ***PRL*** **115** (2015) 212003

Towards tomography of the proton

- CFFs extracted in a VGG fit (local fit: constraint 5 times the predicted value)
- Imaginary part of CFF: $F_{Im}(\xi, t) = F(\xi, \xi, t) \mp F(-\xi, \xi, t)$

— VGG prediction

- - - Ae^{bt}

- H_{Im} slope in t becomes flatter at higher x_B

Valence quarks at centre, sea quarks spread out towards the periphery.

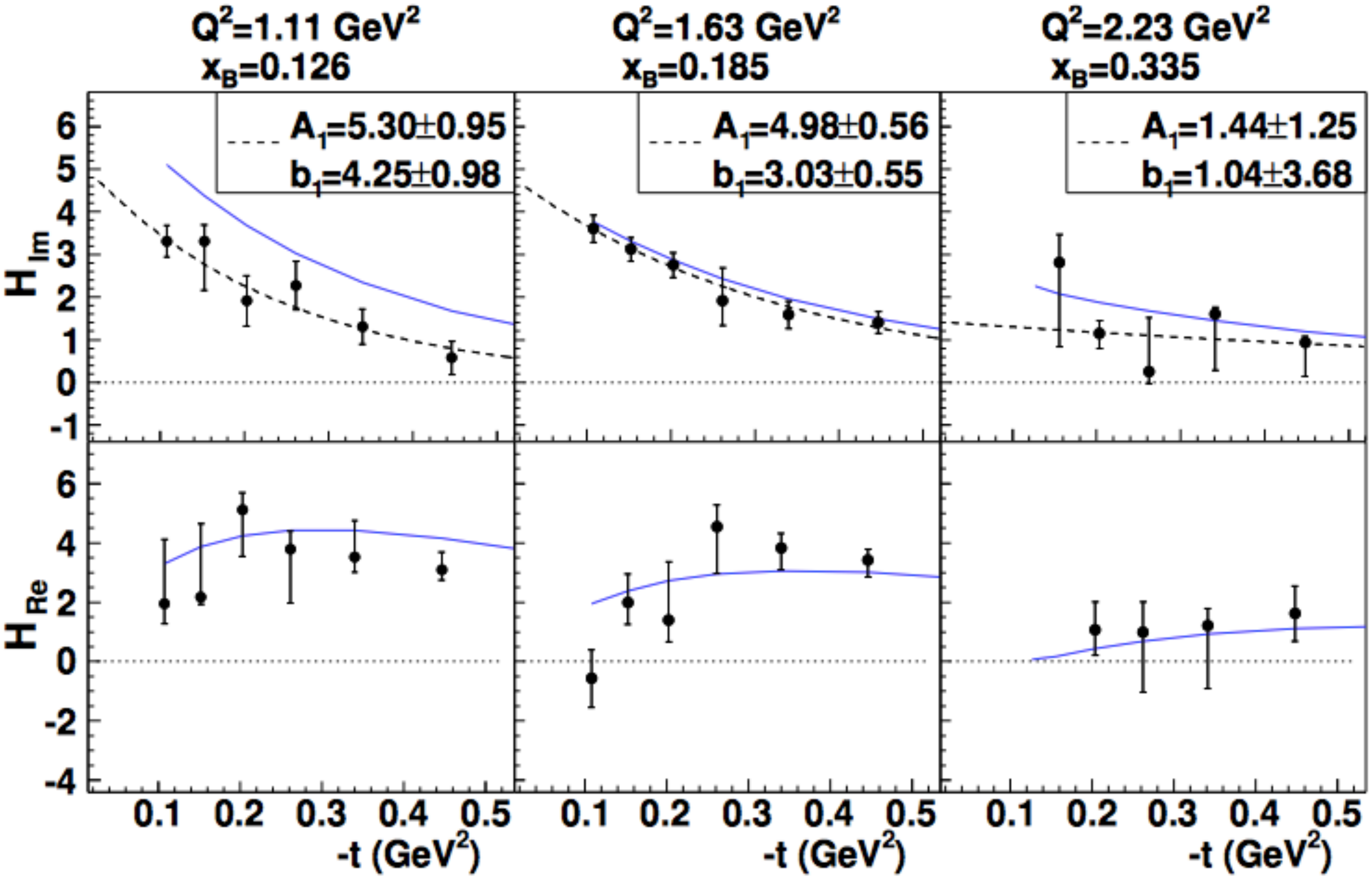

H.-S. Jo *et al* (CLAS Collaboration), ***PRL*** **115** (2015) 212003

CLAS

Beam-spin Asymmetry (A_{LU})

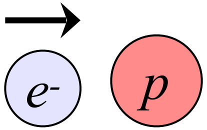

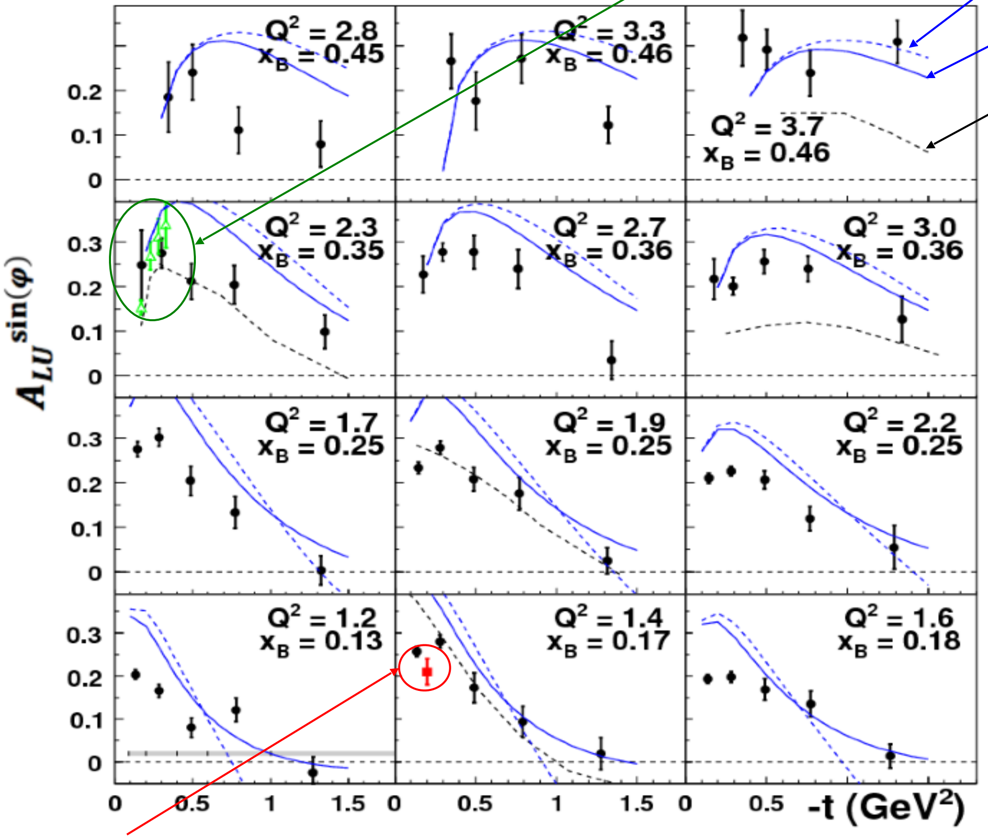

JLab Hall A results

VGG twist-3

VGG twist-2

Regge (JML)

Previous CLAS results

VGG model: Vanderhaeghen, Guichon, Guidal

Follows first CLAS measurement:
S. Stepanyan *et al* (CLAS), ***PRL* 87** (2001) 182002

A_{LU} from fit to asymmetry:

$$A_i = \frac{\alpha_i \sin\phi}{1 + \beta_i \cos\phi}$$

A_{LU} characterised by imaginary parts of CFFs via: $F_1 H + \xi G_M \tilde{H} - \frac{t}{4M^2} E$

Qualitative agreement with models, constraints on fit parameters.

F.-X. Girod *et al* (CLAS), ***PRL* 100** (2008) 162002.

Target-spin Asymmetry (A_{UL})

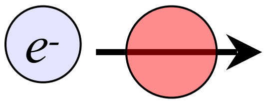

Follows first CLAS measurement:
S. Chen *et al* (CLAS),
***PRL* 97** (2006) 072002

A_{UL} from fit to asymmetry:

$$A_i = \frac{\alpha_i \sin\phi}{1+\beta_i \cos\phi}$$

A_{UL} characterised by imaginary parts of CFFs via:

$$F_1\tilde{H} + \xi G_M\left(H + \frac{x_B}{2}E\right) - \frac{\xi t}{4M^2}F_2\tilde{E} + \ldots$$

High statistics, large kinematic coverage, strong constraints on fits, simultaneous fit with BSA and DSA from the same dataset.

E. Seder *et al* (CLAS), ***PRL* 114** (2015) 032001

S. Pisano *et al* (CLAS), ***PRD* 91** (2015) 052014

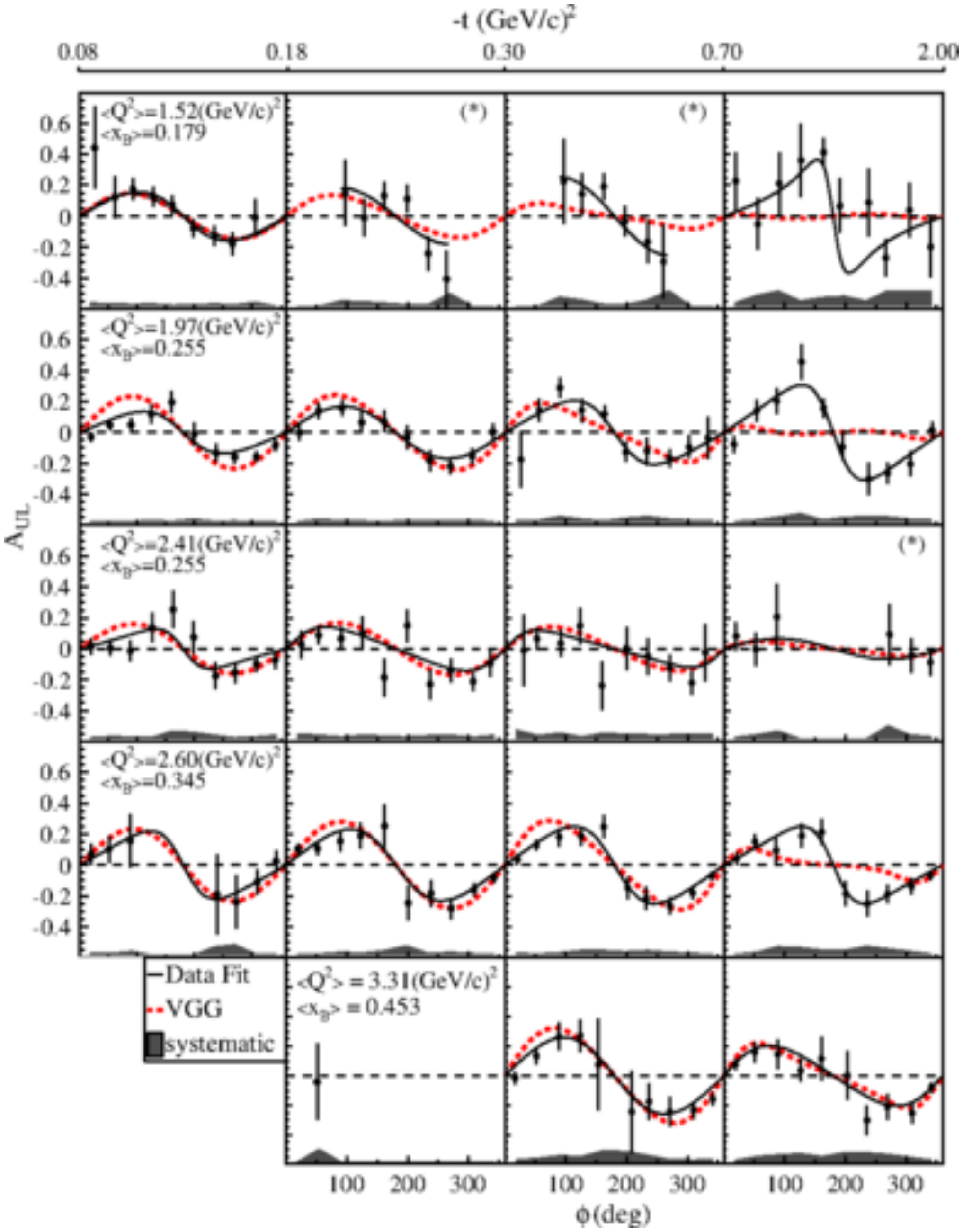

Beam- and target-spin asymmetries

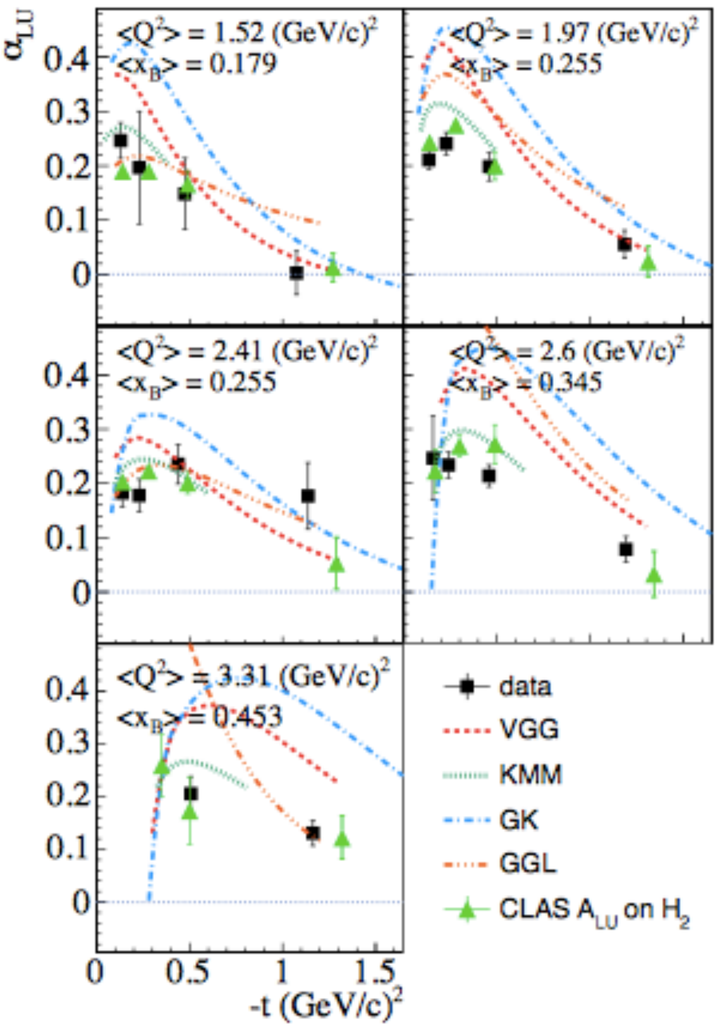

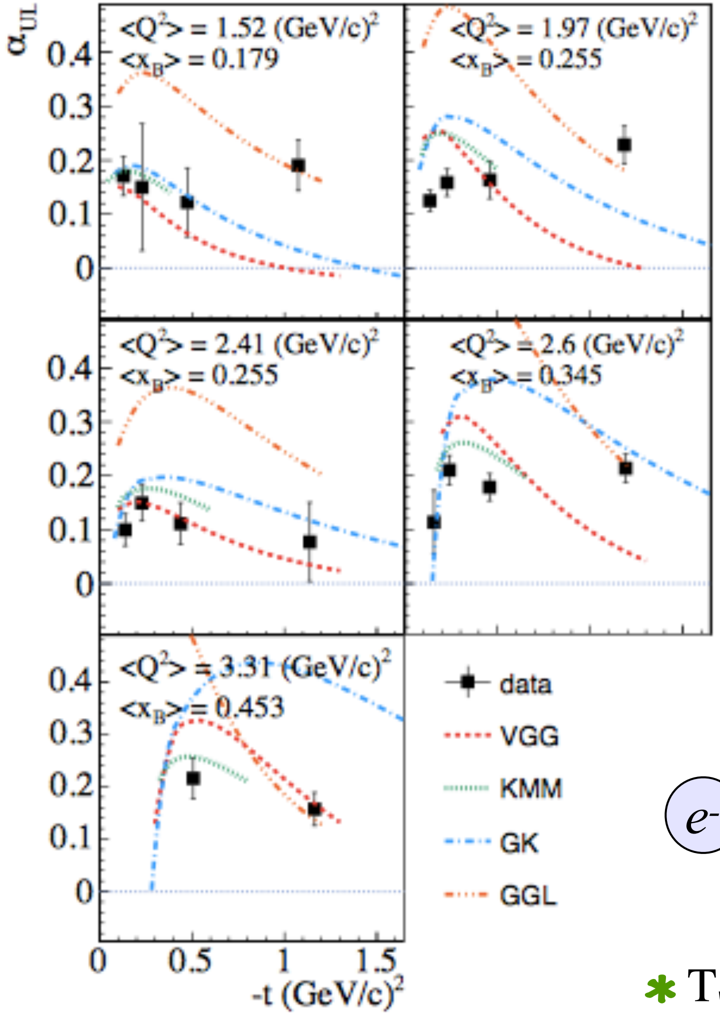

$$A = \frac{\alpha \sin\phi}{1+\beta\cos\phi}$$

GGL: Goldstein, Gonzalez, Liuti

GK: Kroll, Moutarde, Sabatié

KMM: Kumericki, Mueller, Murray

VGG: Vanderhaeghen, Guichon, Guidal

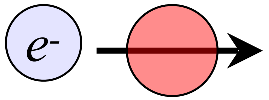

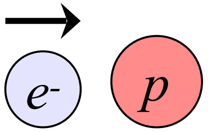

S. Pisano *et al* (CLAS), ***PRD* 91** (2015) 052014
E. Seder *et al* (CLAS), ***PRL* 114** (2015) 032001

- TSA shows a flatter distribution in *t* than BSA.

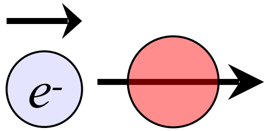

Double-spin Asymmetry (A_{LL})

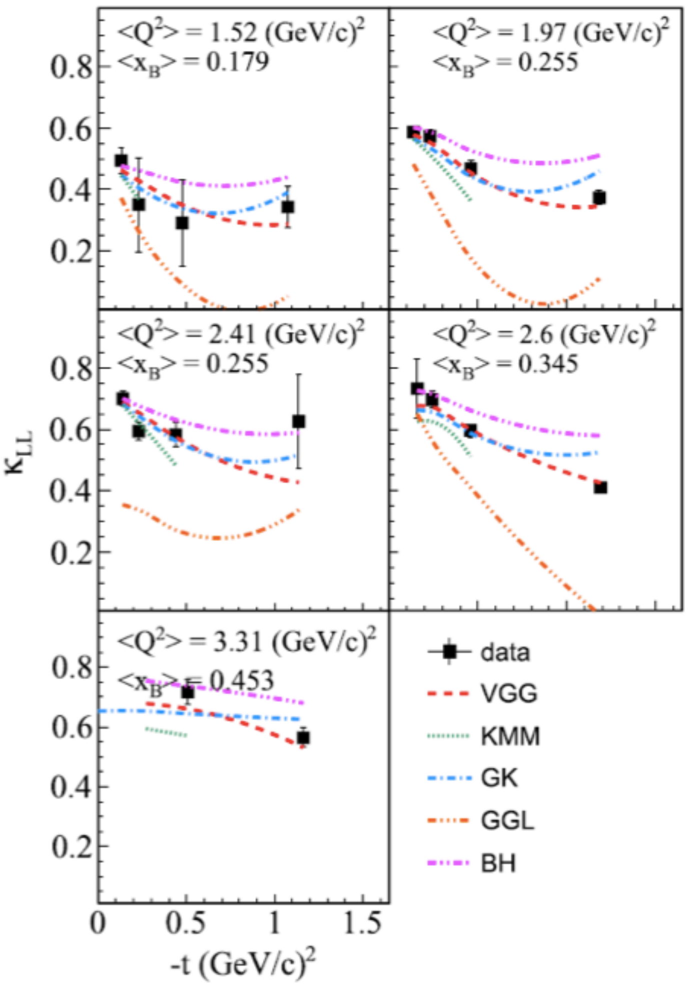

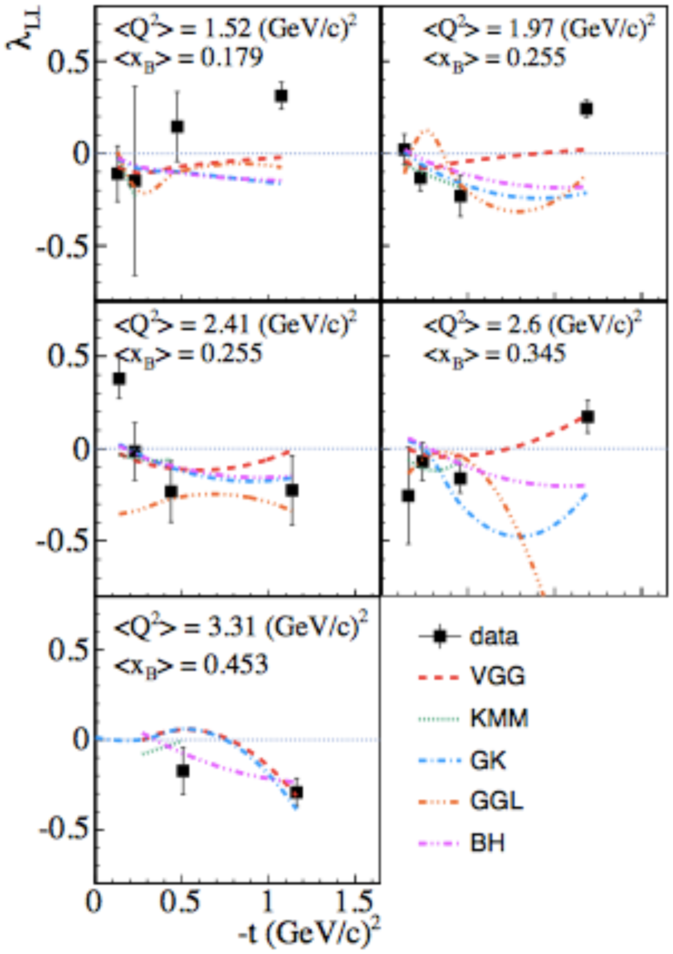

A_{LL} from fit to asymmetry:

$$\frac{\kappa_{LL} + \lambda_{LL}\cos\phi}{1 + \beta\cos\phi}$$

A_{LL} characterised by real parts of CFFs via:

$$F_1\tilde{H} + \xi G_M\left(H + \frac{x_B}{2}E\right) + \ldots$$

- Fit parameters extracted from a simultaneous fit to BSA, TSA and DSA.
- Constant term dominates and is almost entirely BH.

E. Seder *et al* (CLAS), ***PRL* 114** (2015) 032001
S. Pisano *et al* (CLAS), ***PRD* 91** (2015) 052014

CFF extraction from three spin asymmetries at common kinematics.

What can we learn from the asymmetries?

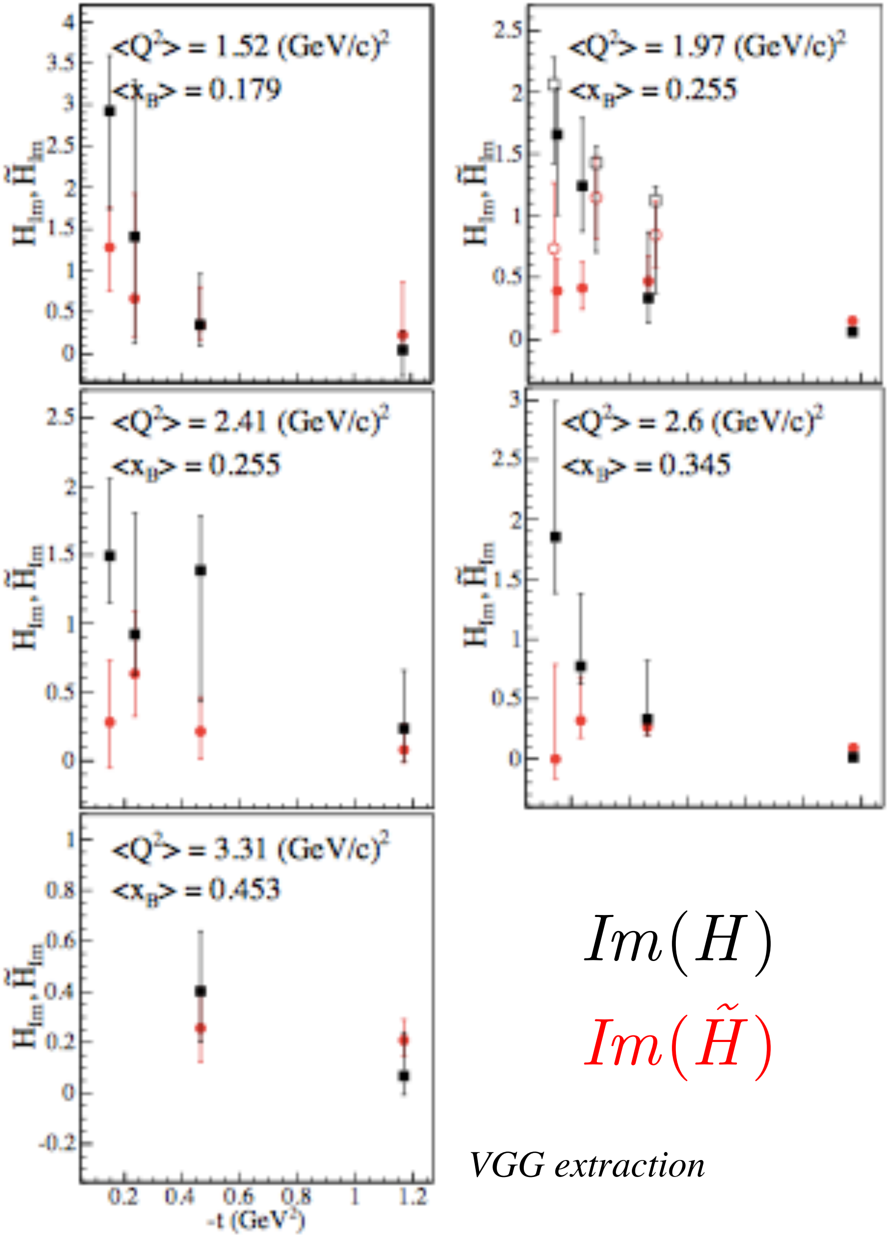

$Im(H)$

$Im(\tilde{H})$

VGG extraction

Answers hinge on a global analysis of all available data.

- Information on relative distributions of quark momenta (PDFs) and quark helicity, $\Delta q(x)$.

$$H(x,0,0) = q(x) \quad \tilde{H}(x,0,0) = \Delta q(x)$$

- Indications that axial charge is more concentrated than electromagnetic charge.

$$\int_{-1}^{+1} H dx = F_1$$

$$\int_{-1}^{+1} \tilde{H}\ dx = G_A$$

E. Seder *et al* (CLAS), ***PRL* 114** (2015) 032001
S. Pisano *et al* (CLAS), ***PRD* 91** (2015) 052014

Towards nucleon tomography

Quasi model-independent extraction of CFFs based on a local fit:

- Set 8 CFFs as free parameters to fit, at each (x_B,t) point, the available observables.
- Limits imposed within +/- 5 times the VGG model predictions (Vanderhaeghen-Guichon-Guidal).
- Leading-twist DVCS amplitude parametrisation based on Double Distributions.

The best constraints in fits to CLAS data were obtained on H_{Im}.

Parametrise its dependence on t:

$$H_{Im}(\xi,t) = A(\xi)e^{B(\xi)t}$$

Relates to quark density

Inverse relation to spatial distribution

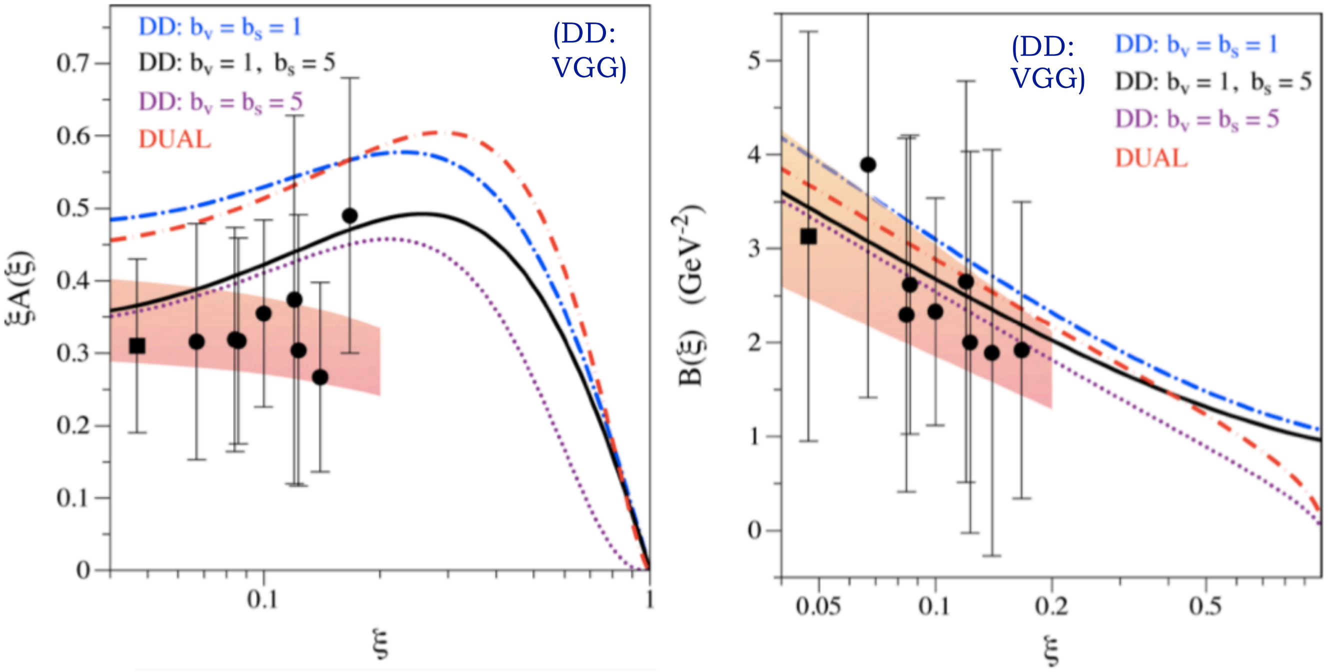

R. Dupré *et al.*, arXiv:1704.07330 [hep-ph]

Towards nucleon tomography

Relating the impact parameter to helicity-averaged transverse charge distribution:

$$\rho^q(x, \mathbf{b}_\perp) = \int \frac{d^2\mathbf{\Delta}_\perp}{(2\pi)^2} e^{-i\mathbf{b}_\perp \cdot \mathbf{\Delta}_\perp} H_-^q(x, 0, -{\mathbf{\Delta}_\perp}^2)$$

Transverse four-momentum transfer to nucleon

$$H_-^q(x, 0, t) \equiv H^q(x, 0, t) + H^q(-x, 0, t)$$

Assuming leading-twist and exponential dependence of GPD on t, using models to extrapolate to the zero skewness point $\xi = 0$ and assuming similar behaviour for u and d quarks there:

$$\langle b_\perp^2 \rangle^q(x) = -4 \frac{\partial}{\partial \mathbf{\Delta}_\perp^2} \ln H_-^q(x, 0, -{\mathbf{\Delta}_\perp}^2) \Big|_{\mathbf{\Delta}_\perp = 0}$$

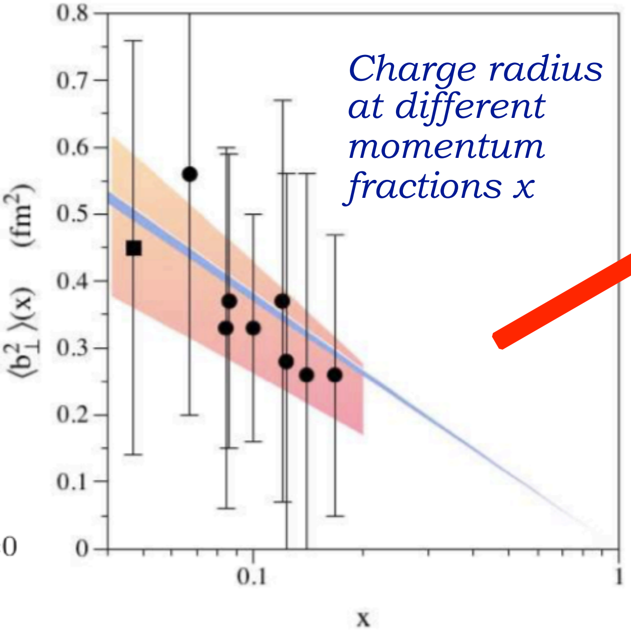

Charge radius at different momentum fractions x

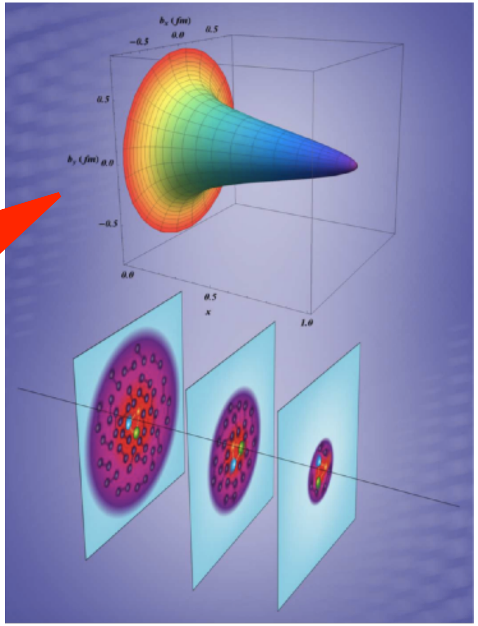

Tentative hints of 3D distributions are emerging.

R. Dupré *et al.*, arXiv:1704.07330 [hep-ph]

Imaging pressure within the nucleon

- GPDs provide indirect access to mechanical properties of the nucleon (encoded in the gravitational form factors, GFFs, of the energy-momentum tensor).

- Three scalar GFFs, functions of *t*: encode pressure and shear forces ($d_1(t)$), mass ($M_2(t)$) and angular momentum distributions ($J(t)$).

- Can be related to GPDs via sum rules:

$$\int x\,[H(x,\xi,t)+E(x,\xi,t)]\,\mathrm{d}x = 2J(t)$$

$$\int xH(x,\xi,t)\mathrm{d}x = M_2(t)+\frac{4}{5}\xi^2 d_1(t)$$

- Possibility of extracting pressure distributions! More data needed.

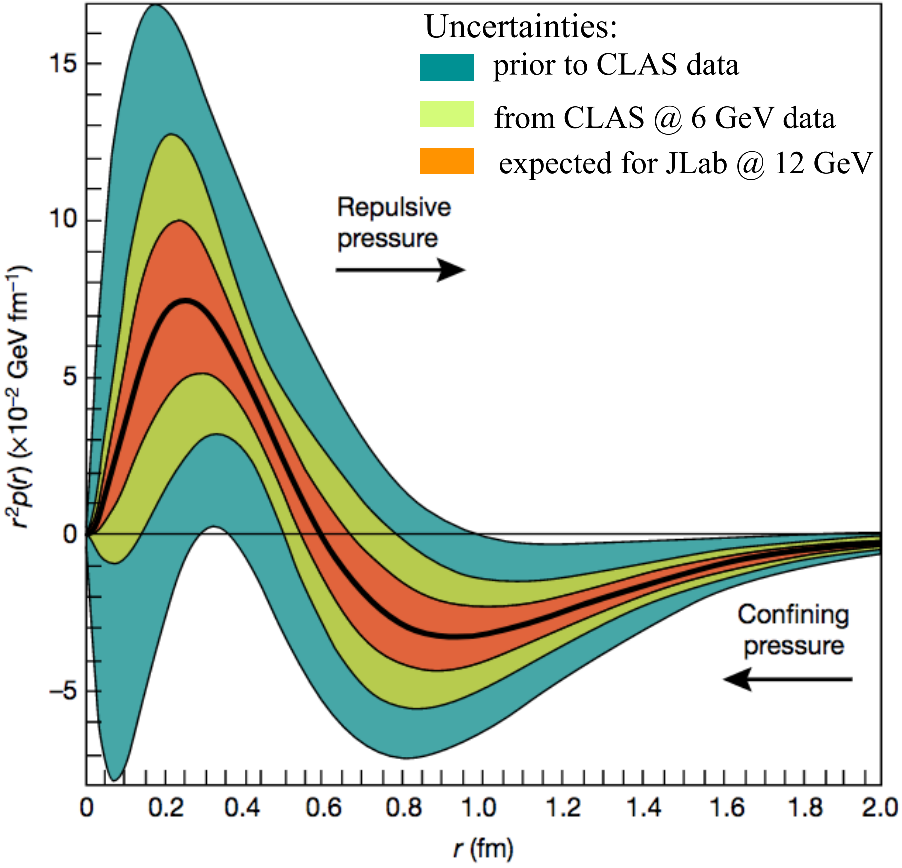

V. Burkert *L. El, F.-X. Girod*, Nature **557**, 396-399 (2018)

DVCS with CLAS12: 11 GeV era

Proton DVCS @ 11 GeV

CLAS12

Experiment E12-06-119

F. Sabatié et al.

$P_{beam} = 85\%$

$L = 10^{35}\ cm^{-2}s^{-1}$

$1 < Q^2 < 10\ GeV^2$

$0.1 < x_B < 0.65$

$-t_{min} < -t < 2.5\ GeV^2$

Kinematics similar for all proton DVCS @ 11 GeV with CLAS12 experiments

Unpolarised liquid H_2 target:

- Statistical error: 1% - 10% on sinφ moments
- Systematic uncertainties: ~ 6 - 8%

A_{LU} characterised by imaginary parts of CFFs via:

$$F_1 H + \xi G_M \tilde{H} - \frac{t}{4M^2} E \longrightarrow \mathit{Im}(H_p)$$

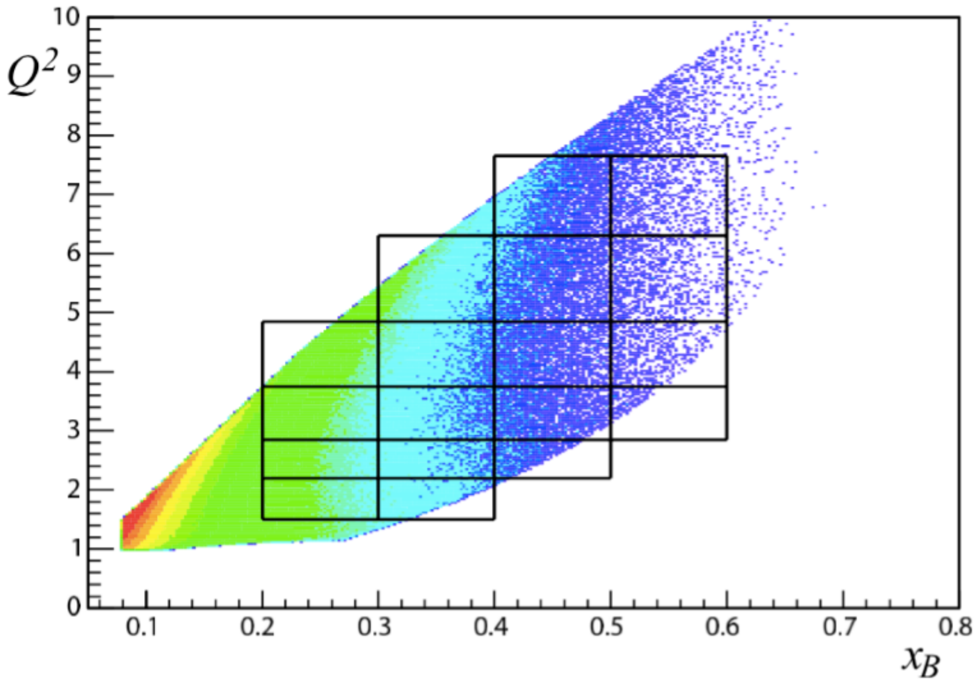

First experiment with CLAS12

Started this February!

Proton DVCS @ 11 GeV

CLAS12

Impact of CLAS12 unpolarised target proton-DVCS data on the extraction of Re(H) and Im(H).

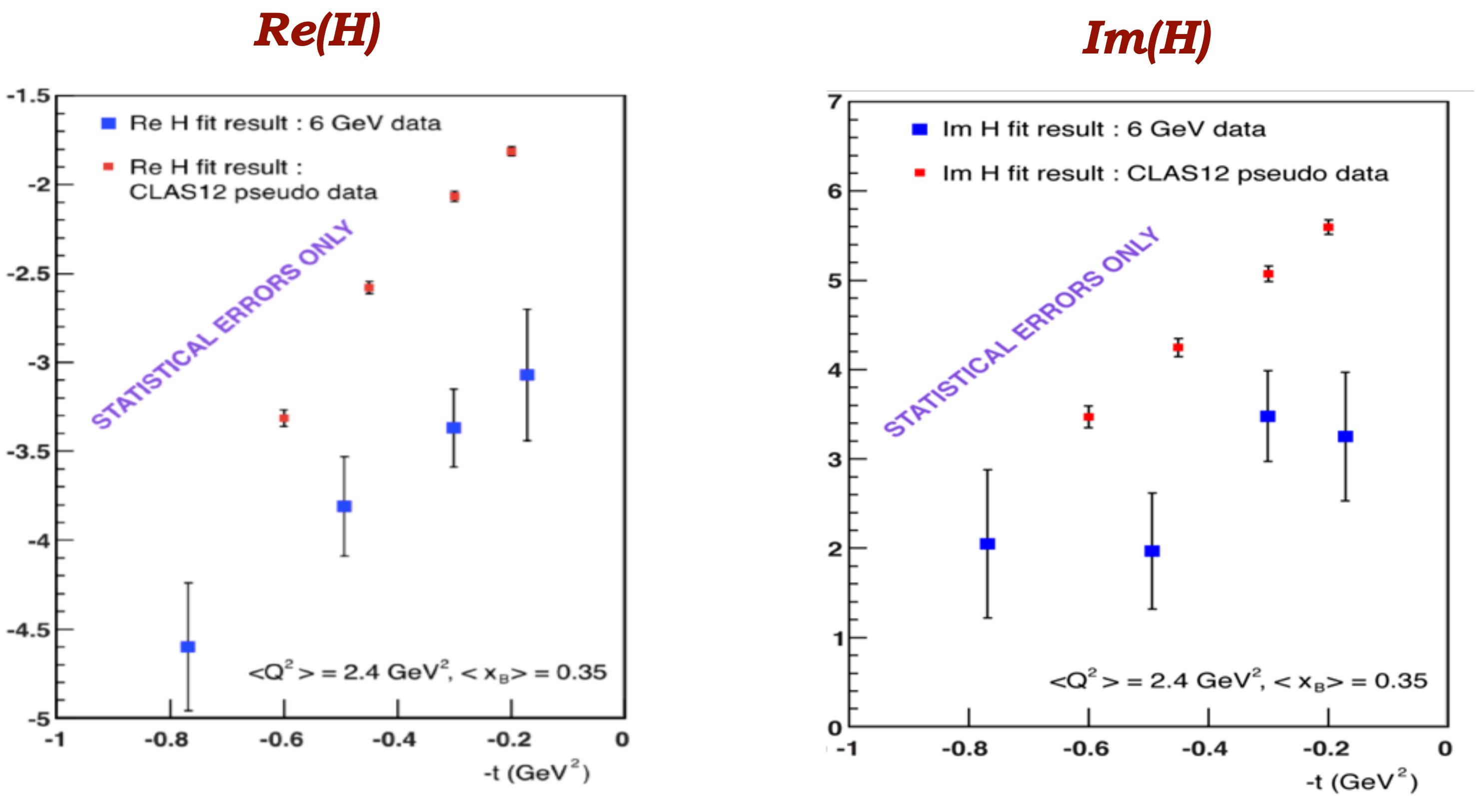
Re(H)

Im(H)

(CLAS 6 GeV extraction H. Moutarde)

DVCS at lower energies with CLAS12

Experiment E12-16-010B
F.-X. Girod et al.

Unpolarised liquid H_2 target:

- Beam energies: 6.6, 8.8 GeV
- Simultaneous fit to beam-spin and total cross-sections.

✱ Rosenbluth separation of interference and $\left|T_{DVCS}\right|^2$ terms in the cross-section

✱ Scaling tests of the extracted CFFs

✱ Model-dependent determination of the D-term in the Dispersion Relation between *Re* and *Im* parts of CFFs: sensitivity to Gravitational Form Factors.

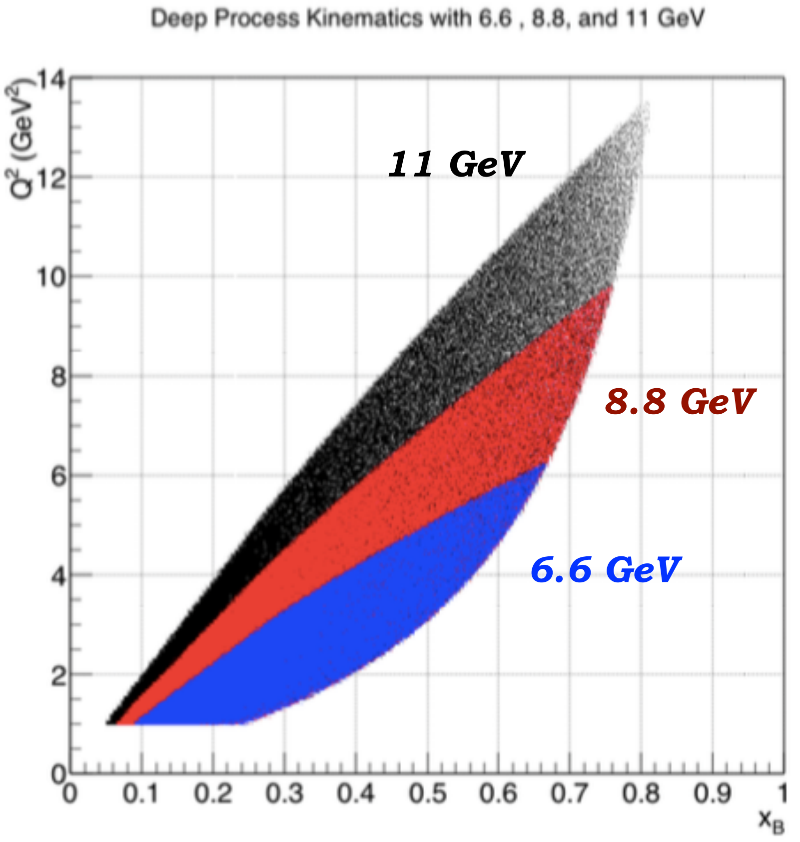

Compare with measurements from Halls A and C: cross-check model and systematic uncertainties.

DVCS at lower energies with CLAS12

Projected extraction of CFFs (red) compared to generated values (green). Three curves on the *Re(H)* show three different scenarios for the D-term.

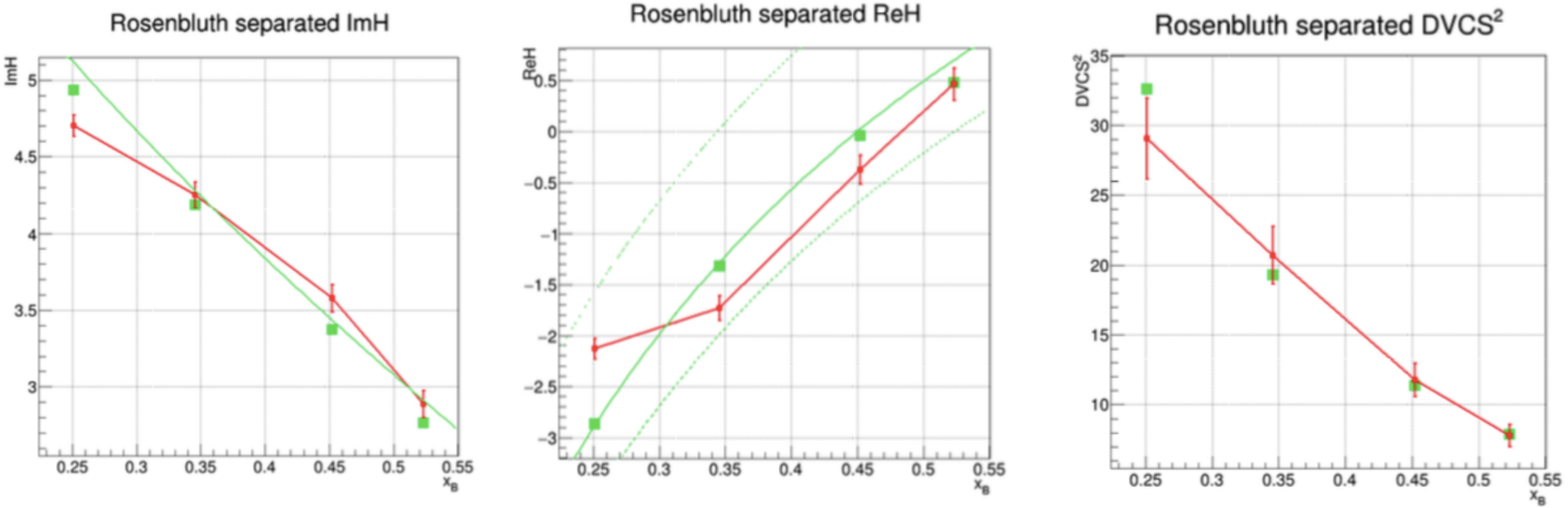

F.-X. Girod et al.

CLAS12

Neutron DVCS @ 11 GeV

Experiment E12-11-003

S. Niccolai, D. Sokhan et al.

$$\Delta\sigma_{LU} \sim \sin\phi\ \mathbf{Im}\{F_1 H + \xi(F_1+F_2)\widetilde{H} - kF_2 E\} d\phi$$

Im (E$_n$) dominates.

Simulated statistical sample:

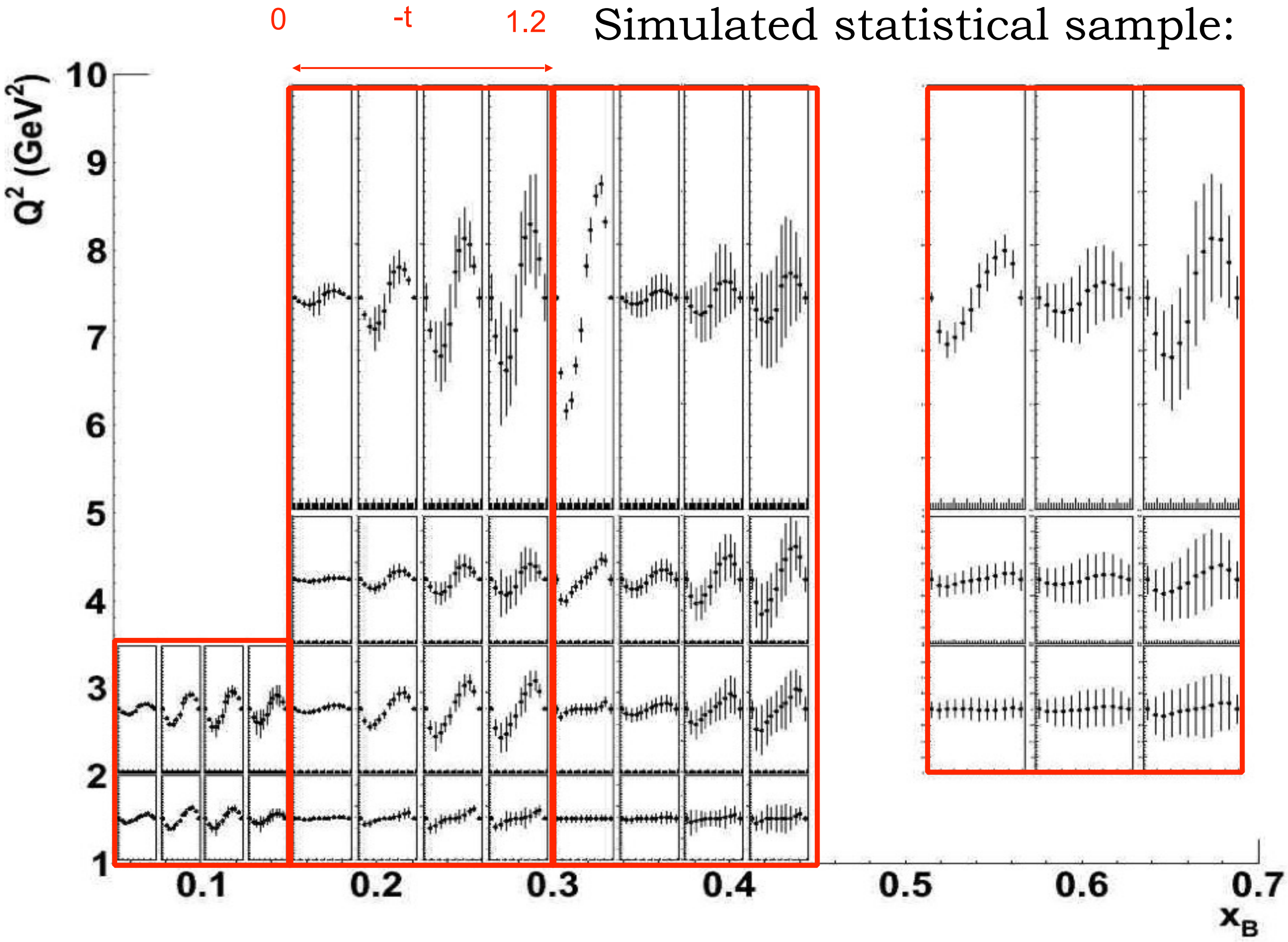

L = 10^{35} cm^{-2}s^{-1}/nucleon

$$e + d \rightarrow e' + \gamma + n + (p_s)$$

CLAS12 +
Forward Tagger +
Neutron Detector

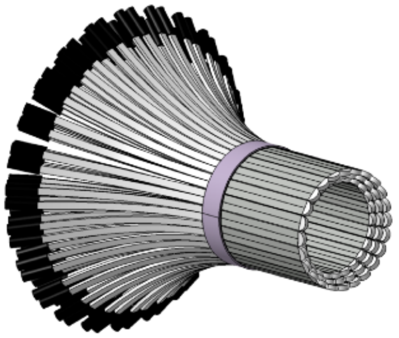

Scheduled: 2019

Beam-spin asymmetry in neutron DVCS @ 11 GeV

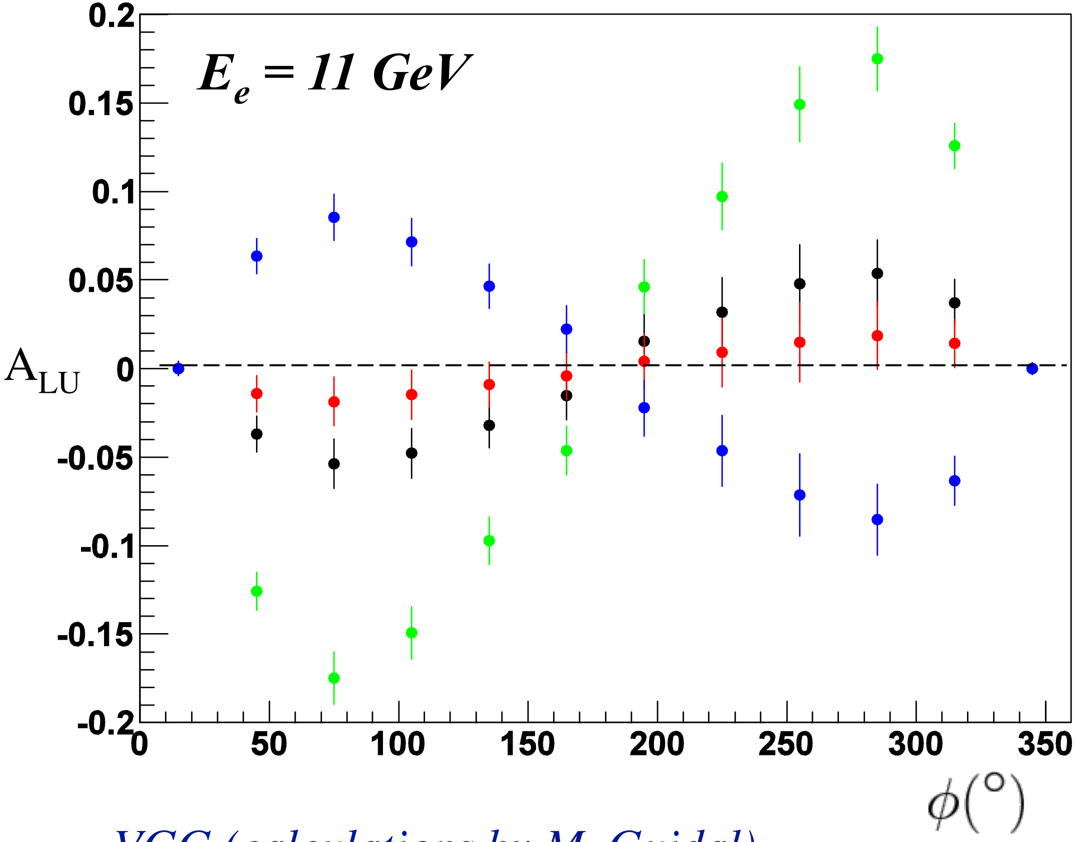

$J_u = 0.3, J_d = -0.1$ $J_u = 0.3, J_d = 0.1$

$J_u = 0.1, J_d = 0.1$ $J_u = 0.3, J_d = 0.3$

VGG (calculations by M. Guidal)

- At 11 GeV, beam spin asymmetry (A_{LU}) in neutron DVCS *is* very sensitive to J_u, J_d
- Wide coverage needed!

Fixed kinematics: $x_B = 0.17 \quad Q^2 = 2\ \text{GeV}^2 \quad t = -0.4\ \text{GeV}^2$

CLAS12

Proton DVCS with a longitudinally polarised target

Experiment E12-06-119

F. Sabatié et al.

A_{UL} characterised by imaginary parts of CFFs via:

$$F_1\tilde{H} + \xi G_M\left(H + \frac{x_B}{2}E\right) - \frac{\xi t}{4M^2}F_2\tilde{E} + \ldots$$

$\longrightarrow$ ***Im*($\widetilde{\mathrm{H}}_{\mathrm{p}}$)**

Longitudinally polarised NH_3 target:

- Dynamic Nuclear Polarisation (DNP) of target material, cooled to 1K in a *He* evaporation cryostat.
- $P_{proton} > 80\%$
- Statistical error: 2% - 15% on sinφ moments
- Systematic uncertainties: ~ 12%

Tentative schedule: 2020

Target cryostat

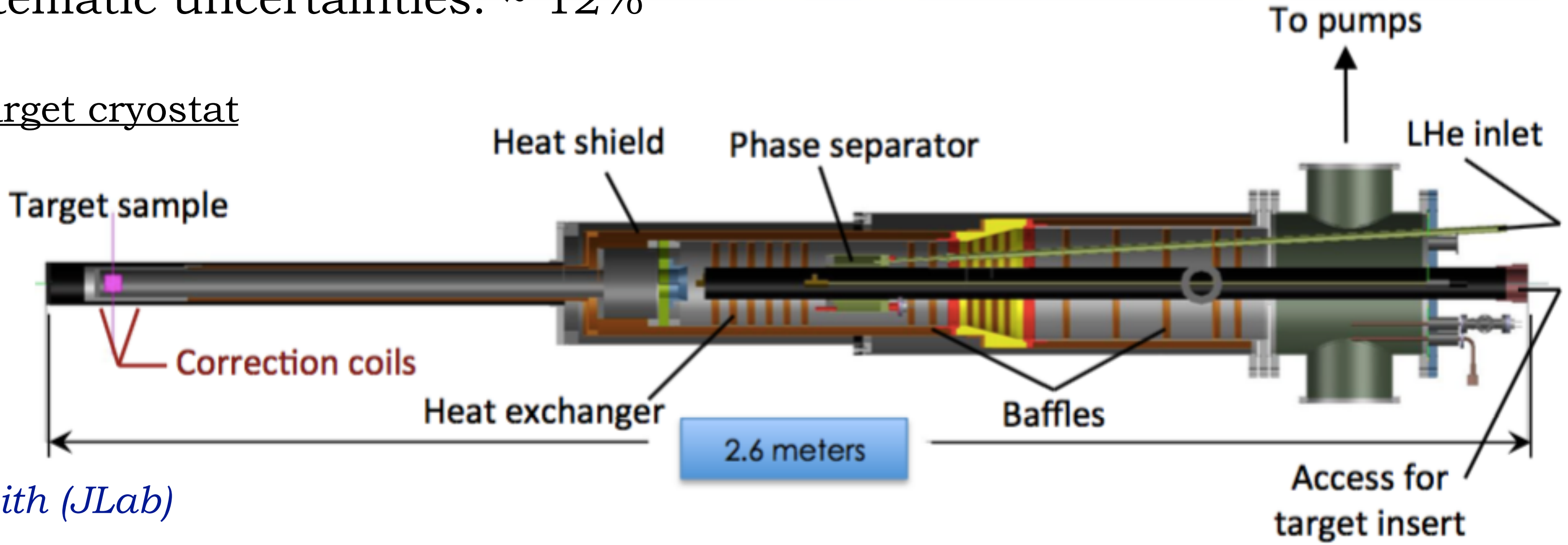

C. Keith (JLab)

CLAS12

Neutron DVCS with a longitudinally polarised target

Experiment E12-06-109A.
S. Niccolai, D. Sokhan et al.

Longitudinally polarised ND_3 target:

- Dynamic Nuclear Polarisation (DNP) of target material in a cryostat shared with the NH_3 target.
- $P_{deuteron}$ up to 50%
- Systematic uncertainties: ~ 12%

A_{UL} characterised by imaginary parts of CFFs via:

$$F_1\tilde{H} + \xi G_M\left(H + \frac{x_B}{2}E\right) - \frac{\xi t}{4M^2}F_2\tilde{E} + \ldots$$

$\longrightarrow$ ***Im*(H$_n$)**

In combination with pDVCS, will allow flavour-separation of the H_q CFFs.

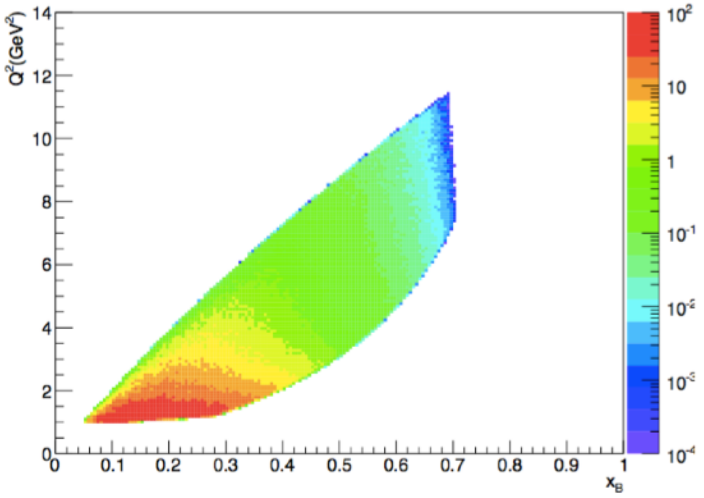

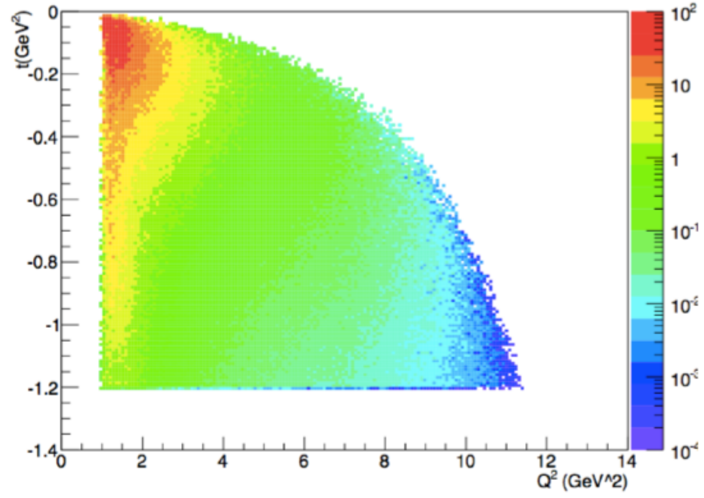

Tentative schedule: 2020

Proton DVCS with transversely polarised target at CLAS12

C12-12-010: with transversely polarised HD target (conditionally approved).

L. Elouardhiri et al.

$\Delta\sigma_{UT} \sim \cos\phi \, \mathrm{Im}\{k(F_2 H - F_1 E) + \ldots.. \} d\phi$

Sensitivity to ***Im(E)*** for the proton.

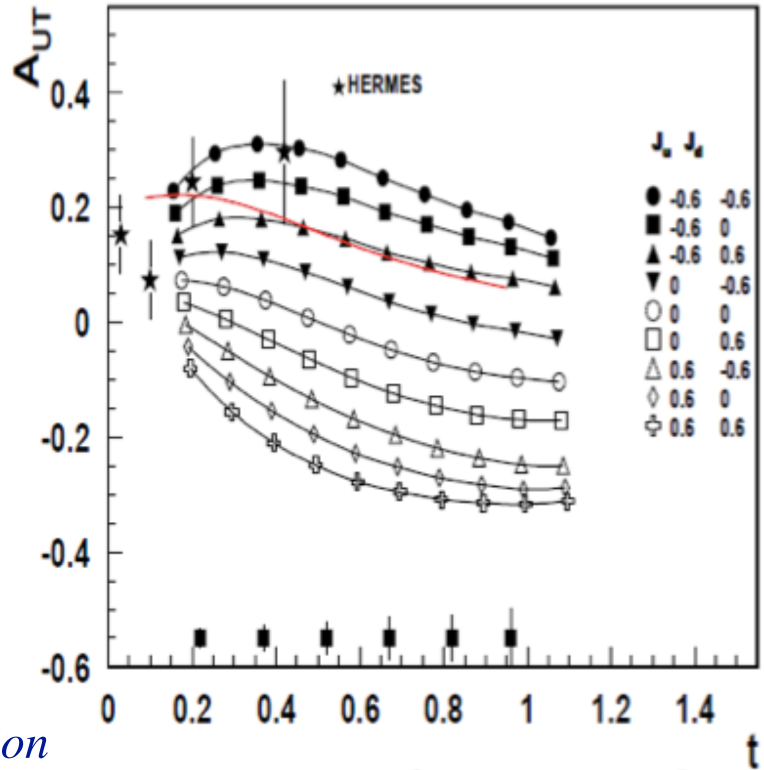

$\langle x \rangle = 0.2, \langle Q^2 \rangle = 2.5\ GeV^2$

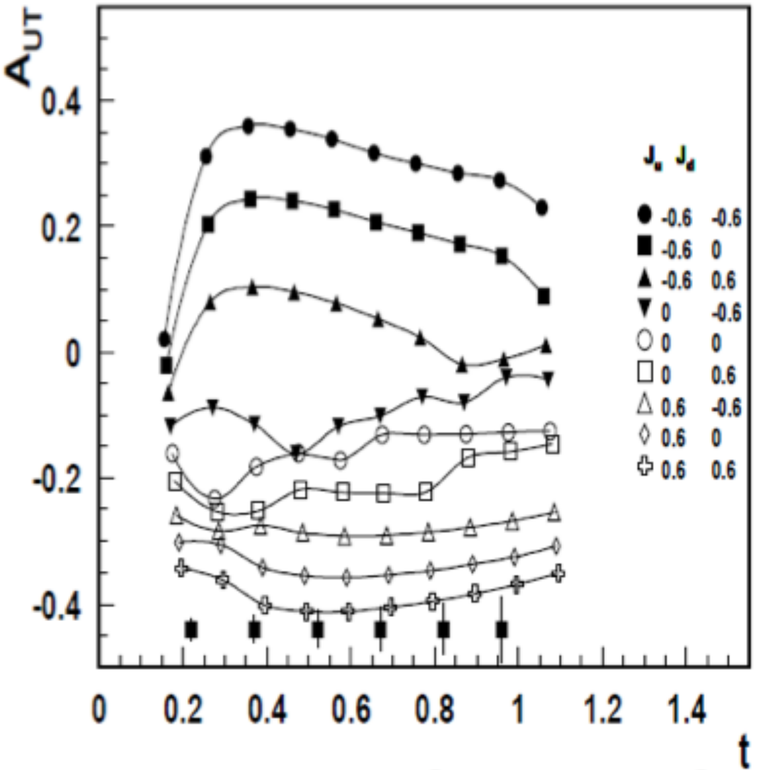

$\langle x \rangle = 0.33, \langle Q^2 \rangle = 2.5\ GeV^2$

VGG extraction (M. Guidal)

Projected sensitivities to *Im(H)* CFF

CLAS12

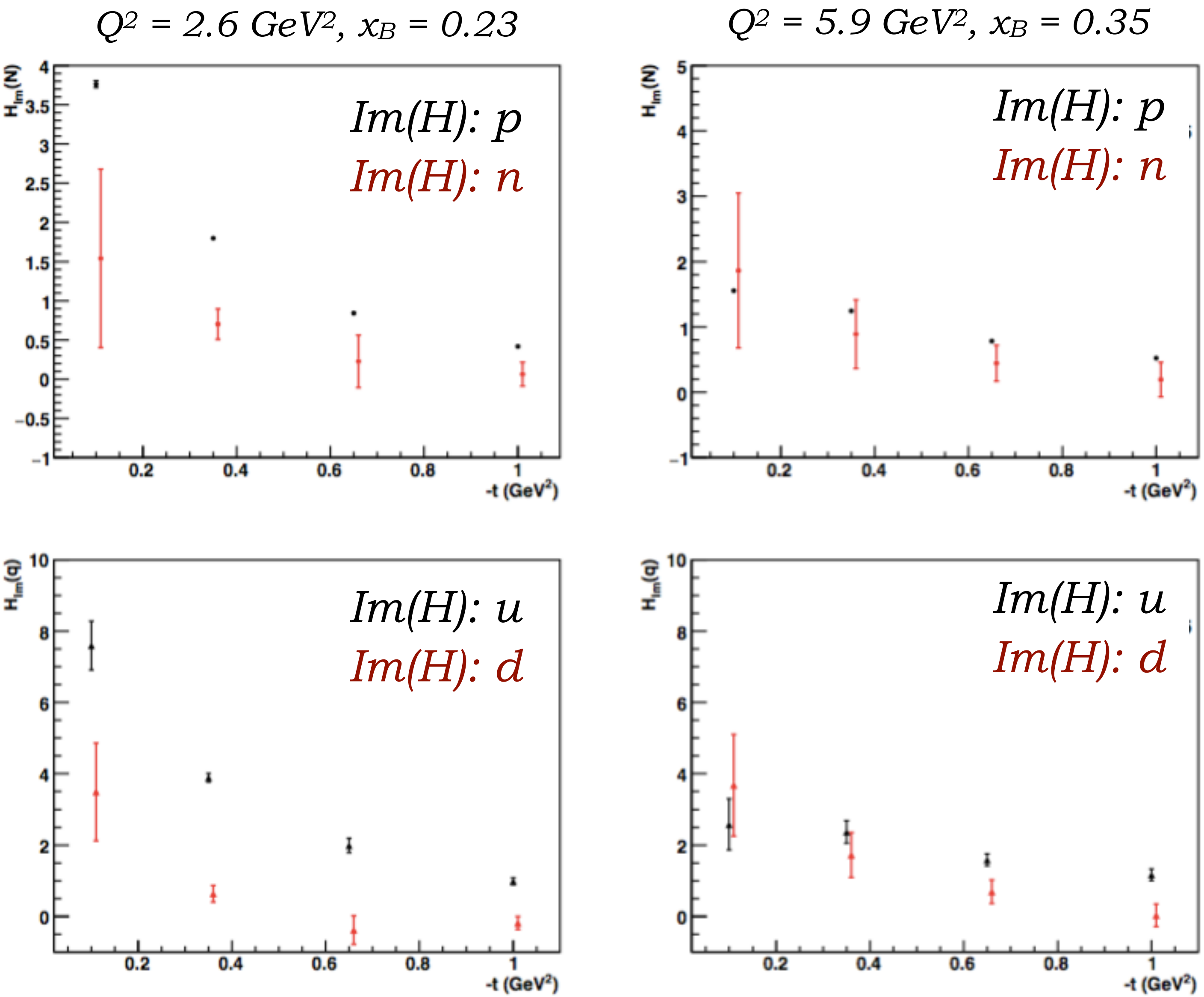
$Q^2 = 2.6$ GeV^2, $x_B = 0.23$

$Q^2 = 5.9$ GeV^2, $x_B = 0.35$

Projections for *Im(H)* neutron and proton and up and down CFFs extracted from approved CLAS12 experiments.

VGG fit (M. Guidal)

Projected sensitivities to *Im(E)* CFF

CLAS12

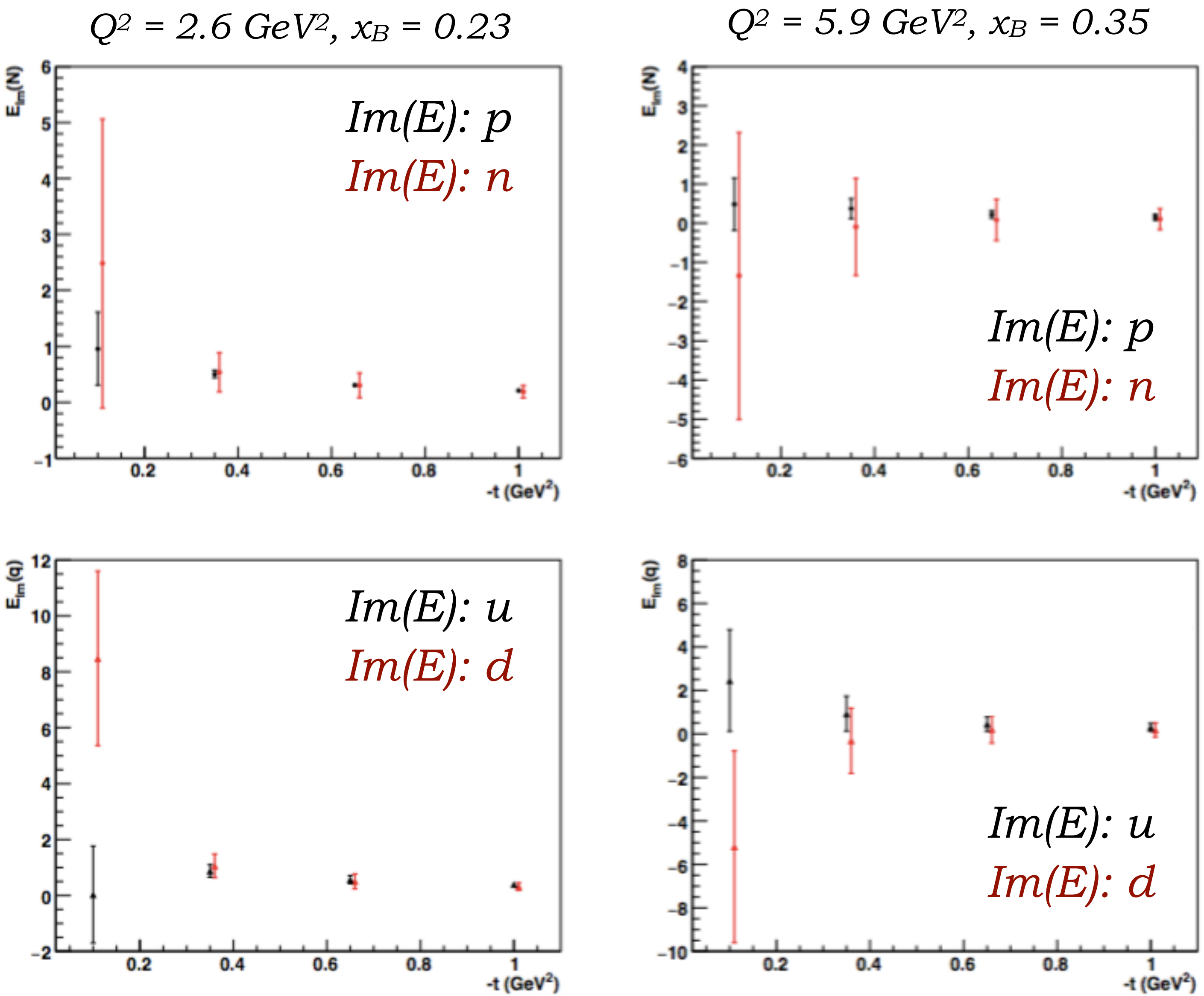

Projections for *Im(E)* neutron and proton and up and down CFFs extracted from approved and conditionally-approved CLAS12 experiments.

VGG fit (M. Guidal)

DVCS on ^{4}He: CLAS12 with ALERT

Experiment E12-17-012:
Z.-E. Meziani et al.

Measurement of BSA in coherent DVCS from a *^{4}He* target: partonic structure of nuclei.

✱ Spin 0 target, so at leading twist only one chiral-even GPD: $\mathbf{H_A}$.

11 GeV beam, 80% polarised.
Gas target straw @ 3 atm
L = 6 x 10^{34} nucleon $cm^{-2}s^{-1}$
with 1000 nA beam.

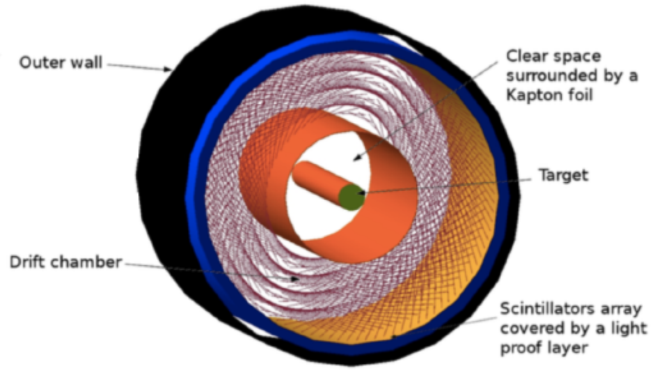

CLAS12 + ALERT: central recoil detector

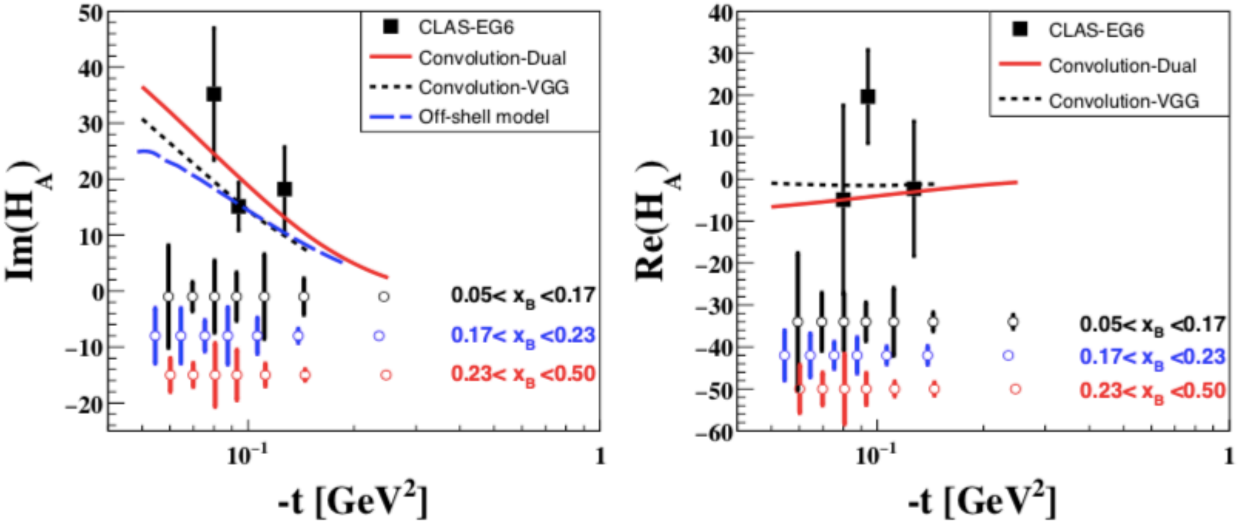

Experiment E12-17-012B
W. Armstrong et al.

Incoherent, spectator-tagged DVCS on *^{4}He* and *d*.

Electron-Ion Collider: from the valence region to the quark-gluon sea

Motivations for the Electron-Ion Collider

- The only facility designed entirely for the study of hadron physics:
  - What is the origin of nucleon mass? How is it generated from the almost massless quarks and massless gluons?
  - What is the quark-gluon origin of the nuclear force?
  - How do hadrons and nuclei emerge from quarks and gluons? What is the nature of confinement?
- 3D tomography of the nucleon: spacial and momentum distributions of partons from the valence quark region to the quark-gluon sea.

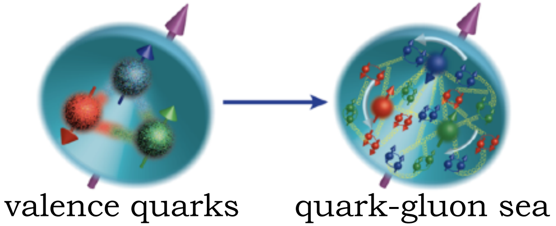

- Nucleon spin puzzle: decomposition of nucleon spin — contribution of gluons.

$$J_q = \frac{1}{2}\Delta\Sigma + L_q + J_g$$

- Structure functions for nucleons and nuclei, effect of nuclear medium on the propagation of a colour charge (hadronisation): insight into the EMC effect.
- Search for gluon saturation: a new form of matter.

The list is NOT exhaustive…

Nucleon at different scales

Valence quarks

Jefferson Lab: fixed-target electron scattering

$0.1 < x_B < 0.7$

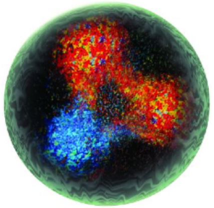

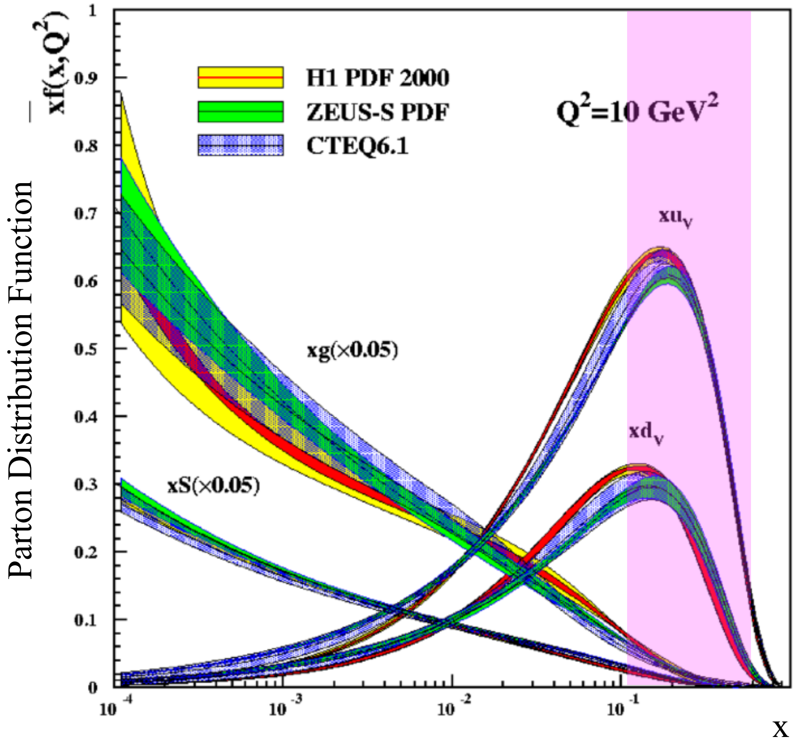

Nucleon at different scales

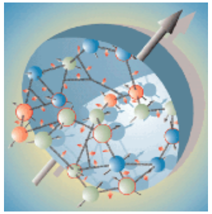

Valence quarks

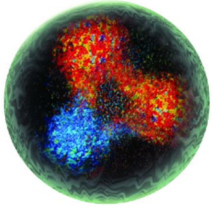

Jefferson Lab: fixed-target electron scattering

$0.1 < x_B < 0.7$

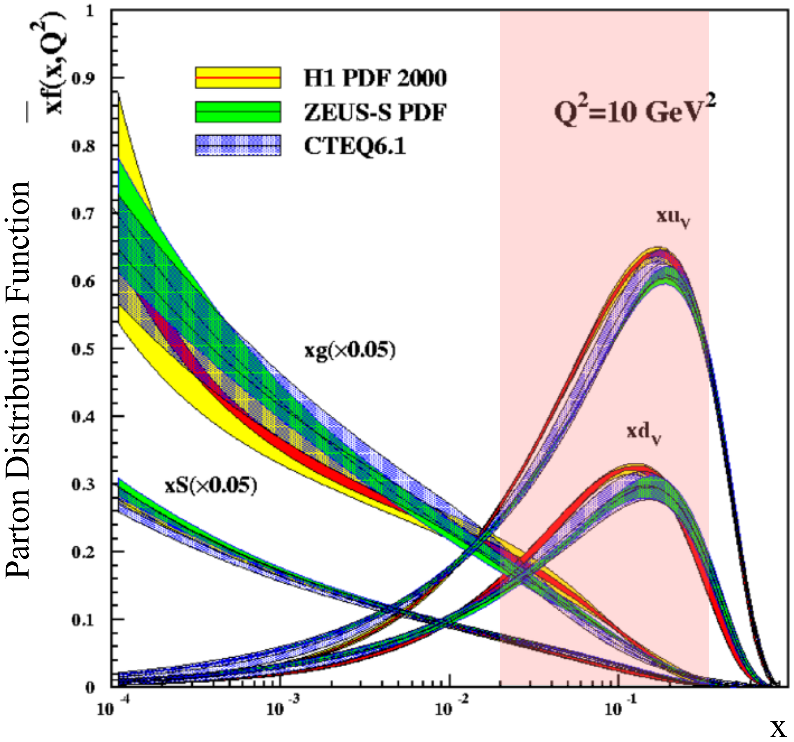

Sea quarks

HERMES: fixed gas-target electron/positron scattering

$0.02 < x_B < 0.3$

Nucleon at different scales

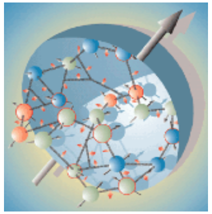

Valence quarks

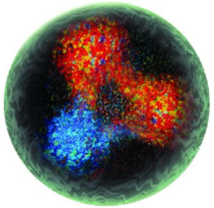

Jefferson Lab: fixed-target electron scattering

$0.1 < x_B < 0.7$

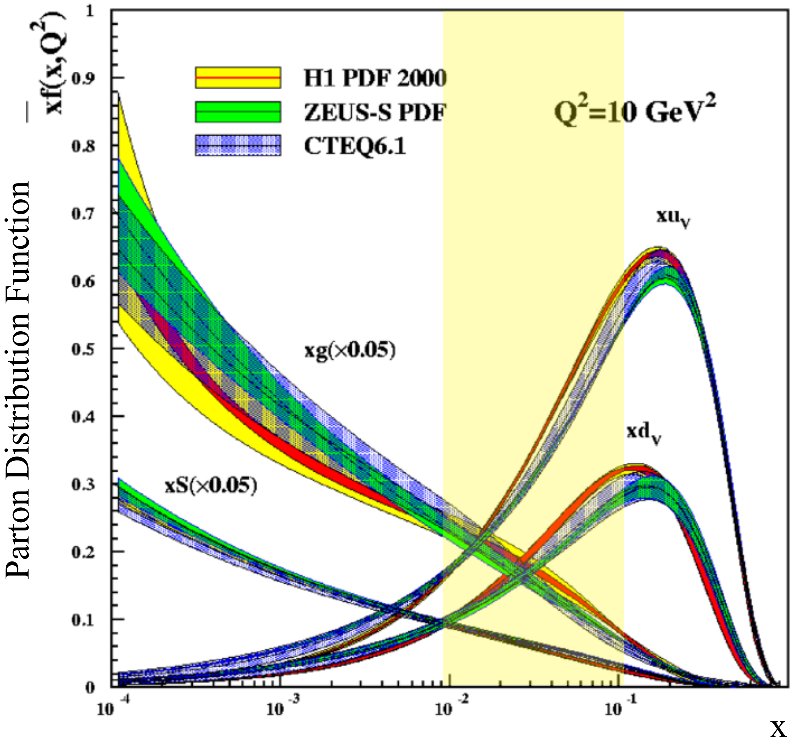

Sea quarks

HERMES: fixed gas-target electron/positron scattering

$0.02 < x_B < 0.3$

COMPASS: fixed-target muon scattering

$0.01 < x_B < 0.1$

Nucleon at different scales

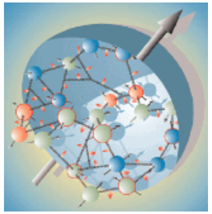

Valence quarks

Jefferson Lab: fixed-target electron scattering

$0.1 < x_B < 0.7$

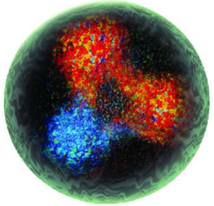

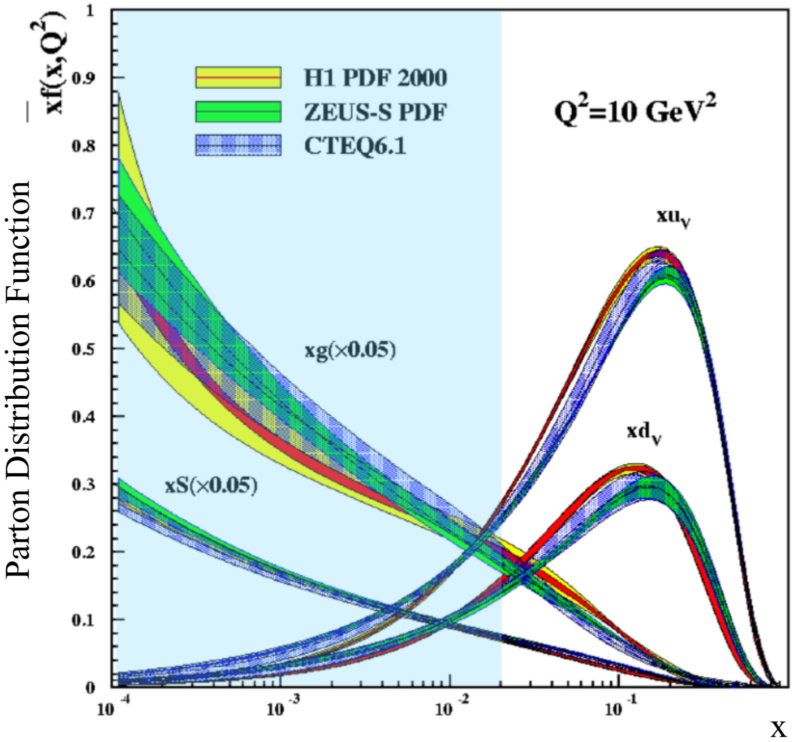

Sea quarks

HERMES: fixed gas-target electron/positron scattering

$0.02 < x_B < 0.3$

COMPASS: fixed-target muon scattering

$0.01 < x_B < 0.1$

The glue

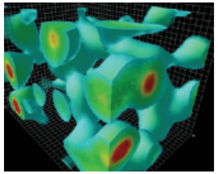

Derek Leinweber

ZEUS/H1: electron/positron-proton collider

$10^{-4} < x_B < 0.02$

Nucleon at different scales

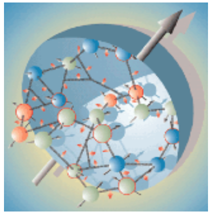

Valence quarks

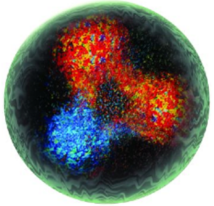

Jefferson Lab: fixed-target electron scattering

$0.1 < x_B < 0.7$

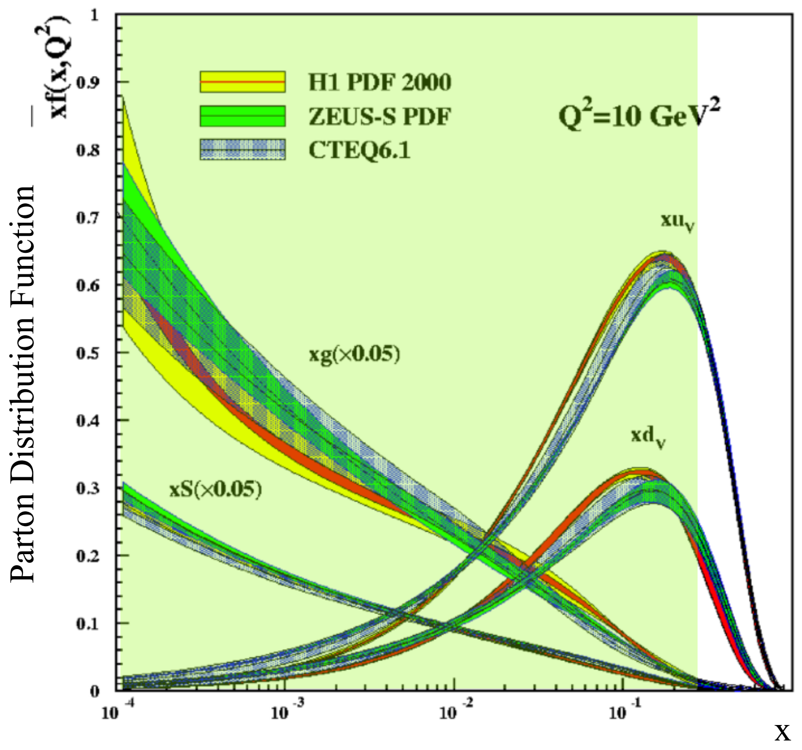

Sea quarks

HERMES: fixed gas-target electron/positron scattering

$0.02 < x_B < 0.3$

COMPASS: fixed-target muon scattering

$0.01 < x_B < 0.1$

The glue

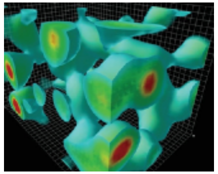

Derek Leinweber

ZEUS/H1: electron/ positron-proton collider

$10^{-4} < x_B < 0.02$

EIC: $10^{-4} < x_B < 0.3$

Luminosity 100 - 1000 times that of HERA

EIC in context

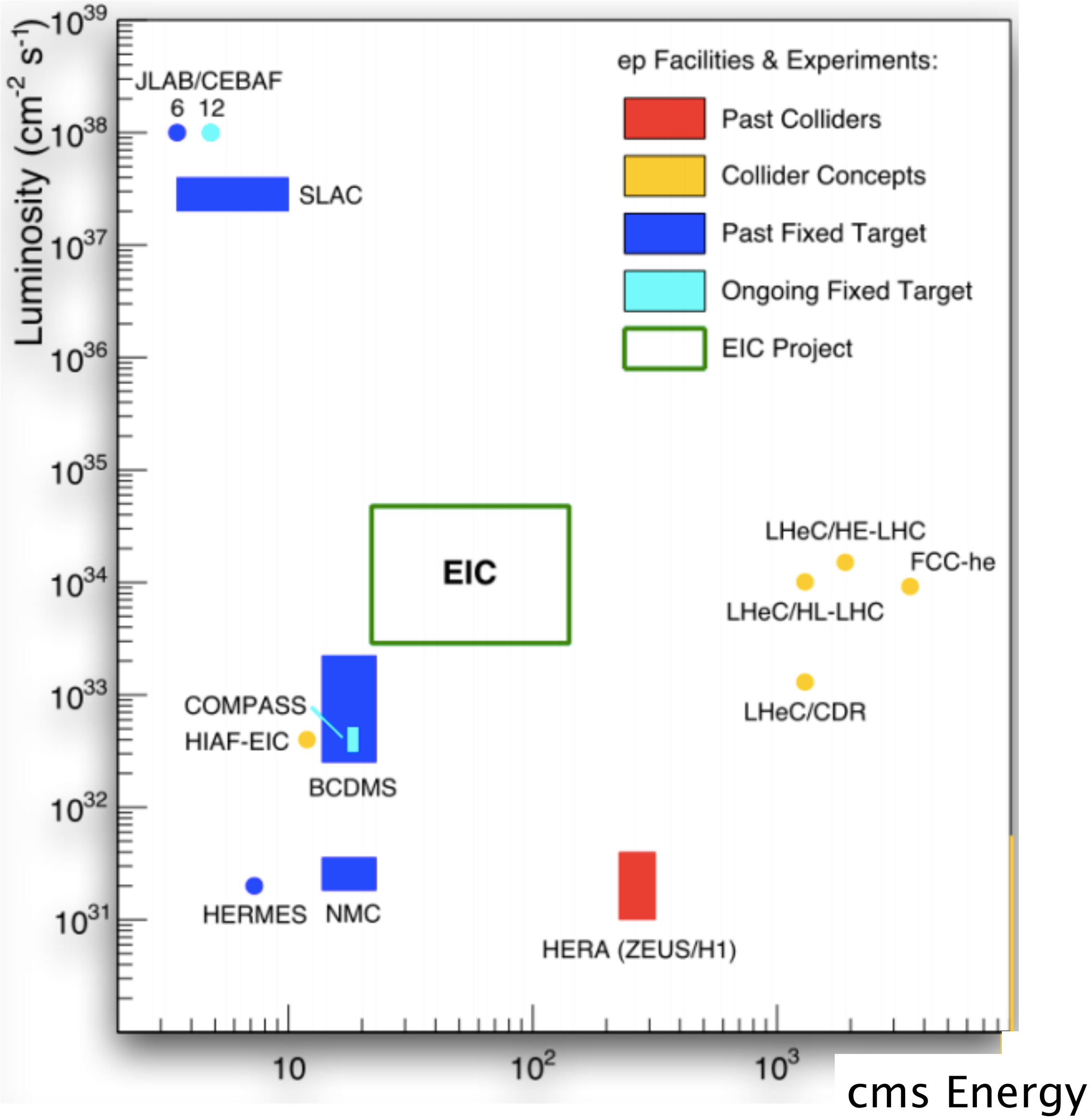

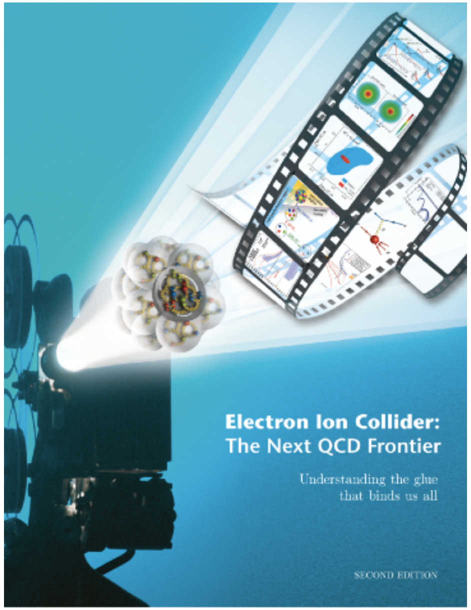

2012 EIC White Paper,
Eur. Phy. J. A 52, 9 (2016)

EIC box includes different baseline designs

Electron-Ion Collider in the making

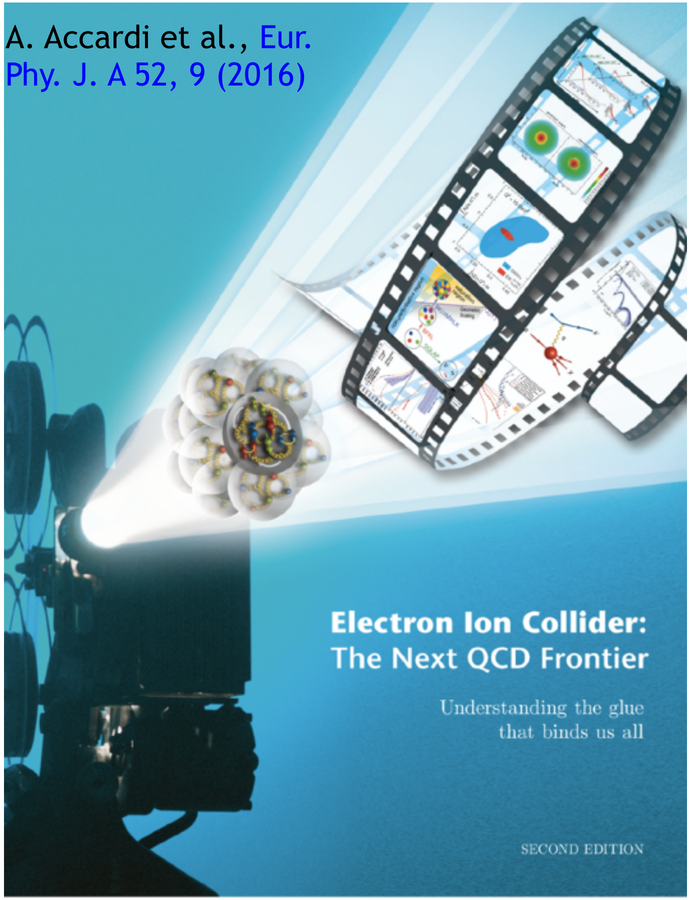

A. Accardi et al., Eur. Phy. J. A 52, 9 (2016)

Electron Ion Collider:
The Next QCD Frontier

Understanding the glue
that binds us all

SECOND EDITION

- ***2007 Nuclear Physics Long Range Plan***: *"The EIC is embodying the vision of reaching the next QCD frontier"*
- ***2012 EIC White Paper***, *Eur. Phy. J. A 52, 9 (2016)*
- ***2015 Nuclear Physics Long Range Plan***: *"high-energy, high-luminosity polarised EIC as the highest priority for new facility construction following completion of FRIB"*
- ***2017-18 National Academies of Science (NAS) Review:*** *"the science questions that an [EIC] would answer are central to completing our understanding of atomic nuclei"*

  *"An EIC can **uniquely** address three profound questions about nucleons … and how they are assembled to form the nuclei of atoms:*

  - *How does the **mass** of the nucleon arise?*
  - *How does the **spin** of the nucleon arise?*
  - *What are the **emergent properties of dense systems of gluons**?"*

July 2018

https://www.nap.edu/catalog/25171/an-assessment-of-us-based-electron-ion-collider-science

Nucleon tomography: imaging quarks

- Quark GPDs through DVCS

DVCS kinematic reach at the EIC:

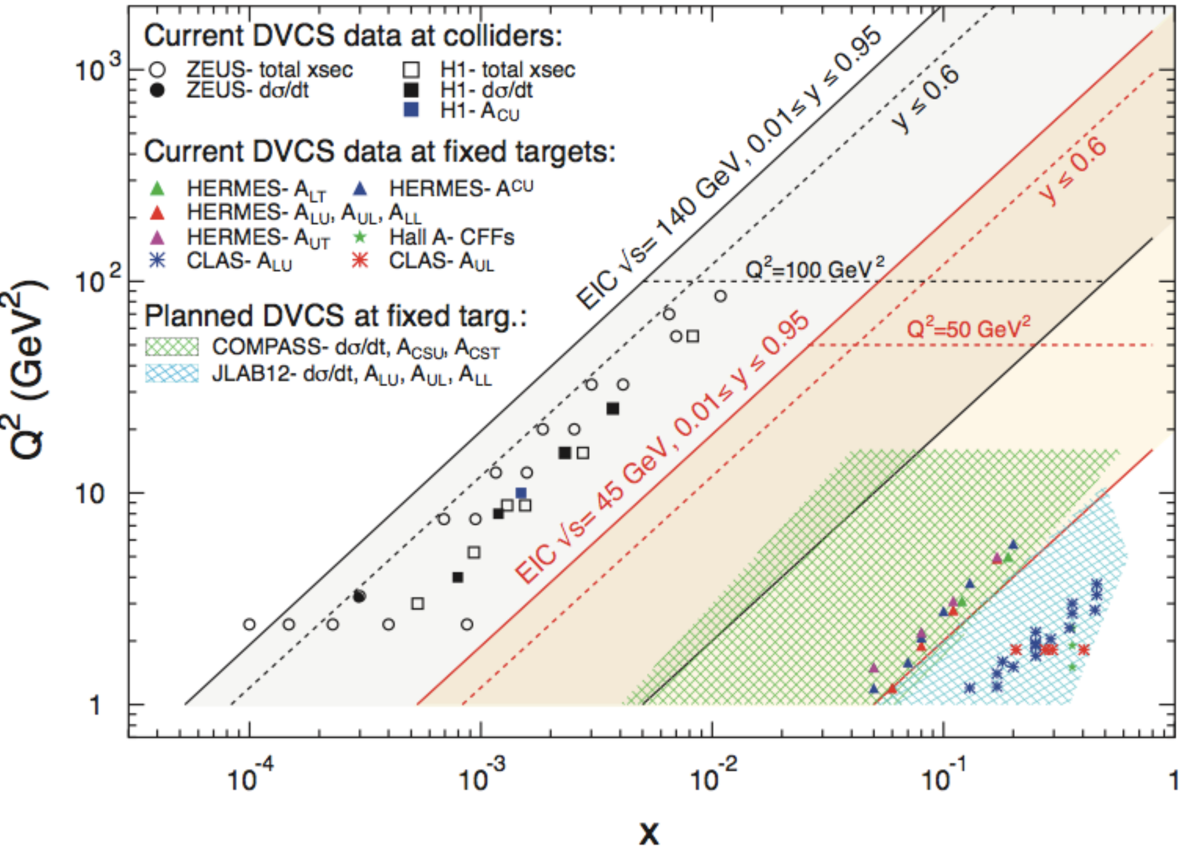

EIC White Paper, *Eur. Phy. J. A 52, 9 (2016)*

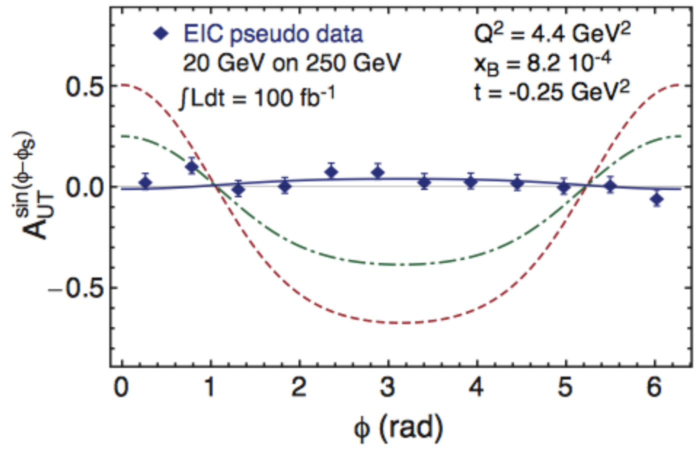

- Scan in *t* enables transverse position mapping. Expected accuracy:

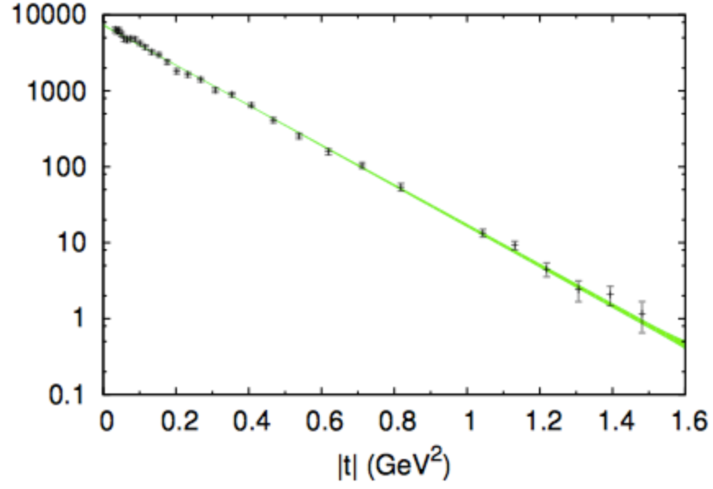

Nucleon tomography: imaging glue

- Gluon GPDs can be accessed through deeply virtual meson production (DVMP), eg: J/Ψ
- Access to spatial distributions of gluons at different longitudinal momentum fractions:

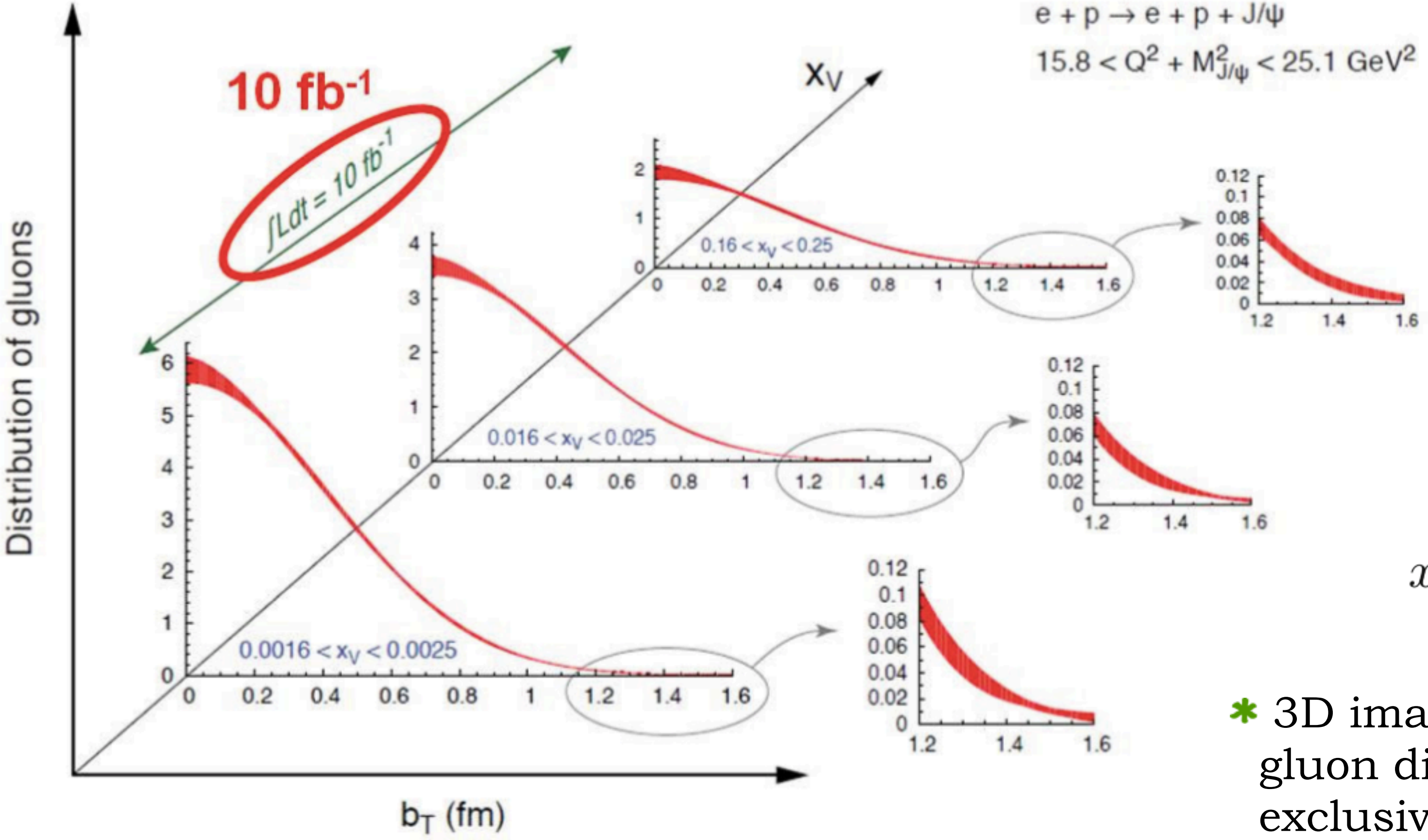

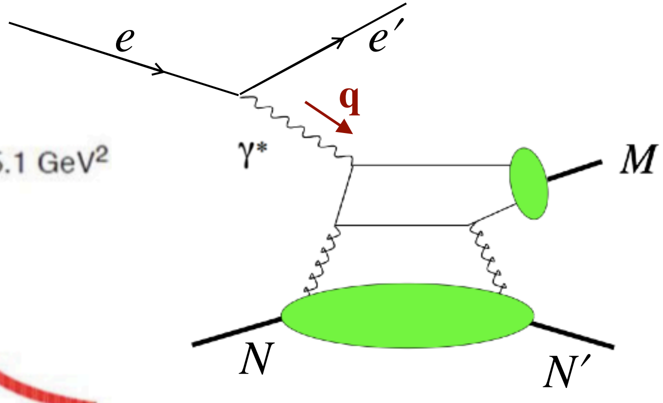

M. Diehl

Gluon momentum fraction related to:

$$x_V = x_B(1 + M^2_{J/\Psi}/Q^2)$$

- 3D images of sea quark and gluon distributions from exclusive reactions: DVCS and DVMP.

EIC White Paper, *Eur. Phy. J. A 52, 9 (2016)*

Gluon spin

- DIS and SIDIS will contribute extremely precise measurements of the helicity distributions of sea-quarks and gluons.

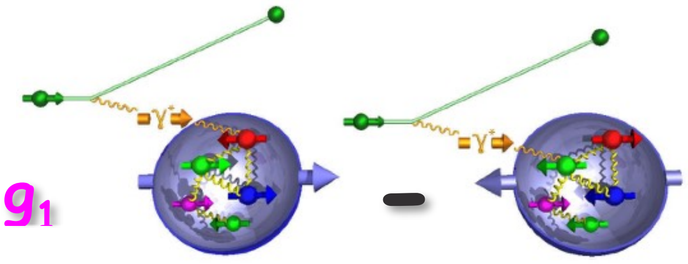

$$\Delta\Sigma(Q^2) = \int_0^1 g_1(x,Q^2)\,dx = \int_0^1 \Delta q_f(x,Q^2)\,dx$$

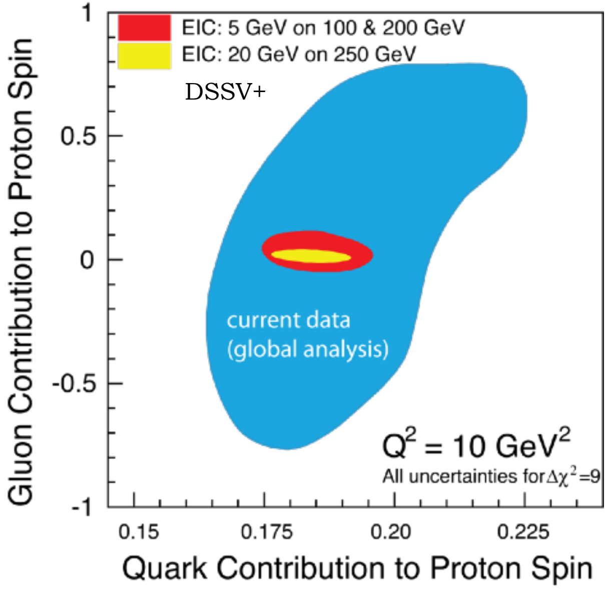

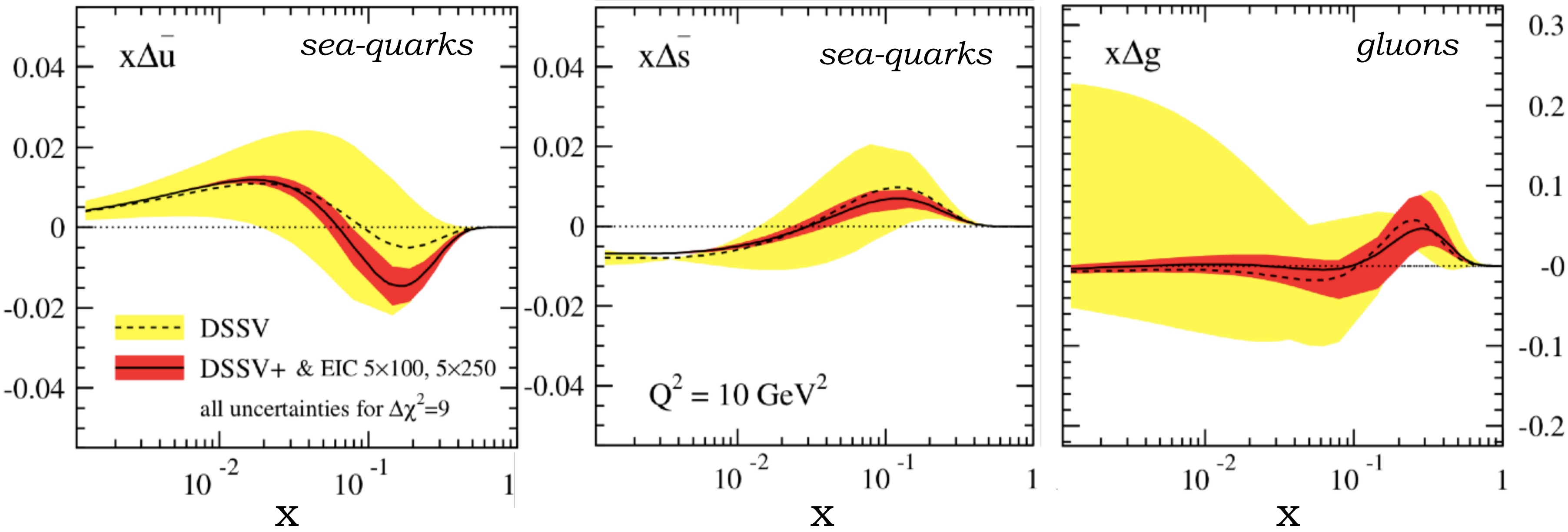

E. Aschenauer *et al.*,
Phys. Rev. D 86, 054020 (2012)

DSSV: D. de Florian, R. Sassot, M. Stratmann, W. Vogelsang, Phys. Rev. **D 80**, 034030 (2009).

DSSV+: arXiv:1112.0904 [hep-ph]

Hadronisation

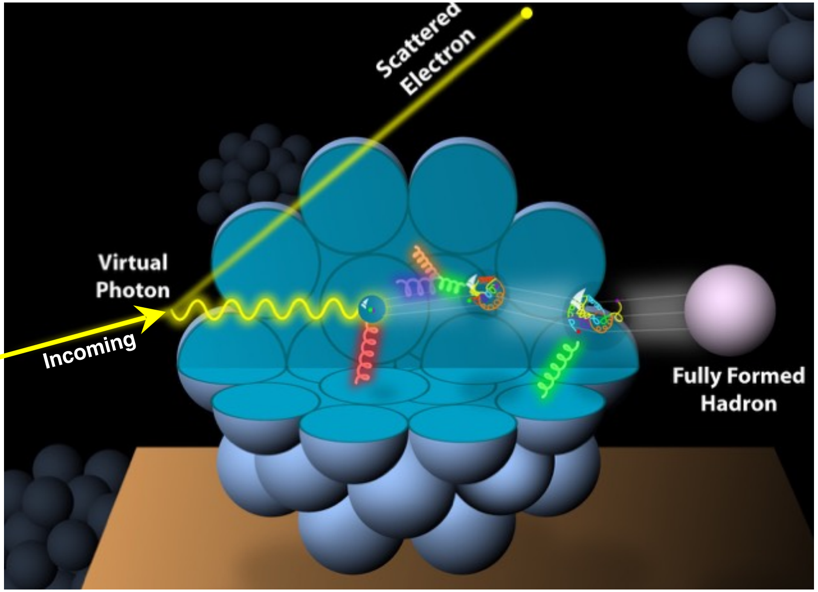

Courtesy of E. Aschenauer

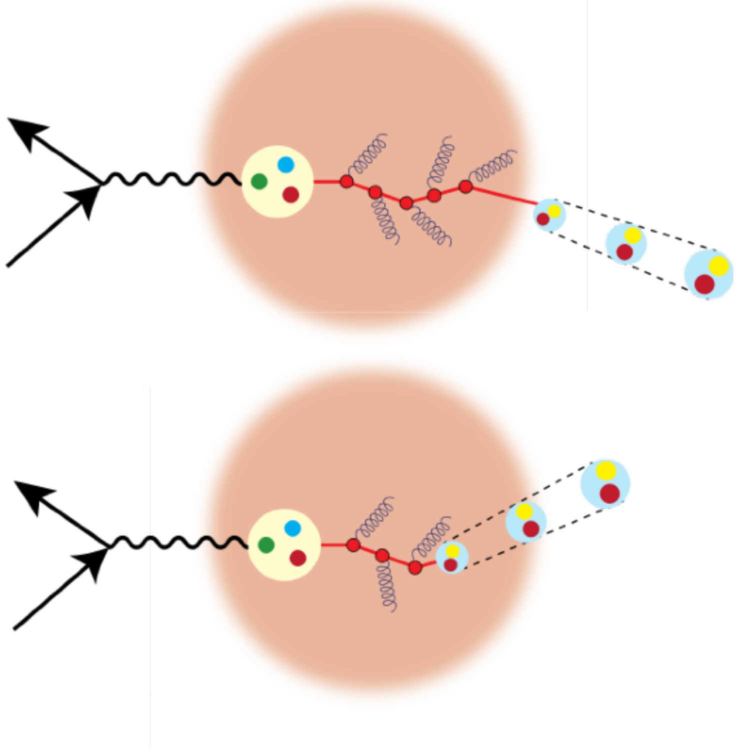

- How does the nuclear environment affect the distributions of quarks and gluons and their interactions inside nuclei?
- How does nuclear matter respond to fast moving color charge passing through it?
- Are there differences for light and heavy quarks?

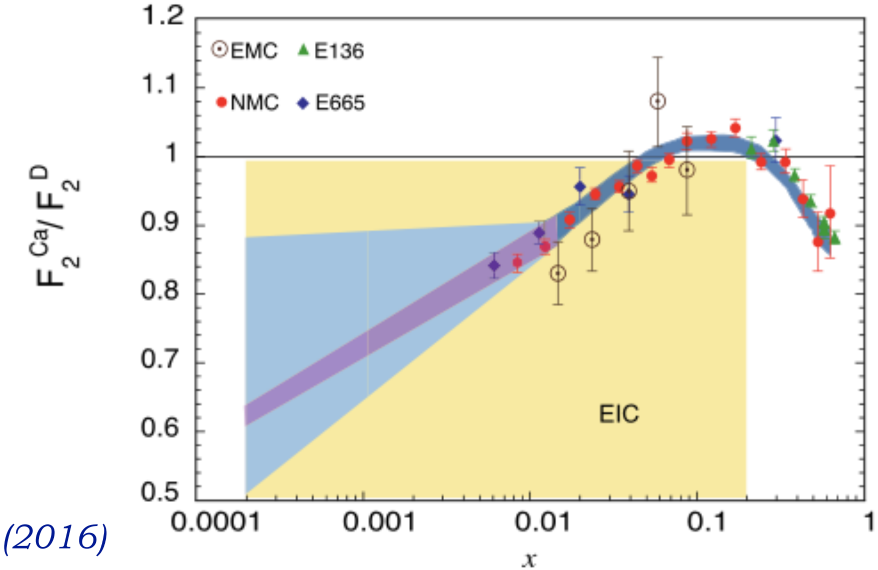

EIC White Paper, *Eur. Phy. J. A 52, 9 (2016)*

Runaway glue

- Nucleon probed at low Q^2, high x.

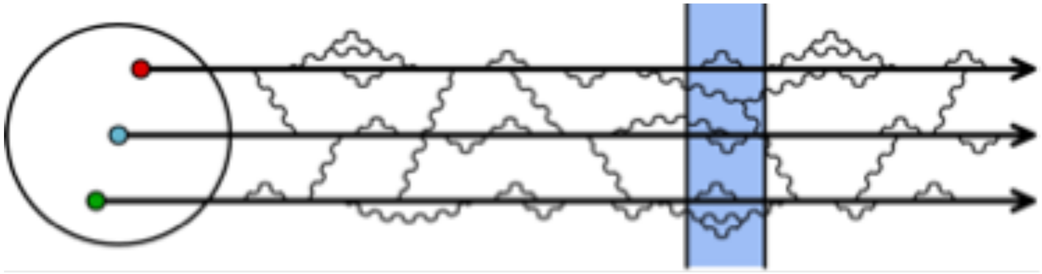

- Nucleon probed at large Q^2, low x.

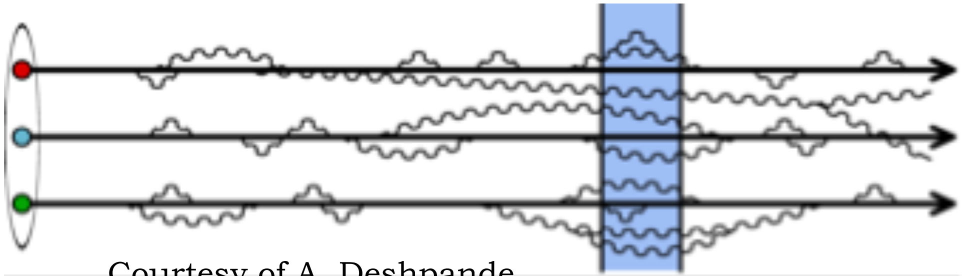

Courtesy of A. Deshpande

- Gluons are charged under colour: can generate (and absorb) other gluons.

- Nucleon probed at high energies, time dilation of strong interaction processes: gluons appear to live longer, emitting more and more gluons. Runaway growth! Runaway growth?

Saturation of gluon density

- Runaway growth of glue at low-x:

"…A small color charge in isolation builds up a big color thundercloud…."

F. Wilczek, in "Origin of Mass"
Nobel Prize, 2004

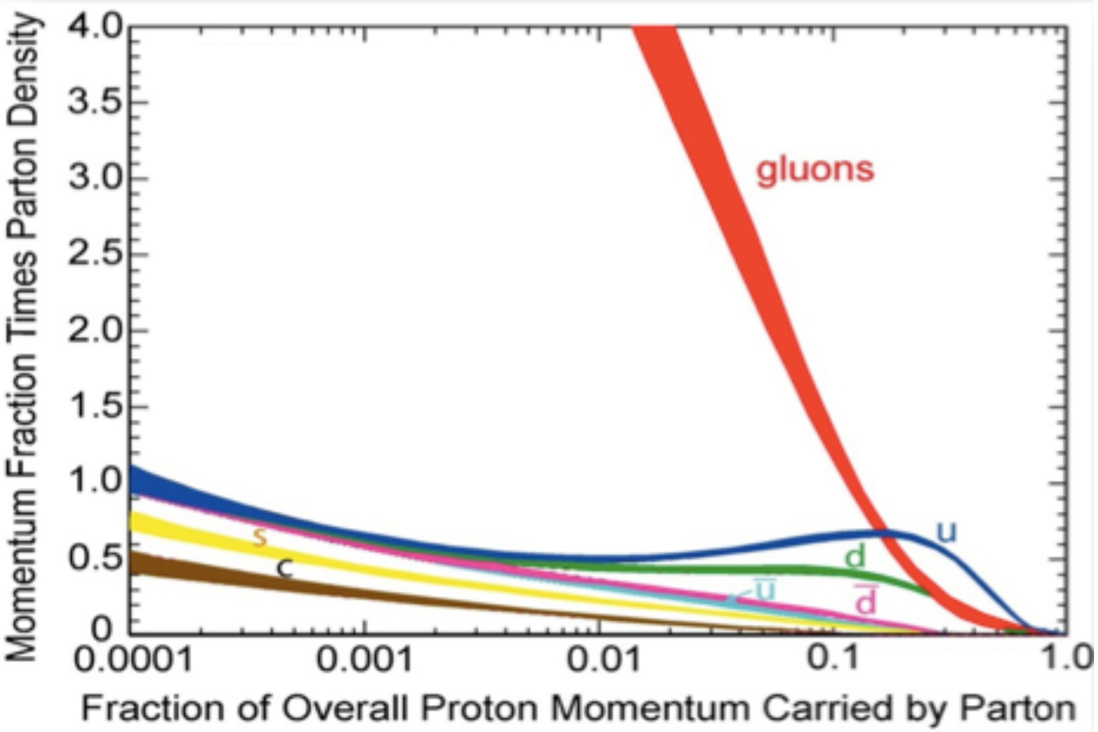

But somewhere it must saturate…

rate of 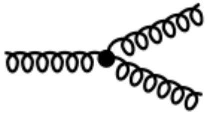 = rate of 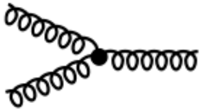

Recombination of gluons leads to saturation of gluon densities. Possible effective theory: Colour Glass Condensate.

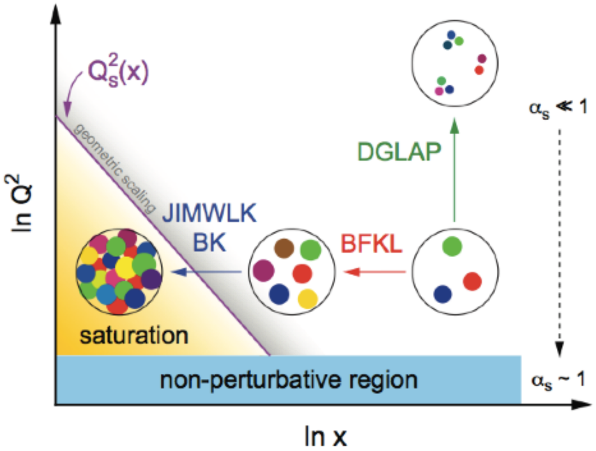

Courtesy of A. Deshpande

Can we reach saturation at EIC?

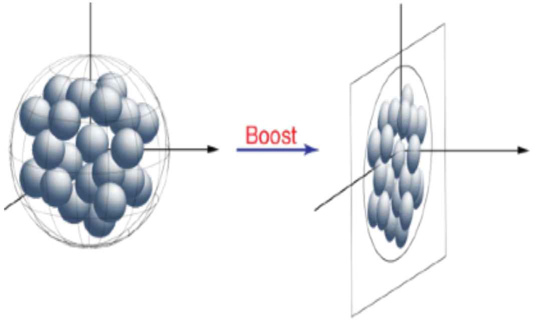

Saturation regime would be accessible at much lower energy in *e-A* collisions than *e-p*. You do not need a TeV collider!

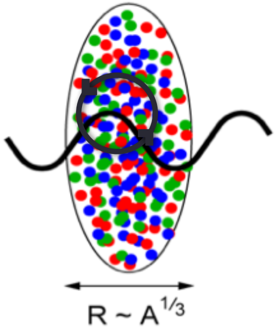

$$(Q_s^A)^2 \approx cQ_0^2 \left[\frac{A}{x}\right]^{1/3}$$

saturation scale

A powerful signature is diffractive cross-sections:

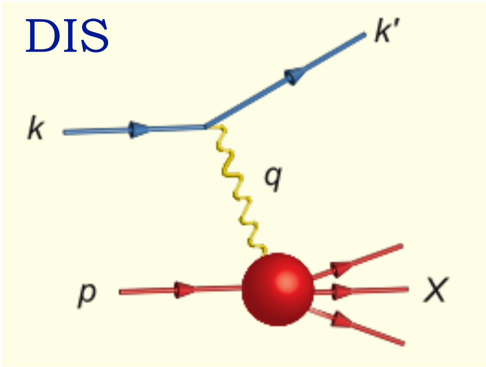

Saw ~10% diffractive events at HERA.

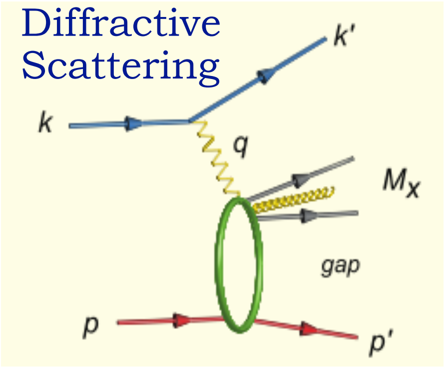

$$\sigma_{\rm diff} \propto [g(x,Q^2)]^2$$

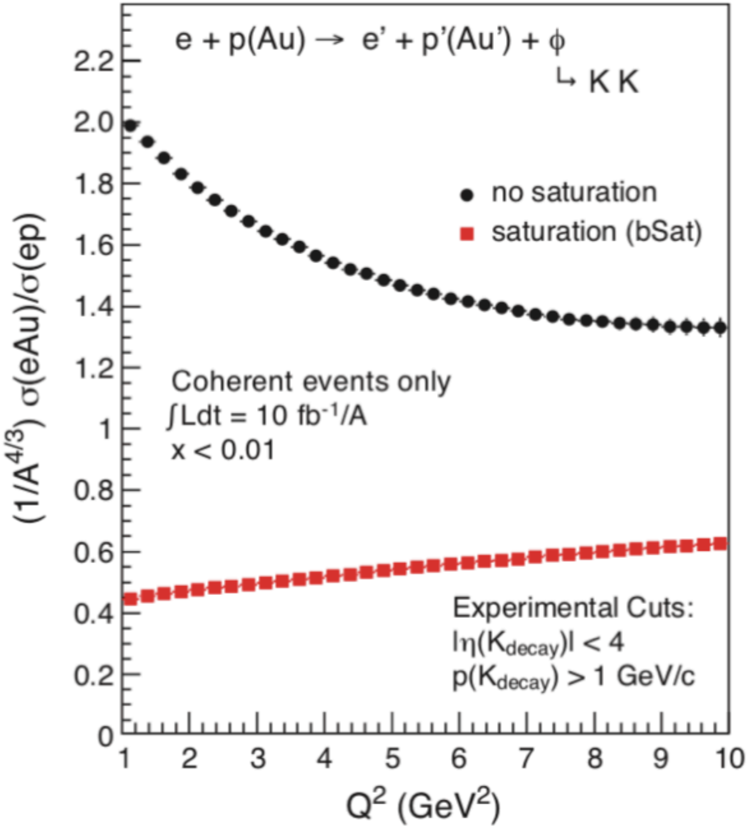

EIC White Paper, *Eur. Phy. J. A 52, 9 (2016)*

What do we want from the machine?

- Parton imaging in 3D: high luminosity, 10^{33-34} cm^{-2} s^{-1} and above.
- Wide coverage of phase space from low to high x and up to high Q^2: variable centre of mass energy.
- Spin structure: high polarisation of electrons (0.8) and light nuclei (0.7).
- Studies of hadronisation, search for saturation at high gluon densities: a wide range of ion species up to the heaviest elements (p -> U).
- Flavour tagging: large acceptance detectors with good PID capabilities.

What will we be able to do?

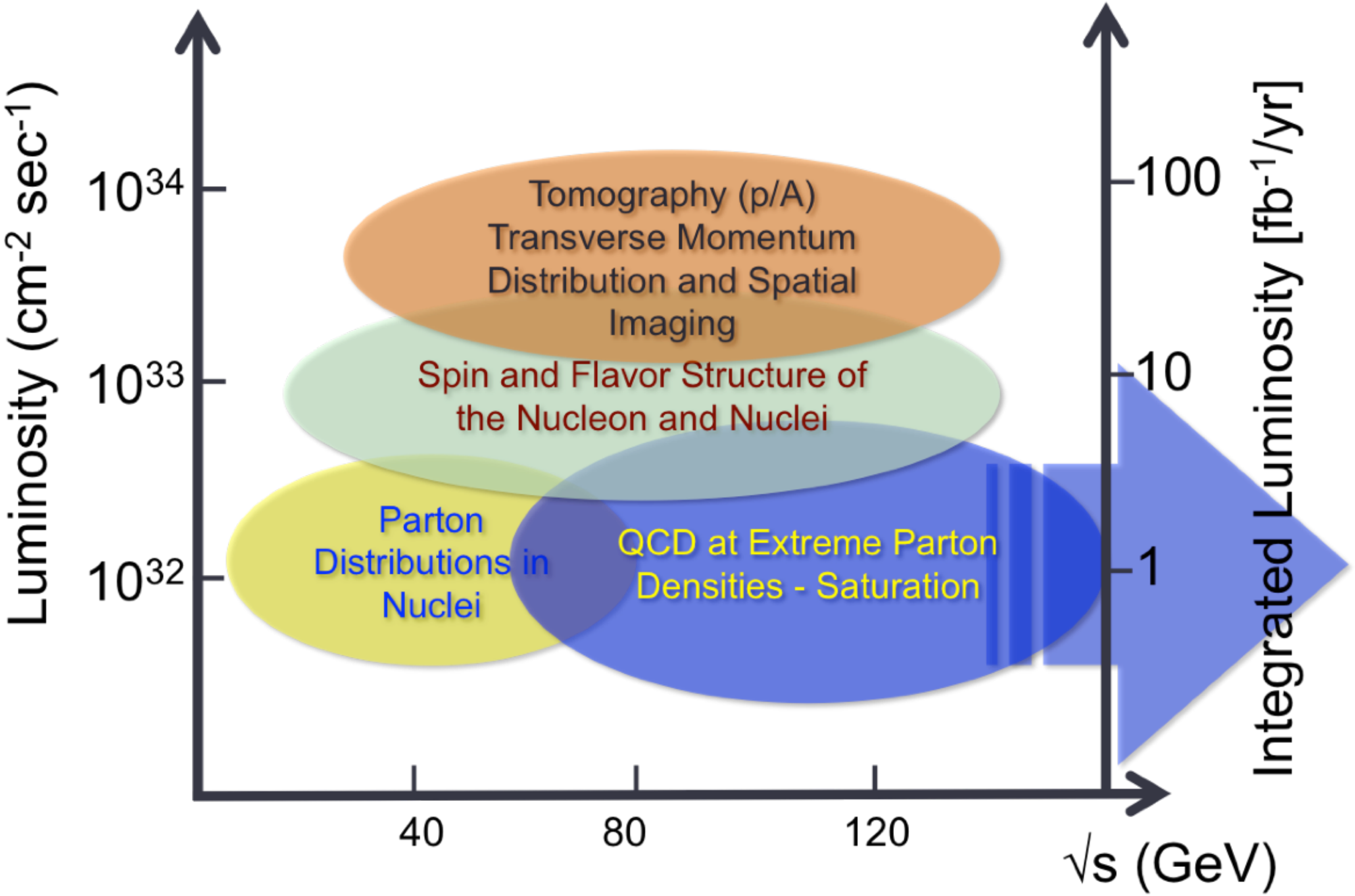

year =10^7 sec

The two proposed sites

World's first polarized electron-proton/light ion and electron-Nucleus collider:

- Polarized beams: e, p, d/^{3}He
- Wide range of nuclei
- 20 - 100 (upgradable to 140) GeV variable CoM
- Polarisation ~ 70%

Two proposals:

- **JLEIC**: 3 - 10 GeV e-, up to 100 GeV/u ions, Luminosity L ~ 10^{34} cm^{-2}s^{-1}
- **eRHIC**: 5 - 18 GeV e$^-$/e$^+$, 50-275 GeV (p) and <100 GeV/u ions, L ~ 10^{33} cm^{-2}s^{-1}

JLEIC @ Jefferson Lab

arXiv:1504.07961

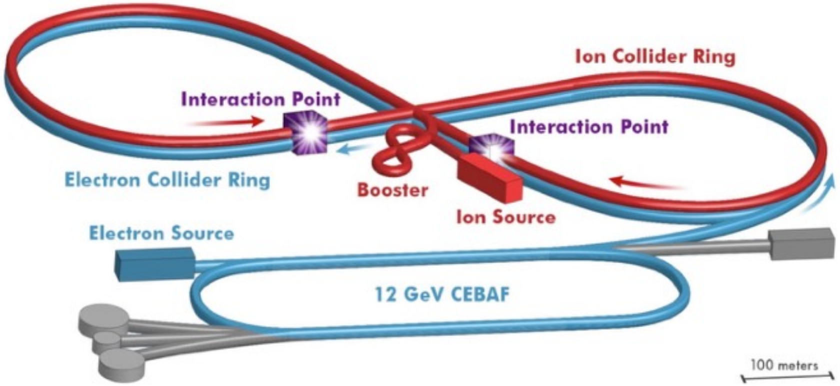

eRHIC @ Brookhaven National Lab

arXiv:1409.1633

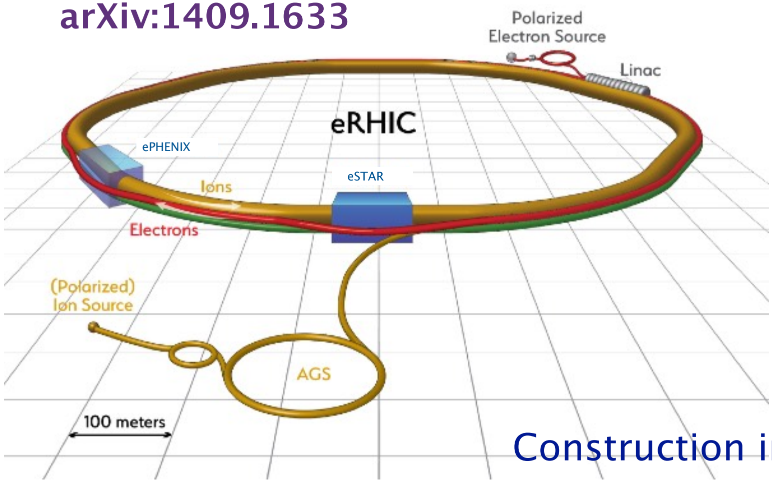

Construction in 2020s

Design in flux: physics case evolving, machine and detector design developing.

JLEIC Reach

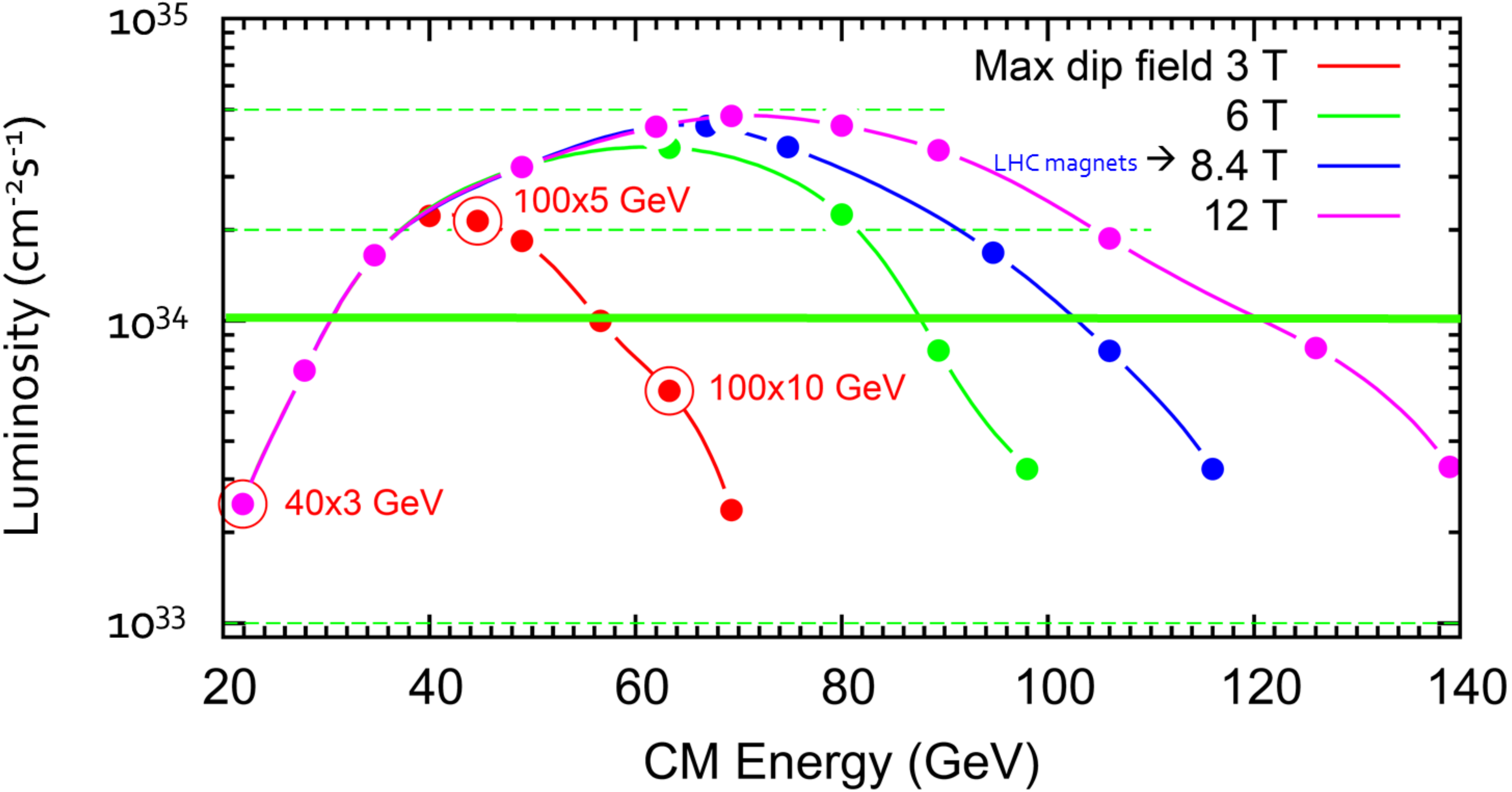

Courtesy of V. Morozov (JLab)

eRHIC Reach

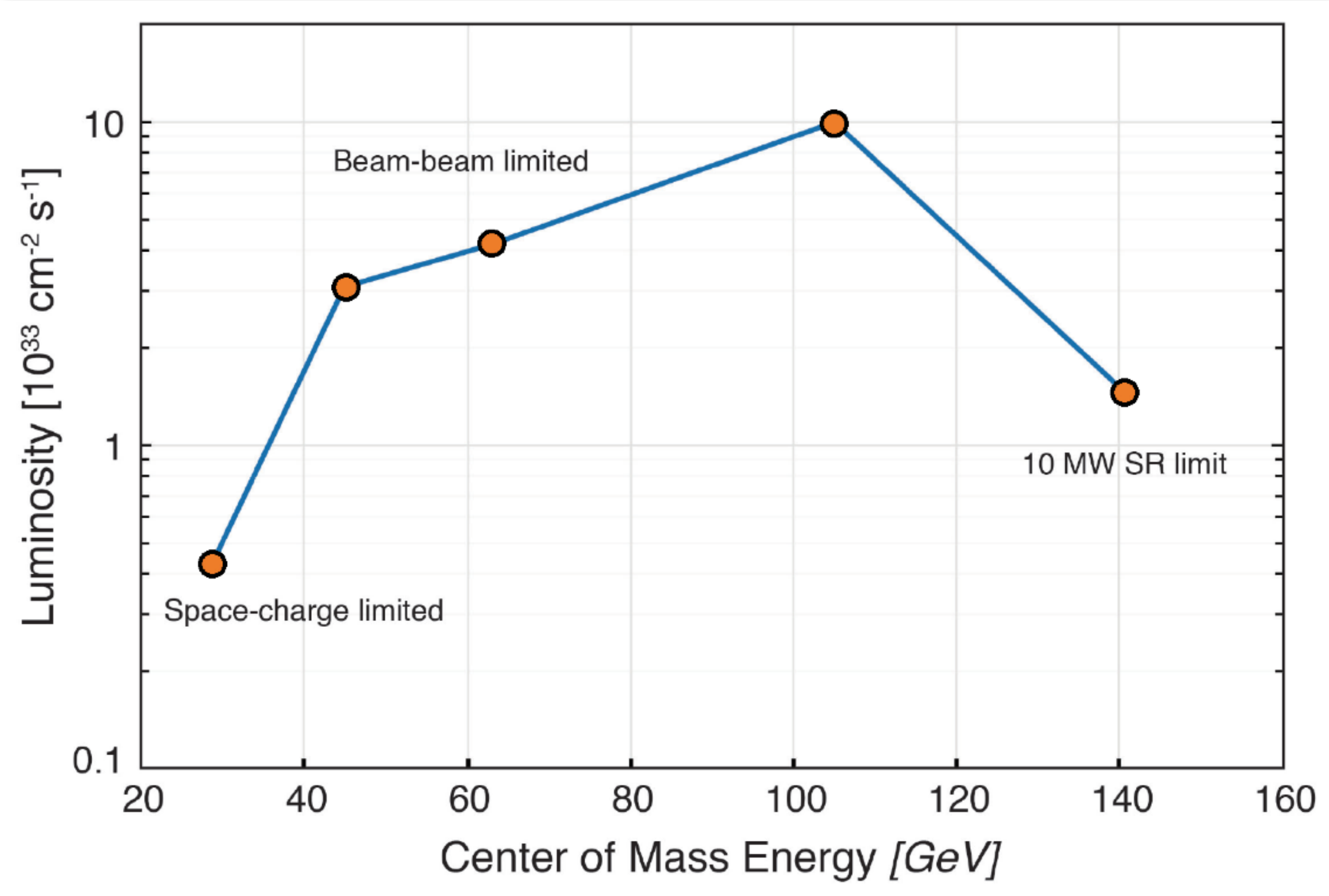

Courtesy of E. Aschenauer (BNL)

Interaction Region

Possible to get ~100% acceptance for the whole event

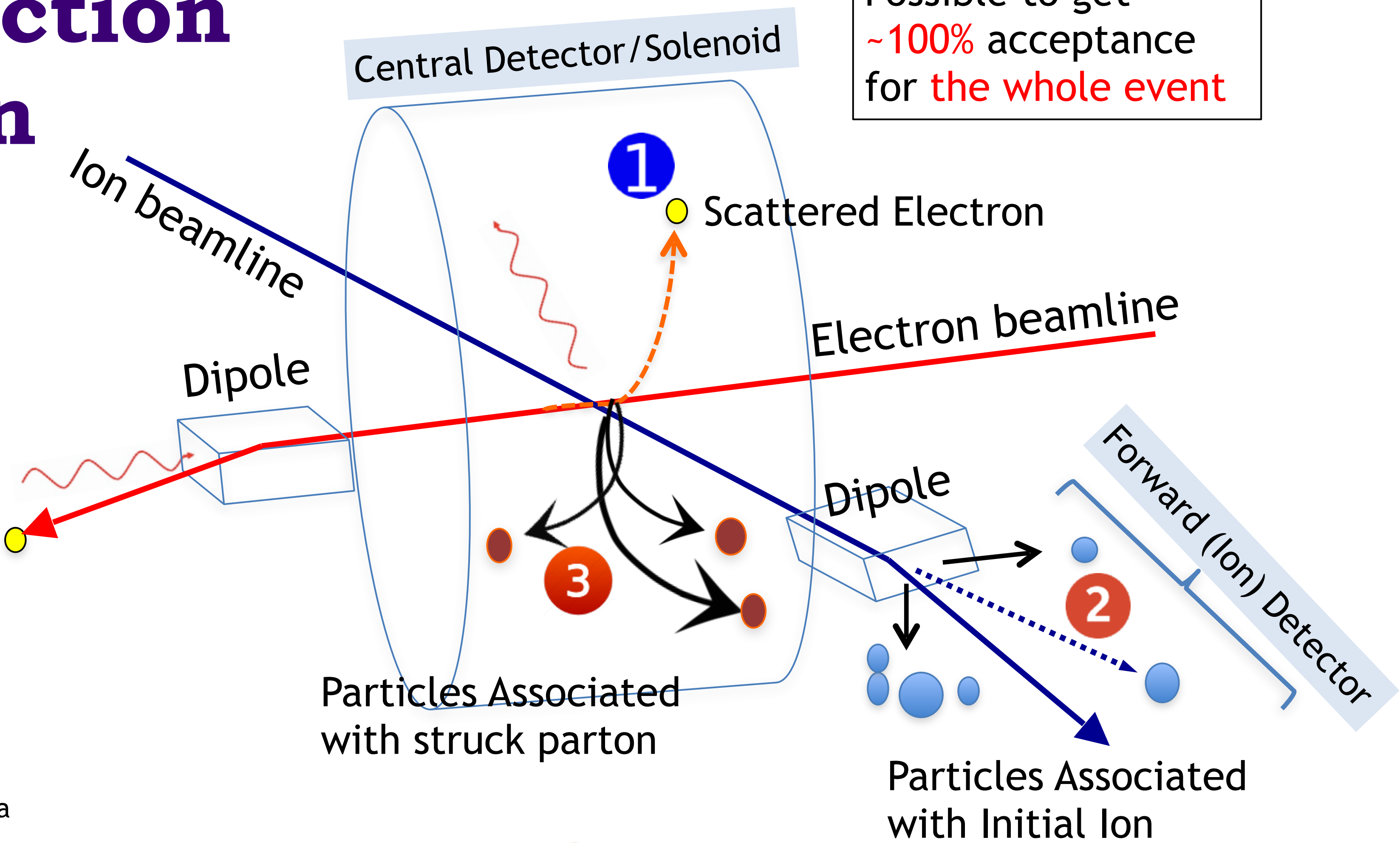

Courtesy of R. Yoshida

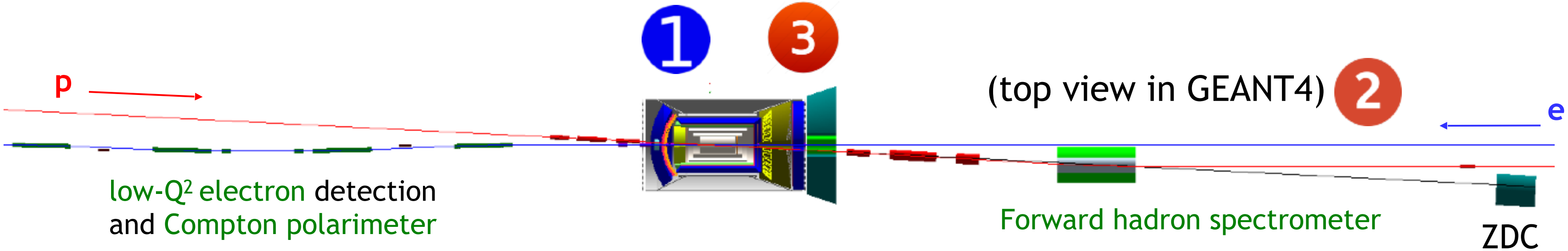

Main detector designs

JLEIC detector (JLab)

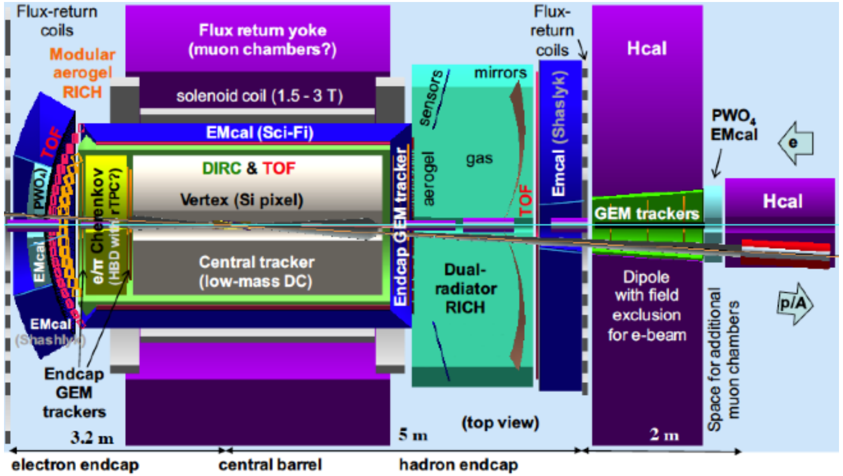

BEAST (BNL)

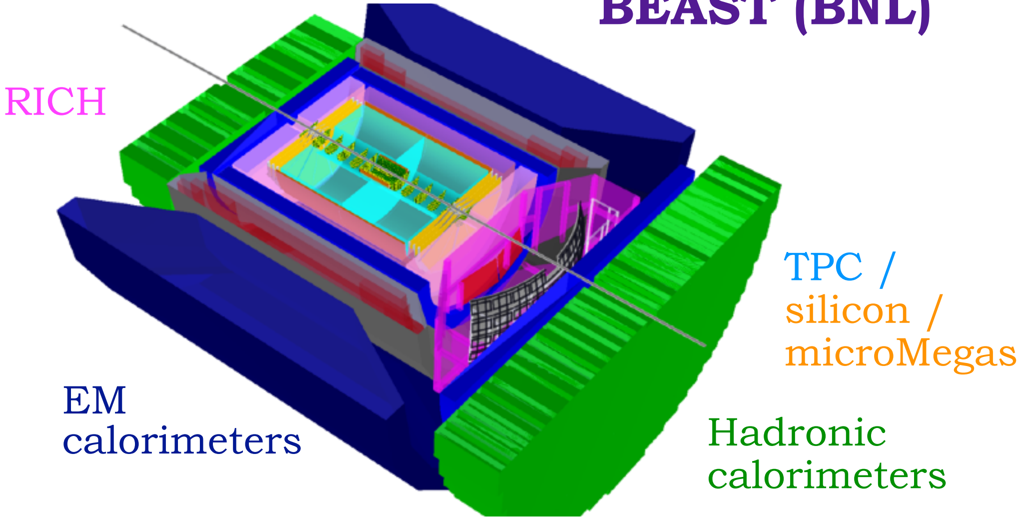

TOPside (Argonne)

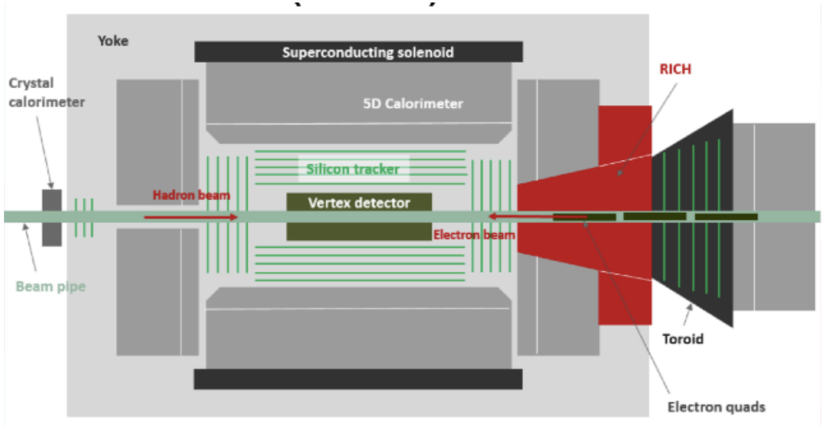

ePHENIX (BNL)

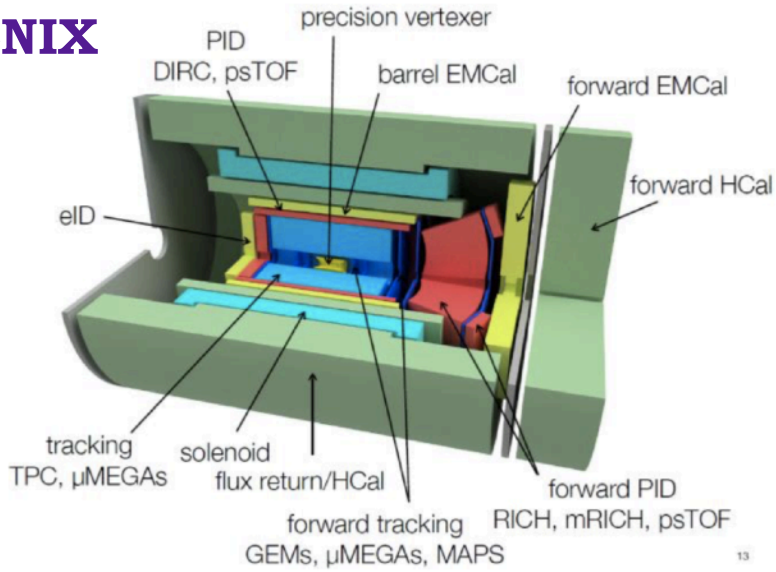

The EIC Users Group

821 members, 173 Institutes, 30 Countries

475 experimentalists, 162 theorists, 142 accelerator-physicists, 42 other

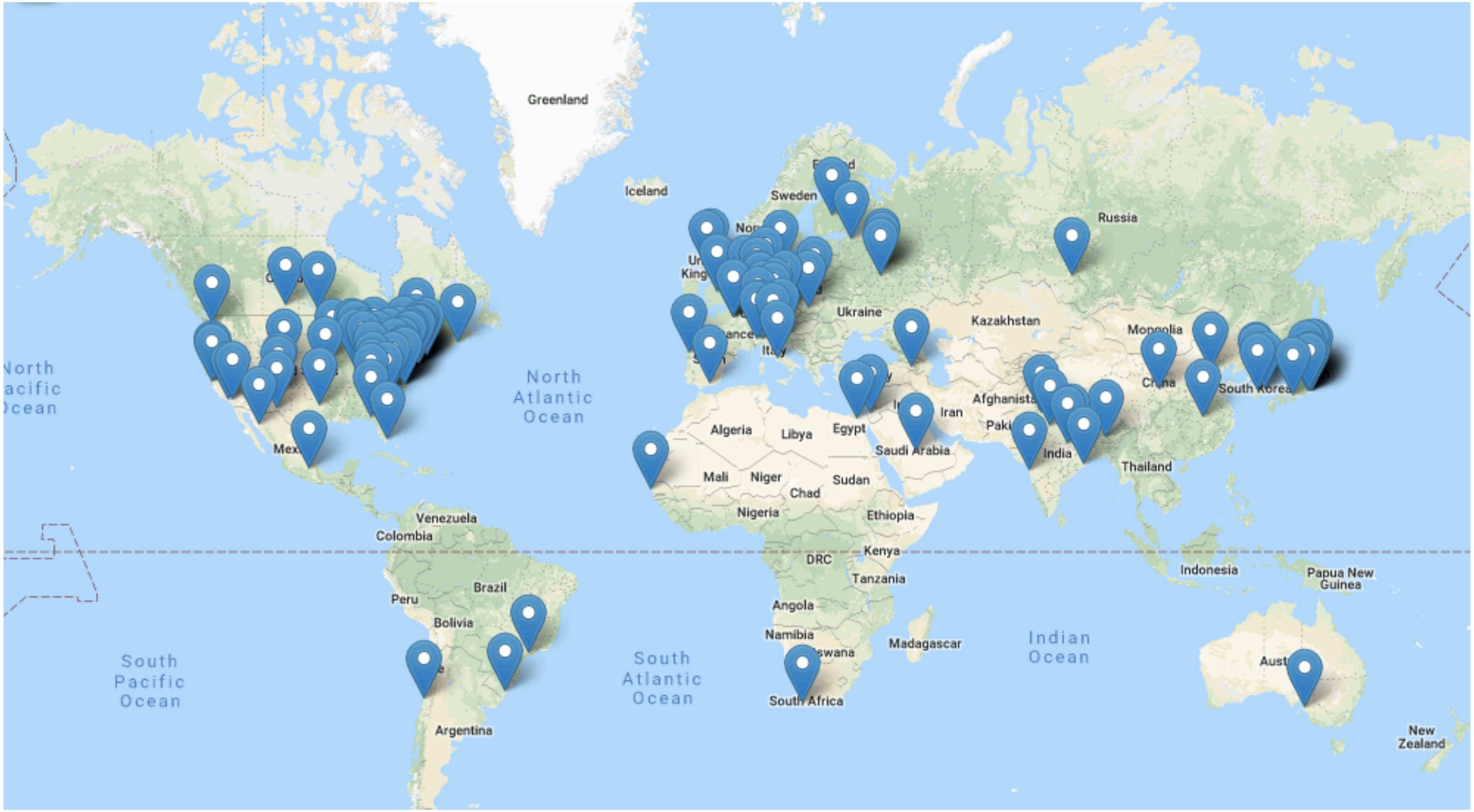

www.eicug.org

and growing…

To conclude

- Success of the initial DVCS programme using **CLAS at Jefferson Lab with 6 GeV beams** — measurements of the cross-section, beam- target- and double-spin asymmetries in proton DVCS, constraints on CFF fits, first steps towards nucleon tomography and pressure distributions within nucleons.

- JLab 12 GeV upgrade: 11 GeV to Hall B with **CLAS12**, opens a new region of phase space — high luminosity, high precision. **DVCS measurements** are a flagship part of the new programme, approved proposals aimed at greatly constraining CFF fits in a global analysis:
  - extraction of H and E from proton and neutron DVCS,
  - flavour separation of CFFs,
  - separation of pure DVCS amplitude from the interference term,
  - measurements at higher precision and statistics,
  - sensitivity to higher-twist contributions.

- The EIC will be the first electron-ion collider providing polarised electrons and light ions, and unpolarised heavy ions. Two possible sites: JLab and BNL.

- Combing a large variable centre-of-mass energy reach and an extremely high luminosity, it will allow measurements of very low cross-section processes from the valence quark region to the quark-gluon sea.

- NAS Review report (July 2018) is extremely positive — expect CD0 stage (establishing mission need) ~ 2019, construction in the 2020s.

Thank you!

Back-up and sundry

The DVCS/BH amplitude

$$\mathcal{T}^2 = |\mathcal{T}_{\mathrm{BH}}|^2 + |\mathcal{T}_{\mathrm{DVCS}}|^2 + \mathcal{I} \longleftarrow$$

Interference term for DVCS/BH

$$|\mathcal{T}_{\mathrm{BH}}|^2 = \frac{e^6}{x_B^2 y^2 (1+\epsilon^2)^2 t\, \mathcal{P}_1(\phi)\mathcal{P}_2(\phi)} [c_0^{\mathrm{BH}} + \sum_{n=1}^{2} c_n^{\mathrm{BH}} \cos n\phi + s_1^{\mathrm{BH}} \sin\phi]$$

$$|\mathcal{T}_{\mathrm{DVCS}}|^2 = \frac{e^6}{y^2 \mathcal{Q}^2} \{c_0^{\mathrm{DVCS}} + \sum_{n=1}^{2} [c_n^{\mathrm{DVCS}} \cos n\phi + s_n^{\mathrm{DVCS}} \sin n\phi]\}$$

$$\mathcal{I} = \frac{e^6}{x_B y^3 t \mathcal{P}_1(\phi)\mathcal{P}_2(\phi)} \{c_0^{\mathcal{I}} + \sum_{n=1}^{3} [c_n^{\mathcal{I}} \cos n\phi + s_n^{\mathcal{I}} \sin n\phi]\}$$

Intermediate lepton propagators

Coefficients depending on Compton Form Factors

From asymmetries to CFFs

At leading twist, beam-spin asymmetry (BSA) can be expressed as:

$$A_{\mathrm{LU}}(\phi) \sim \frac{s^{\mathcal{I}}_{1,\mathrm{unp}} \sin\phi}{c^{\mathrm{BH}}_{0,\mathrm{unp}} + (c^{\mathrm{BH}}_{1,\mathrm{unp}} + c^{\mathcal{I}}_{1,\mathrm{unp}} + \ldots)\cos\phi \ldots}$$

higher-twist terms…

The leading coefficient is related to the imaginary part of the Compton Form Factors:

$$s^{\mathcal{I}}_{1,\mathrm{unp}} \propto \Im\mathrm{m}[F_1 \boxed{\mathcal{H}} + \xi(F_1 + F_2)\widetilde{\mathcal{H}} - \frac{t}{4M^2} F_2 \mathcal{E}]$$

At CLAS kinematics, this dominates

F_1, F_2: Dirac, Pauli form factors

Likewise, for the target-spin asymmetry (TSA):

$$A_{\mathrm{UL}}(\phi) \sim \frac{s^{\mathcal{I}}_{1,\mathrm{LP}} \sin\phi}{c^{\mathrm{BH}}_{0,\mathrm{unp}} + (c^{\mathrm{BH}}_{1,\mathrm{unp}} + c^{\mathcal{I}}_{1,\mathrm{unp}} + \ldots)\cos\phi + \ldots}$$

$$s_{1,\mathrm{LP}} \propto \Im\mathrm{m}[F_1 \boxed{\widetilde{\mathcal{H}}} + \xi(F_1 + F_2)(\boxed{\mathcal{H}} + \frac{x_B}{2}\mathcal{E}) - \xi(\frac{x_B}{2}F_1 + \frac{t}{4M^2}F_2)\widetilde{\mathcal{E}}]$$

At CLAS kinematics, these CFFs dominate

✱ Obtain coefficients from fitting the phi-dependence of the asymmetry:

$$A_i = \frac{\alpha_i \sin\phi}{1 + \beta_i \cos\phi}$$

From asymmetries to CFFs

At leading twist, beam-spin asymmetry (BSA) can be expressed as:

$$A_{\mathrm{LU}}(\phi) \sim \frac{s^{\mathcal{I}}_{1,\mathrm{unp}} \sin\phi}{c^{\mathrm{BH}}_{0,\mathrm{unp}} + (c^{\mathrm{BH}}_{1,\mathrm{unp}} + c^{\mathcal{I}}_{1,\mathrm{unp}} + \ldots)\cos\phi \ldots}$$

higher-twist terms…

The leading coefficient is related to the imaginary part of the Compton Form Factors:

$$s^{\mathcal{I}}_{1,\mathrm{unp}} \propto \Im\mathrm{m}[F_1 \mathcal{H} + \xi(F_1 + F_2)\widetilde{\mathcal{H}} - \frac{t}{4M^2} F_2 \mathcal{E}]$$

At CLAS kinematics, this dominates

F_1, F_2: Dirac, Pauli form factors

Likewise, for the target-spin asymmetry (TSA):

$$A_{\mathrm{UL}}(\phi) \sim \frac{s^{\mathcal{I}}_{1,\mathrm{LP}} \sin\phi}{c^{\mathrm{BH}}_{0,\mathrm{unp}} + (c^{\mathrm{BH}}_{1,\mathrm{unp}} + c^{\mathcal{I}}_{1,\mathrm{unp}} + \ldots)\cos\phi + \ldots}$$

$$s_{1,\mathrm{LP}} \propto \Im\mathrm{m}[F_1 \widetilde{\mathcal{H}} + \xi(F_1 + F_2)(\mathcal{H} + \frac{x_B}{2}\mathcal{E}) - \xi(\frac{x_B}{2} F_1 + \frac{t}{4M^2} F_2)\widetilde{\mathcal{E}}]$$

At CLAS kinematics, these CFFs dominate

✱ Obtain coefficients from fitting the phi-dependence of the asymmetry:

$$A_i = \frac{\alpha_i \sin\phi}{1 + \beta_i \cos\phi}$$

Double-spin asymmetry

At leading twist, double-spin asymmetry (DSA) can be expressed as:

$$A_{\mathrm{LL}}(\phi) \sim \frac{c^{\mathrm{BH}}_{0,\mathrm{LP}} + c^{\mathcal{I}}_{0,\mathrm{LP}} + (c^{\mathrm{BH}}_{1,\mathrm{LP}} + c^{\mathcal{I}}_{1,\mathrm{LP}})\cos\phi}{c^{\mathrm{BH}}_{0,\mathrm{unp}} + (c^{\mathrm{BH}}_{1,\mathrm{unp}} + c^{\mathcal{I}}_{1,\mathrm{unp}} + \ldots)\cos\phi \ldots}$$

$$c^{\mathcal{I}}_{0,\mathrm{LP}}, c^{\mathcal{I}}_{1,\mathrm{LP}} \propto \Re\mathrm{e}[F_1\widetilde{\mathcal{H}} + \xi(F_1 + F_2)(\mathcal{H} + \frac{x_B}{2}\mathcal{E}) - \xi(\frac{x_B}{2}F_1 + \frac{t}{4M^2}F_2)\widetilde{\mathcal{E}}]$$

At CLAS kinematics, leading-twist dominance of these CFFs

- ✱ Fit function for the phi-dependence of the asymmetry: $\frac{\kappa_{\mathrm{LL}} + \lambda_{\mathrm{LL}}\cos\phi}{1 + \beta\cos\phi}$

Shares denominator with BSA and TSA!
If measurements at same kinematics, can do a simultaneous fit.

Jefferson Lab: 6 GeV era

CEBAF: Continuous Electron Beam Accelerator Facility.

- Energy up to ~6 GeV
- Energy resolution $\delta E/E_e \sim 10^{-5}$
- Longitudinal electron polarisation up to ~85%

Hall A:

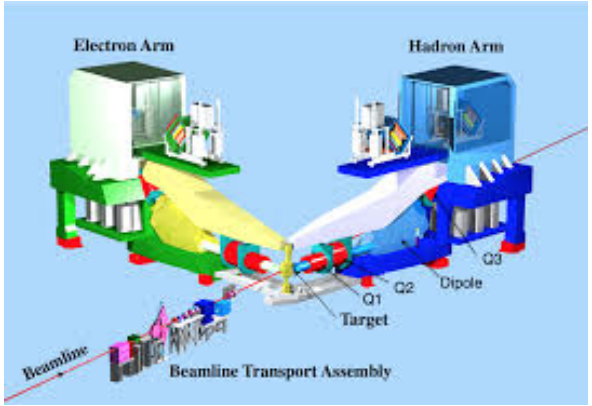

- High resolution($\delta p/p = 10^{-4}$) spectrometers, very high luminosity.

Hall B: CLAS

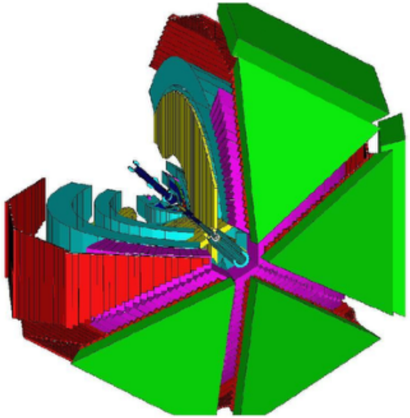

- Very large acceptance, detector array for multi-particle final states.

Hall C:

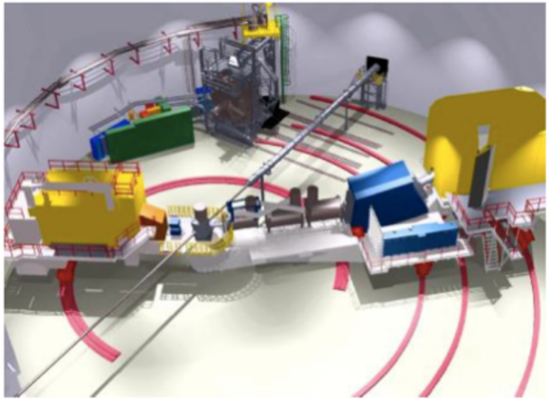

- Two movable spectrometer arms, well-defined acceptance, high luminosity

JLab @ 12 GeV

Hall A

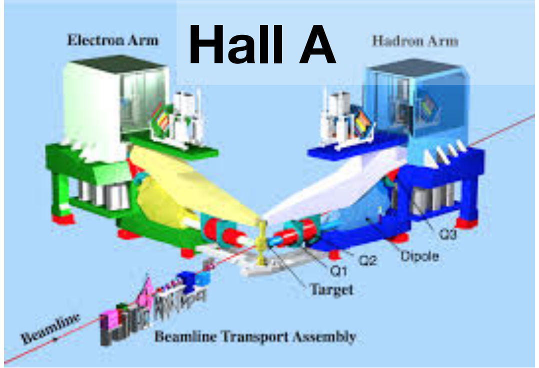

High resolution($\delta p/p = 10^{-4}$) spectrometers, very high luminosity, large installation experiments.

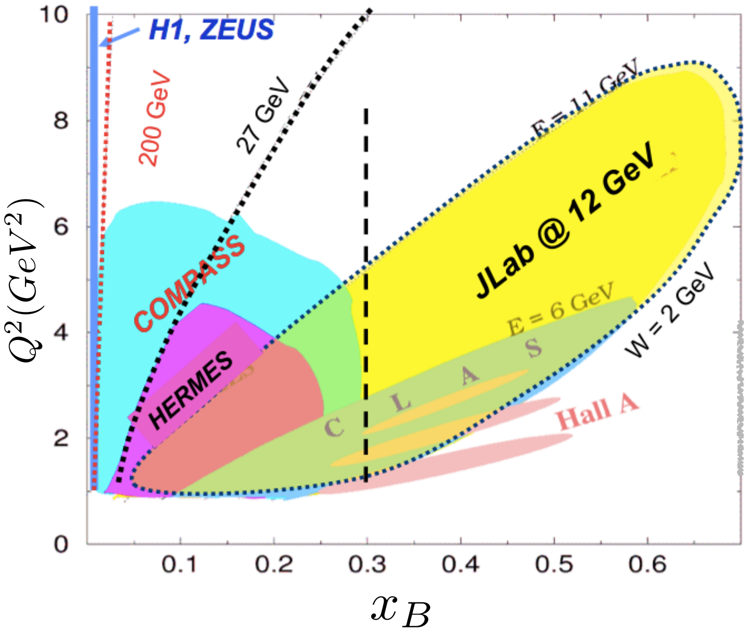

Hall C

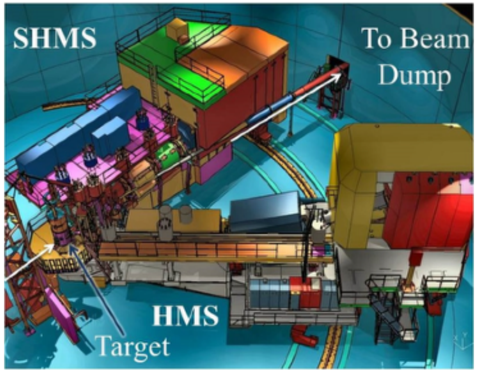

Two movable high momentum spectrometers, well-defined acceptance, very high luminosity.

Hall D

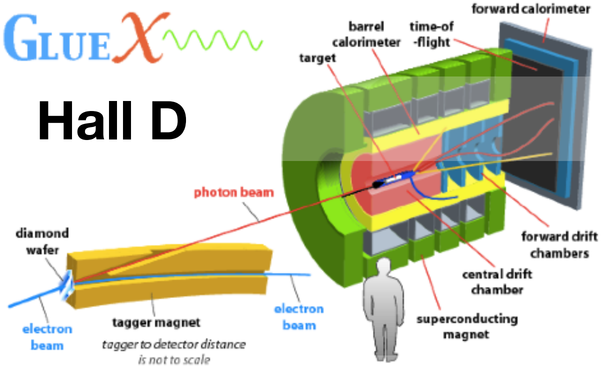

9 GeV tagged polarised photons, full acceptance

Hall B: CLAS12

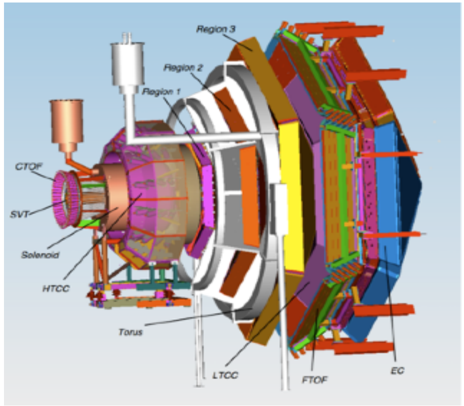

Very large acceptance, high luminosity.

DVCS in Hall A @ 11 GeV

Detect electron in the Left High Resolution Spectrometer (HRS-L): 0.01% momentum resolution

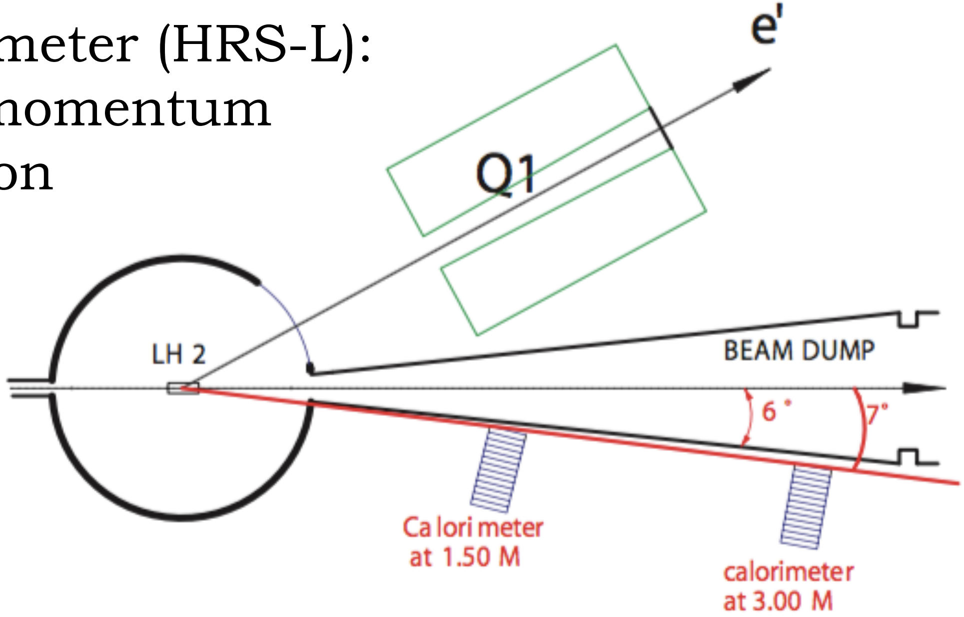

Detect photon in PbF_2 calorimeter: < 3% energy resolution

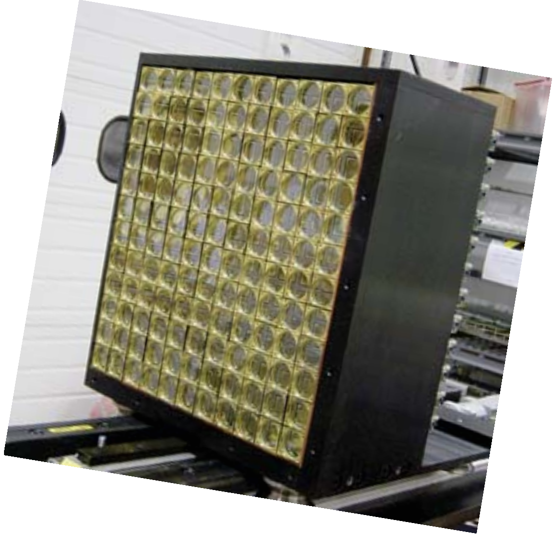

Reconstruct recoiling proton through missing mass.

DVCS in Hall C @ 11 GeV

Detect electron with (Super) High Momentum Spectrometer, (S)HMS.

Detect photon in $PbWO_4$ calorimeter.

Sweeping magnet to reduce backgrounds in calorimeter.

Reconstruct recoiling proton through missing mass.

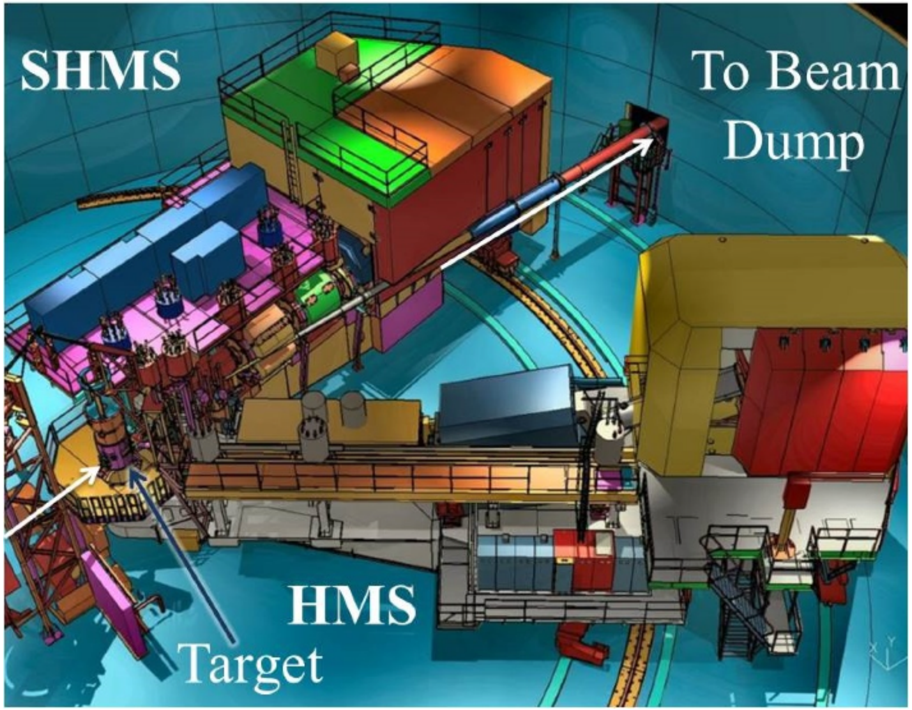

First DVCS cross-sections in valence region

Hall A

- Hall A, ran in 2004, high precision, narrow kinematic range. Q^2: 1.5 - 2.3 GeV^2, $x_B = 0.36$.

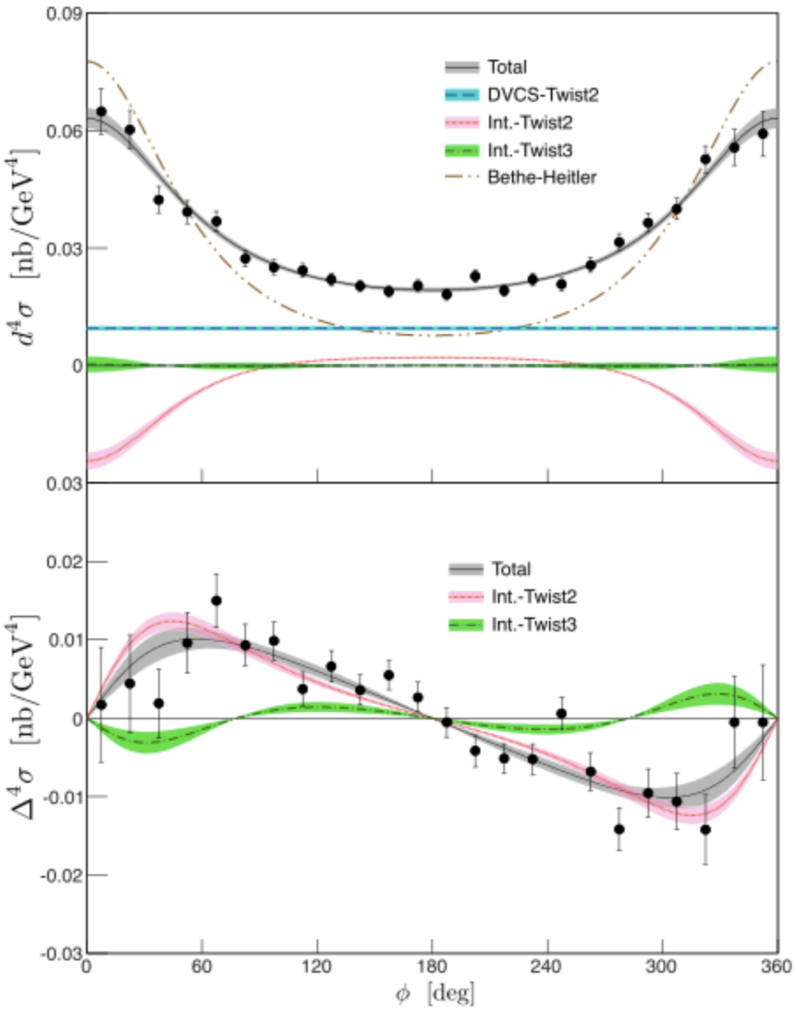

$x_B = 0.36, Q^2 = 2.3\ GeV^2, -t = 0.32\ GeV^2$

- CFFs show scaling in DVCS: leading twist (twist-2) dominance at this moderate Q^2.
- Strong deviation of DVCS cross-section from BH: extraction of $\left|T_{DVCS}\right|^2$ amplitude as well as interference terms.
- Separation of real part of the twist-2 interference term and the $\left|T_{DVCS}\right|^2$ amplitude is very sensitive to relative cross-sections at $\phi = 0^\circ$ and $\phi = 180^\circ$.

M. Defurne *et al*, ***PRC* 92** (2015) 055202.

First DVCS cross-sections in valence region

Hall A

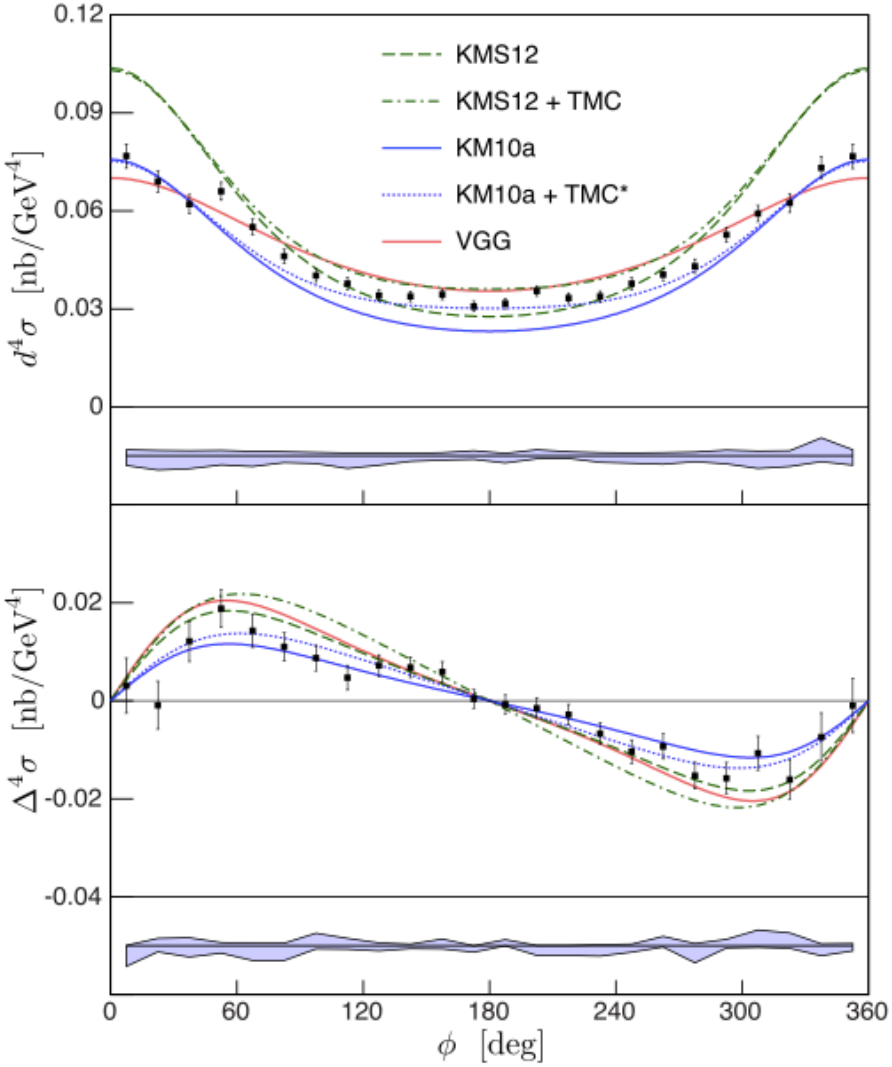

$x_B = 0.36, Q^2 = 1.9\ GeV^2, -t = 0.32\ GeV^2$

- High precision of the data: sensitivity to subtle differences in model predictions.

VGG model: Vanderhaeghen, Guichon, Guidal
KMS model: Kroll, Moutarde, Sabatié
KM model: Kumericki, Mueller

TMC: kinematic twist-4 target-mass and finite-t corrections, calculated for proton DVCS and estimated for KMS12.

- KMS parameters tuned on very low x_B meson-production data: not adapted to valence quarks.

→ TMC*: TMC extracted from the KMS12 model and applied to KM10a.

- TMC improve agreement for KM10a model, especially at $\phi = 180^\circ$. Higher-twist effects?

The devil is in the detail…

M. Defurne *et al*, ***PRC* 92** (2015) 055202.

Here comes the twist...

- Twist: powers of $\frac{1}{\sqrt{Q^2}}$ in the DVCS amplitude. Leading-twist (LT) is twist-2.
- Order: introduces powers of α_s
- LO requires $Q^2 >> M^2$ (M: target mass)

  Bold assumption for JLab 6 GeV kinematics!

- CFFs can be classified according to real and virtual photon helicity:

$\mathcal{F}_{++}$

helicity of real produced photon

helicity of virtual incoming photon

  - Helicity-conserved CFFs — $\mathcal{F}_{++}$
  - Helicity-flip (transverse) — $\mathcal{F}_{-+}$
  - Longitudinal to transverse flip — $\mathcal{F}_{0+}$

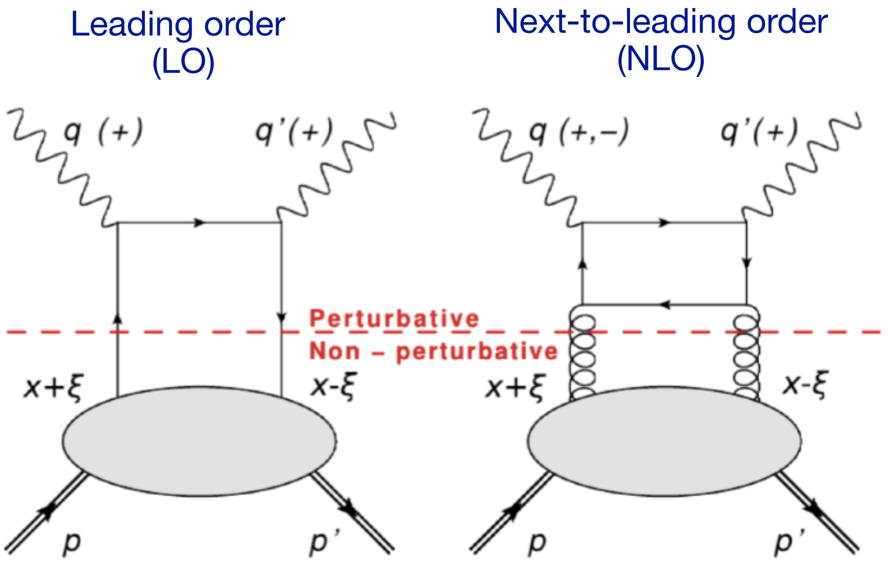

- CFFs contributing to the scattering amplitude:
  - LT in LO: only $\mathcal{F}_{++}$
  - LT in NLO: both $\mathcal{F}_{++}$ and $\mathcal{F}_{-+}$
  - Twist-3: $\mathcal{F}_{0+}$

Here comes the twist…

- At finite Q^2 and non-zero t there's ambiguity in defining the light-cone axis:
  - Traditional GPD phenomenology uses the Belitsky convention, in plane of q and P:

    A. Belitsky *et al*, ***Nucl. Phys. B878*** (2014), 214
  - New, Braun definition using q and q': more natural.

    V. Braun *et al*, ***Phys. Rev. D89*** (2014), 074022

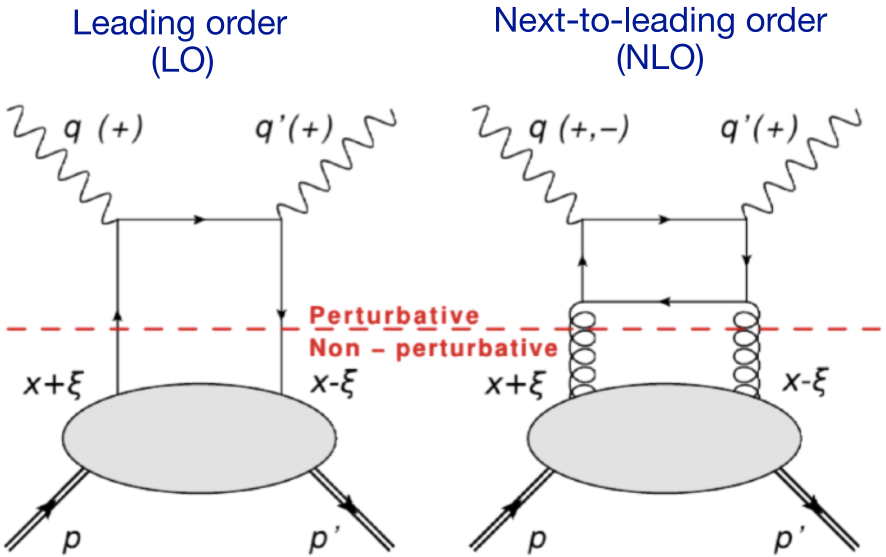

Reformulating CFFs in this frame absorbs most kinematic power corrections (TMC):

$$\mathcal{F}_{++} = \mathbb{F}_{++} + \frac{\chi}{2}\left[\mathbb{F}_{++} + \mathbb{F}_{-+}\right] - \chi_0 \mathbb{F}_{0+}$$

$$\mathcal{F}_{-+} = \mathbb{F}_{-+} + \frac{\chi}{2}\left[\mathbb{F}_{++} + \mathbb{F}_{-+}\right] - \chi_0 \mathbb{F}_{0+}$$

$$\mathcal{F}_{0+} = -\left(1 + \chi\right)\mathbb{F}_{0+} + \chi_0\left[\mathbb{F}_{++} + \mathbb{F}_{-+}\right]$$

Belitsky CFFs

Braun CFFs

Assuming LO and LT in the Braun frame leaves higher-twist, higher-order contributions in the Belitsky frame, scaled by kinematic factors χ and χ_0.

Non-negligible at the Q^2 and x_B of the Hall A cross-section measurement!

M. Defurne *et al*, ***Nature Communications 8*** (2017) 1408.

Hints of higher twist or higher orders

Hall A

- Strong deviation of the measured cross-section from Bethe-Heitler: a beam-energy scan can be used to identify pure DVCS and interference terms in a Rosenbluth-like separation, and to look for higher-twist effects.

→ E07-007: Hall A experiment to measure helicity-dependent and -independent cross-sections at two beam energies and constant x_B and t.

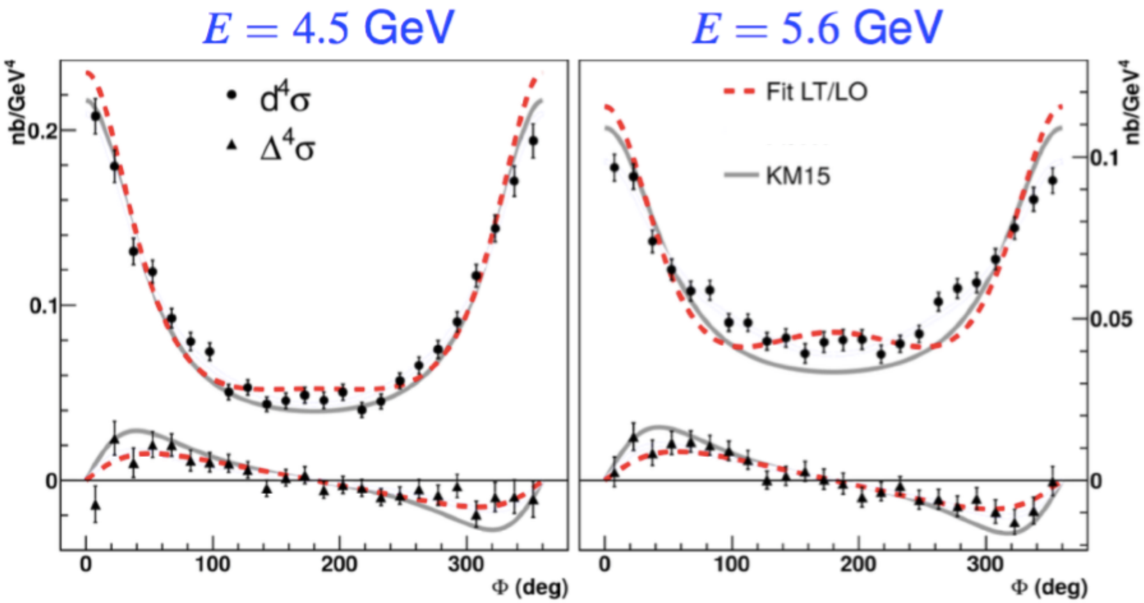

$E = 4.5$ GeV

$E = 5.6$ GeV

- Simultaneous fit to cross-sections at both energies and three values of Q^2 using only leading twist and leading order (LT/LO) do not describe the cross-sections fully: **higher twist/order effects?**

Using Braun's decomposition, $\mathbb{H}_{-+}$ and $\mathbb{H}_{0+}$ can't be neglected.

M. Defurne *et al*, ***Nature Communications* 8** (2017) 1408.

Hints of higher twist or higher orders

Hall A

- Including either higher order or higher twist effects (HT) improves the match with data:

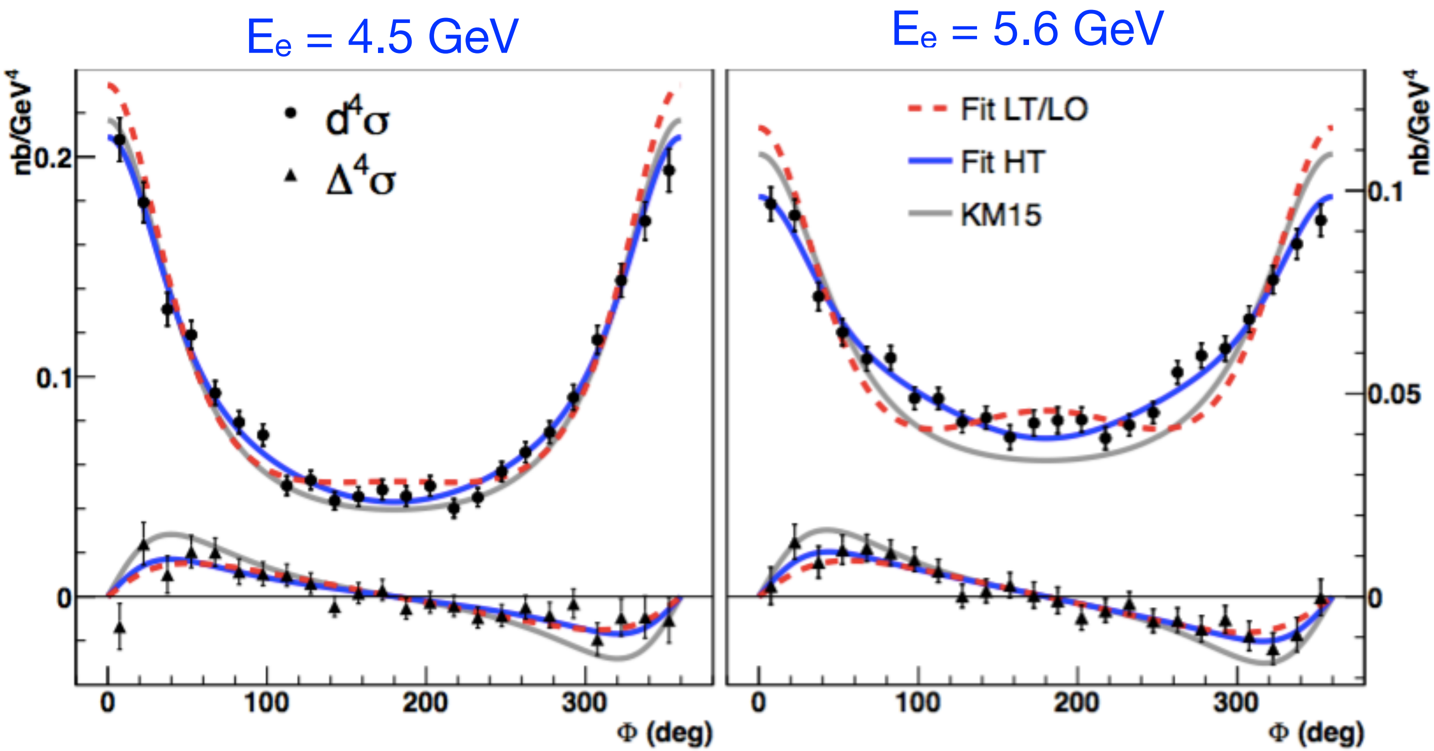

Higher-order and / or higher-twist terms are important! A glimpse of gluons.

Wider range of beam energy needed to identify the dominant effect → **JLab at 11 GeV.**

M. Defurne *et al*, ***Nature Communications* 8** (2017) 1408.

Rosenbluth separation of DVCS² and BH-DVCS terms

Hall A

- Generalised Rosenbluth separation of the DVCS² and the BH-DVCS interference terms in the cross-section is possible but NLO and/or higher-twist required.

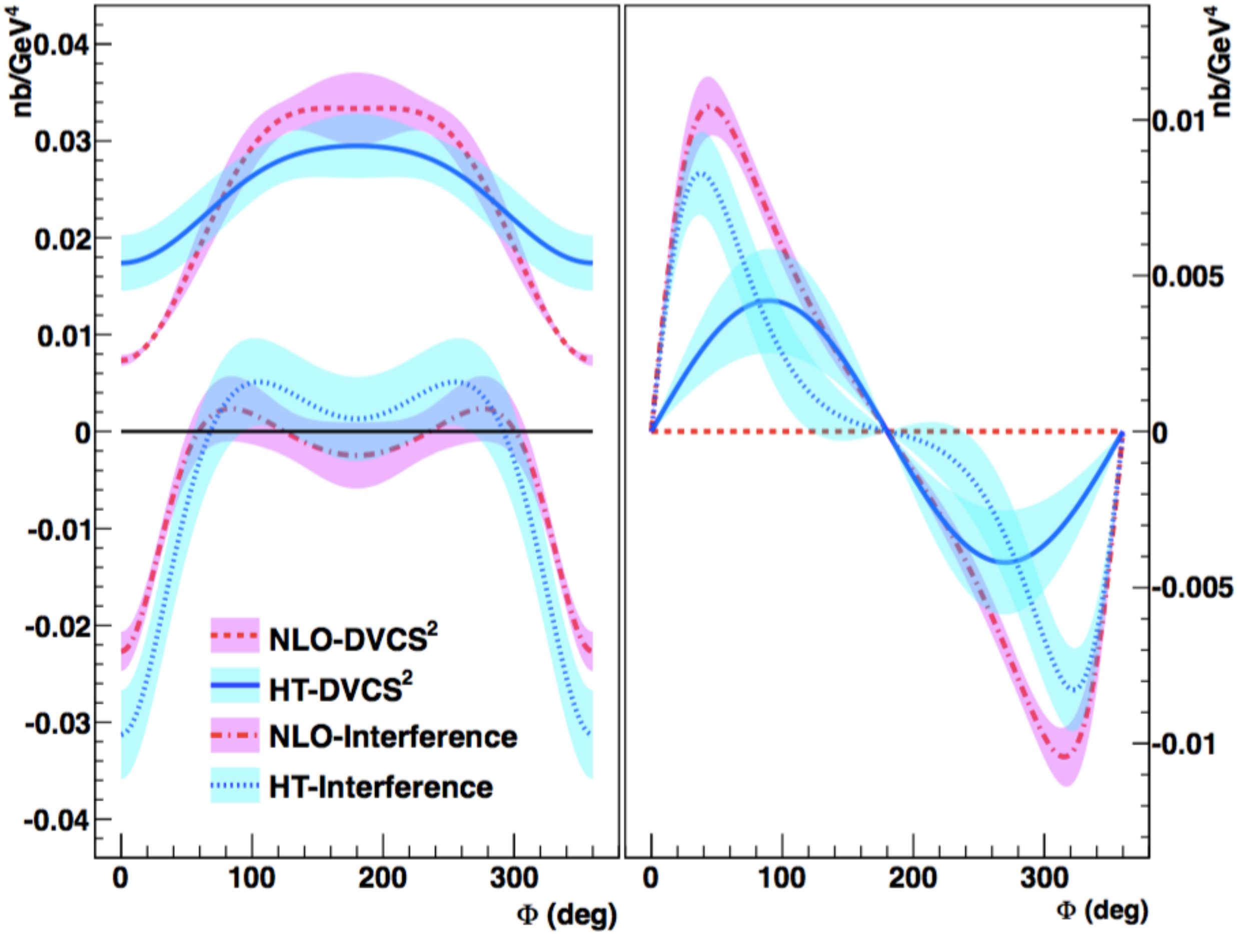

- Significant differences between pure DVCS and interference contributions.
- Helicity-dependent cross-section has a sizeable DVCS² contribution in the higher-twist scenario.
- Separation of HT and NLO effects requires scans across wider ranges of Q^2 and beam energy: JLab12!

M. Defurne *et al*, ***Nature Communications 8*** (2017) 1408.

DVCS Cross-sections: Halls A and C

Experiments:
E12-06-114 (Hall A, 100 days),
E12-13-010 (Hall C, 53 days)
C. Muñoz Camacho et al.,
C. Hyde et al.

Unpolarised liquid H_2 target:

- Beam energies: 6.6, 8.8, 11 GeV
- Scans of Q^2 at fixed x_B.
- Hall A: aim for absolute cross-sections with 4% relative precision.

✱ Azimuthal, energy and helicity dependencies of cross-section to separate $|T_{DVCS}|^2$ and interference contributions in a wide kinematic coverage.

✱ Separate *Re* and *Im* parts of the DVCS amplitude.

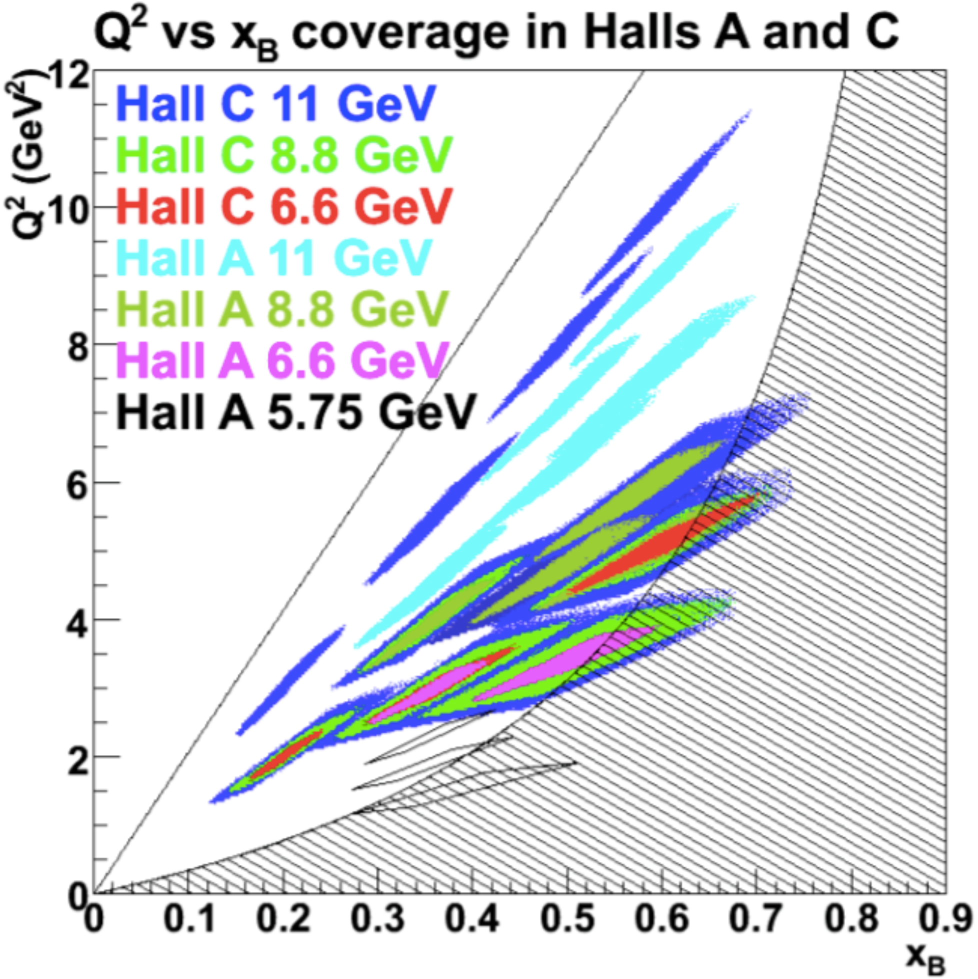

Hall A started taking data last spring!

Interpretations of the nucleon

What do spatial distributions tell us?

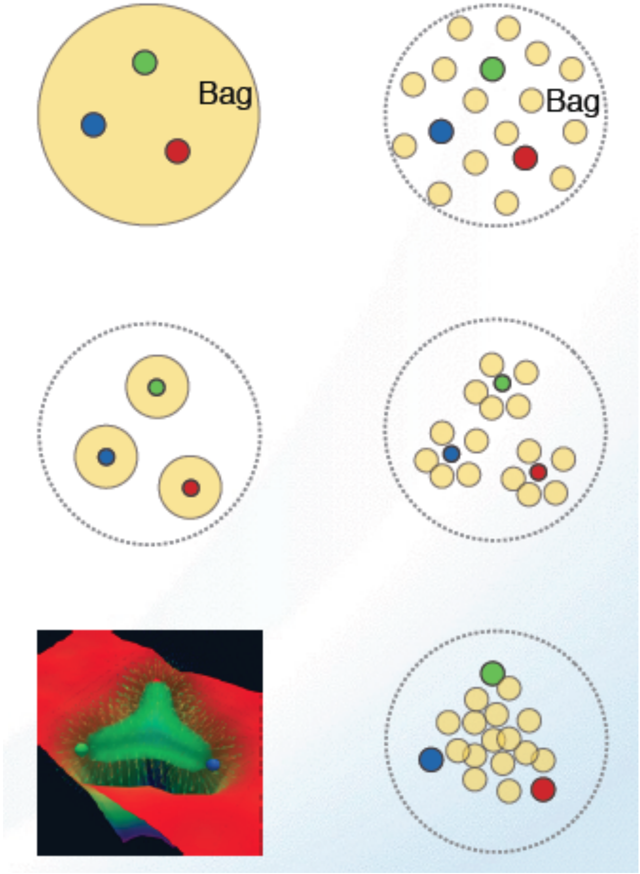

Courtesy of A. Deshpande

Bag Model: Gluon field distribution is wider than the fast moving quarks.

Gluon radius > Charge Radius

Constituent Quark Model: Gluons and sea quarks hide inside massive quarks.

Gluon radius ~ Charge Radius

Lattice Gauge theory (with slow moving quarks), gluons more concentrated inside the quarks:

Gluon radius < Charge Radius

Need transverse images of the quarks and gluons in confinement

JLEIC

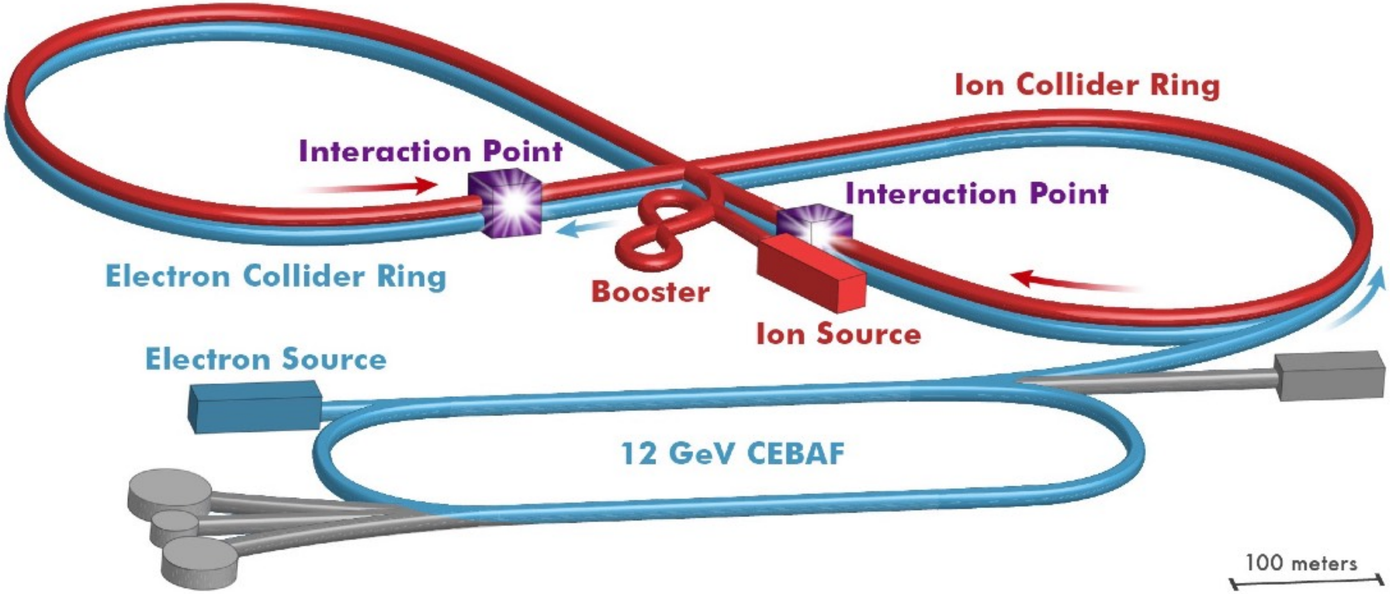

- Use CEBAF as full-energy injector (polarisation ~85%). Addition of an ion source, booster, and a figure-of-8 collider ring for electrons and ions.
- High luminosity reached through small beam size (small emittance through cooling and low bunch charge with high repetition).
- High polarisation through figure-of-8 design (net spin precession is zero, spin controlled with small magnets)

eRHIC

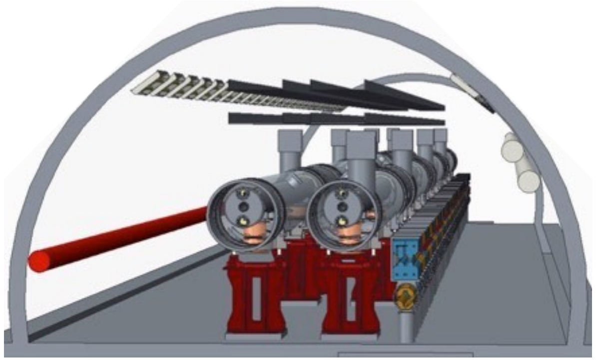

- Exploit current 275 GeV proton collider by adding a 5-18 GeV electron storage ring in the same tunnel.
- High luminosity requires novel technologies of hadron cooling — currently most promising is micro-bunched electron-beam cooling with 2 plasma amplification stages.
- 29 - 141 GeV CoM energies
- Polarised electron source and 400 MeV SLAC-type injector LINAC, 10 nA.
- Harmonic spin matching for higher polarisation (~80%).
- Highest risk in the design: hadron cooling for high luminosity (factor of ~3).